UK Atomic Energy Authority

UKAEA-R(15)30
October 2015

Michael Fleming
Jean-Christophe Sublet
Jiri Kopecky
Dimitri Rochman
Arjan Koning

Probing experimental & systematic trends of the neutron-induced TENDL-2014 nuclear data library

Probing experimental & systematic trends of the neutron-induced TENDL-2014 nuclear data library

Michael Fleming
Jean-Christophe Sublet
Jiri Kopecky[1]
Dimitri Rochman[2]
Arjan Koning[3]

October 2015

UK Atomic Energy Authority
Culham Science Centre, Abingdon, OX14 3DB
[1] Juko Research
Kalmanstraat 4, 1817 HX Alkmaar, The Netherlands
[2] Paul Scherrer Institut
OHSA/D05, Ch-5232 Villigen PSI, Switzerland
[3] IAEA Nuclear Data Section
Vienna International Centre, A-1400 Vienna, Austria

Contacts Dr Michael Fleming
Dr Jean-Christophe Sublet

UK Atomic Energy Authority
Culham Science Centre, Abingdon, OX14 3DB, UK

Telephone: +44 (0)1235-466884
email: michael.fleming@ccfe.ac.uk

Telephone: +44 (0)1235-466400
email: jean-christophe.sublet@ccfe.ac.uk

Facsimile: +44 (0)1235-463435

Website: http://www.ccfe.ac.uk/EASY.aspx

Disclaimer

Executive Summary

TENDL is a truly general-purpose nuclear data library, assembled from the outputs of the TALYS nuclear model code system for direct use in both basic physics and engineering applications. The most recent TENDL-2014 version is based on both default and adjusted parameters of the most recent T6 codes: TALYS, TAFIS, TANES, TARES, TEFAL and TASMAN, wrapped into a Total Monte-Carlo loop for uncertainty quantification. TENDL-2014 contains complete neutron-incident evaluations for all target nuclides with half-life longer than 1 second (2632 isotopes), up to 200 MeV, with covariances and all daughter products of half-life greater than 0.1 second. With the added High Fidelity Resonance (HFR) approach, all resonances are unique, following statistical rules.

The completeness not only in energy range, but also in open channels and targets, of TENDL-2014 dwarfs not only other libraries but also the experimental databases that are available to compare with. TENDL-2014 extends the nuclear landscape: having reached the proton drip-line it is now probing the neutron one. It does so with a technological methodology, so that the evaluated data are now more influenced by model parameters than excitation function adjustment.

The validation of the TENDL-2014 neutron-induced library against standard, evaluated, microscopic and integral cross sections is performed against a newly compiled UKAEA database of thermal and resonance integral cross sections. This has been assembled using the most up-to-date, internationally-recognised data sources including the Atlas of Resonances, CRC, evaluated EXFOR and EAF database. Excellent agreement with TENDL-2014 values is found except for a very small set of discrepancies due to TENDL-2014 input parameter errors.

The microscopic cross section systematics used in previous EAF library validations have been implemented and those for 14 MeV incident neutrons on major reaction channels are compared against TENDL-2014 using a variety of visualisation methods. Many differences are found which are due to the limitations of the systematics which were never designed for a complete library such as TENDL. The addition of more open reaction channels, extension further from stability and inclusion of the most sophisticated nuclear input parameter libraries places TENDL-2014 well beyond the reach of simple polynomial systematics and therefore the systematic comparisons are complemented with surveys of microscopic cross sections.

Contents

1 Introduction

The TALYS-generated [1, 2] TENDL-2014 [3] is a general-purpose nuclear data library which includes neutron-induced files of all target nuclides with half-life greater than 1 second and all reaction channels up to 200 MeV. In comparison with the well-known legacy nuclear data libraries and activation libraries, it sets a completely different standard for comprehensiveness. The boldness of this approach is inherently connected to another unique feature of the TENDL data: it is *completely* updated annually with improved models, input parameters and corrections. This gives TENDL a tremendous advantage in a field of nuclear data libraries which are generally incomplete (in files, channels, emitted data, uncertainties, *etc*), are slow to improve (and correct) and contain many legacy, application-specific 'features'.

Any nuclear data library, and particularly a complete one, must reconcile the detailed data over all energies and emitted parameters with the limited experimental information available. The limitations come in two types:

1 Experimental data only exists for a specific energies of importance (or convenience) on the few nuclides which are of particular interest (mostly for specific applications).

2 Where the data are available, they are unique (and renormalised to) or require some evaluation to select a reference value.

In the validation of TENDL-2014, the available experimental inputs are required as an evaluated database. For this report the main references are the *Atlas of Neutron Resonances* [4], most recent CRC handbook [5] and EAF compilation database [6] which are cross-checked and supplemented with a few modern experimental results and evaluated EXFOR entries. The resulting UKAEA database of microscopic thermal and resonance integral cross sections is then compared with the TENDL-2014 values to validate the library, building upon previous validations for high-energy and astrophysical integral cross sections [7, 8]. Together these form a broad range of validations over the available experimental data in a variety of complementary energies and with multiple integral values.

The more difficult issue of missing experimental data presents a problem for nuclear data validation, but the need for this data in many simulations requires TENDL to extend well beyond the stability line and include channels beyond the energies of experimental support, or indeed channels which have no experiments whatsoever. The approach favoured for legacy activation libraries has been to generate systematic functions through the use of some theoretical models of nuclear interactions in order to choose a functional form and then select parameters with a statistical fit to the available experimental data. These systematics could then be used for renormalisations of data. This approach has been quite successful in previous work, but suffers from two major drawbacks:

1 The models considered are invariably less physically realistic than those within TALYS and draw upon a small subset of the available input parameters.

2 While interpolation of statistical fits to experimental data may be valid between the nuclides near stability, it cannot be extrapolated far from stability where new models and open channels are required.

The role for systematics in nuclear data has now become as a verification tool, finding agreement in local/global trends and identifying outliers which may be due to errors in input data or coding bugs. In this regard systematics with a reasonable amount of sophistication can be quite useful near the stability line. Far from stability and when odd/even or magic effects become prominent, systematics become less reliable and simple surveys of microscopic cross sections must suffice. Still, these can be successful in identifying suspicious trends and outliers, as is demonstrated in this report.

2 Experimental data

2.1 Thermal cross sections

Cross sections for thermal Maxwellian energies of standard laboratory and reactor temperatures are (relative to many other energies) easy to measure and a large set of reaction channels have experimental data. Many of these are not precise differential measurements, but effective, integral cross sections which are obtained within a Maxwell distribution at some temperature such as 293 K (equivalent to average neutron energy of 0.0253 eV or a neutron moving at 2200 m/s). The Maxwellian-averaged cross section

$$\sigma_{maxw}(kT) = \frac{2}{(kT)^2\sqrt{\pi}} \int \sigma(E)\, E\, e^{-E/kT}\, dE \tag{1}$$

is typically quite similar to the differential value at $E = kT$,

$$\sigma_{maxw}(kT) \equiv g_w\, \sigma(kT) \tag{2}$$

with the Wescott factor g_w defined as the ratio between the two. For most reactions the cross section over the energies covered by the Maxwellian vary as $1/v$ and the collapsed value is very near to the differential, *ie* $g_w \approx 1$. This is not true in general and there are many reactions, such as the well-known ^{135}Xe, ^{149}Sm and ^{239}Pu captures, which are significantly different from $1/v$ in the thermal energy region. All of the thermal cross sections summarised in the Appendix A are marked as either differential or averaged over a Maxwellian spectrum.

The *Atlas of Neutron Resonances* [4] is the main source for the thermal cross section data selected for this validation with a few additional values from the CRC handbook [5]. In a few cases the values in these sources were found to be in disagreement with the experimental data and were replaced with data taken from the best available experiments referenced in EXFOR. In some cases a variety of different values were published in the experimental database which also conflicted with the *Atlas* and/or the CRC. In these cases (particularly for isomeric production ratios) evaluated EXFOR values were selected for this compilation.

Table 1: Reactions with updated data not from the *Atlas*, CRC or previous compilations [6].

Target	Reaction	Source	Target	Reaction	Source
^{22}Na	(n,γ) total	Werner 1972 [9]	**^{59}Ni**	(n,p) total	Eval. EXFOR
^{78}Se	(n,γ)g,m	Eval. EXFOR	**^{80}Se**	(n,γ)g,m	Eval. EXFOR
^{82}Se	(n,γ)g,m	Eval. EXFOR	**^{78}Kr**	(n,γ)g,m	Eval. EXFOR
^{84}Kr	(n,γ)g,m	Eval. EXFOR	**^{85}Rb**	(n,γ)g,m	Eval. EXFOR
^{89}Y	(n,γ)m	Eval. EXFOR	**^{90}Zr**	(n,γ)m	Eval. EXFOR
^{106}Pd	(n,γ)m	Eval. EXFOR	**^{110}Cd**	(n,γ)g,m	Eval. EXFOR
^{116}Sn	(n,γ)m	Krane 2006 [10]	**^{120}Sn**	(n,γ)m	Eval. EXFOR
^{122}Sn	(n,γ)m	Krane 2006 [10]	**^{123}Sb**	(n,γ)g,m	Eval. EXFOR
^{124}Te	(n,γm	Eastman 2008 [11]	**^{126}Te**	(n,γ)g,m	Eval. EXFOR
^{128}Xe	(n,γ)g,m	Eval. EXFOR	**^{130}Xe**	(n,γ)g,m	Eval. EXFOR
^{132}Xe	(n,γ)g,m	Eval. EXFOR	**^{134}Xe**	(n,γ)g,m	Eval. EXFOR
^{151}Er	(n,γ)g,m,n	Eval. EXFOR	**^{176}Lu**	(n,γ)g,m	Eval. EXFOR
^{177}Hf	(n,γ)n	Karamian 2006 [12]	**^{181}Ta**	(n,γ)g,m,n	Eval. EXFOR
^{237}U	(n,f) total	Eval. EXFOR	**^{238}U**	(n,f) total	Eval. EXFOR
^{239}Np	(n,f) total	Eval. EXFOR	**^{243}Am**	(n,γ)g,m	Eval. EXFOR

2.2 Integral resonance values

Resonance integral data is a standard, but simplistic, method for comparing the reaction probabilities in the complex resonance ranges. For the operation of fission reactors the capture or fission cross sections of this region are simplified into one value using a neutron spectrum which is approximately $1/E$ between the thermal Maxwellian and fission spectrum. The standard integral is given in this spectrum, as

$$I = \int_{E_1}^{E_2} \frac{\sigma(E)}{E}\, dE, \tag{3}$$

where the integration limits are taken as E_1=0.5 eV and E_2=100 keV. The references for these values are mostly taken from the *Atlas*, which provides values calculated using all of the resonance within that text, as well as a contribution from the $1/v$ cross section background. Some of these values are experimental while others are derived from the resonance parameters included in the *Atlas*. Since these calculated values are dependent upon the accuracy of the set of resonance parameters between 0.5 eV and 100 keV, the integral resonance cross section provides more of a verification against another 'library' of resonances. When both are provided and differ substantially, such as the ^{196}Pt (n,γ) integral resonance, experimental values are generally preferred for this validation.

2.3 Maxwellian-averaged cross sections

Stellar nucleosynthesis involves a variety of nuclear reactions, of which neutron capture plays a central role in the production of heavy nuclides. The combination of neutron capture and beta decay of neutron-rich nuclides results in the synthesis of progressively heavier nuclei. The *slow* s-process runs through the valley of stability and these capture reactions have been the focus of many experimental efforts.

The KADoNiS database [13] is largely built upon the compilation of Bao *et al* [14] and provides temperature-dependent Maxwellian-averaged cross sections for kT=1 to kT=100 keV. The validation of TENDL-2014 over all of these nuclides and temperatures was the subject of another UKAEA report [8], which describes the collapse and broadening methods employed. The reaction rates in this case vary considerably over the Maxwellian energy region and are highly sensitive to the resonances, as shown in the ^{87}Rb example of Figure 1. These values clearly depend upon the resonance parameters covered over a variety of complementary spectra and the full report with temperature-dependent analysis provides a more detailed picture. The collapse is the same as with Equation (1), but the complex resonance features will ensure that the effective g_w is generally not near one. In this report only the 30 keV data are considered as an additional non-threshold integral value.

Note that 80 of the 357 cross sections within KADoNiS (22%) are due to statistical model calculations, although they are generally informed by detailed studies with multiple different codes and systematics. These are identified in the detailed report, which should be referred to for more information.

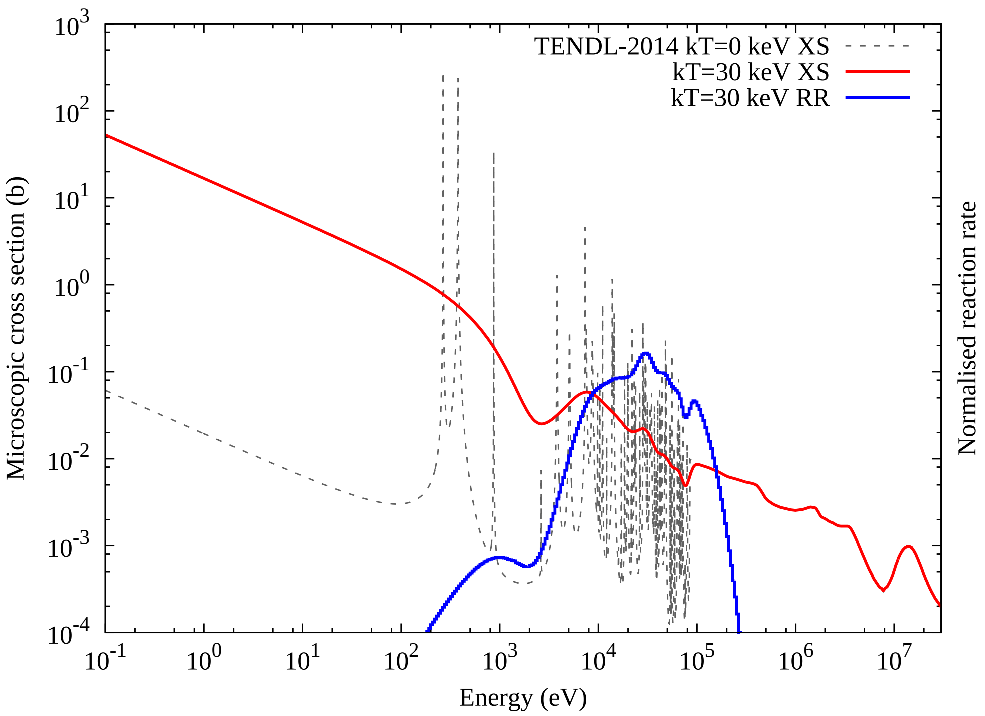

Figure 1: Microscopic cross section for ^{87}Rb neutron capture at 0 and 30 keV, with a normalised, energy-dependent reaction rate superimposed.

3 Codes and Library

This report considers all available thermal cross section and resonance integral measurements, as well as the capture cross sections from s-process nuclides within the KADoNiS database. It benefits from the completeness of TENDL-2014 [3], which does not miss any of the target nuclides and contains all reaction channels. The low-Z nuclides ^{1,2,3}H, ^{3,4}He, ^{6,7}Li, ^{9}Be, ^{10,11}B, ^{nat}C, ^{14,15}N, ^{16}O and ^{19}F are not generated by the TALYS code suite, but taken directly from the ENDF/B-VII.1 libraries [15], except natural carbon which is taken from JENDL-4.0 [16].

In order to extract, process and collapse the microscopic and integral cross sections from nuclear data files, a combination of energy-dependent neutron capture cross sections and codes which can broaden and collapse these data with the corresponding neutron spectra are required. The three codes used for these purposes are:

- **PREPRO-2015** [17] The ENDF pre-processing code used to produce the TENDL-2014 pointwise data with the appropriate Doppler broadening.
- **maxwav** [18] A Fortran code developed by the Japanese Atomic Energy Research Institute to perform resonance region integration with high temperature Maxwellian spectra. Used for the calculations in [19].
- **inter** [20] The ENDF Utility Code which is a standard in the field of nuclear data. This code extracts many quantities from the processed pointwise files including differential and integral, effective cross sections in a variety of neutron spectra. The built-in Maxwellian spectra can be set at arbitrary temperatures. It is also used to extract other microscopic cross sections for global cross section verification.

4 Comparisons with experimental values

The comparison of TENDL-2014 with the newly compiled UKAEA database uncovers several errors in the original experimental databases as well as the TENDL data. These errors can be broken down into a few varieties:

- One non-threshold channel incorrectly attributed to another (typically to capture)
- Total absorption transformed into a specific channel
- Isomeric production omitted and read as total
- b vs. mb vs. μb mis-attribution
- Simple typographical errors

Since the TALYS code suite contains its own version of the thermal cross section database, the errors contained within it are most likely the source of these discrepancies and use of the newly generated database from this report should greatly improve future libraries.

In all figures and tables,

$$A = N + Z$$

is the sum of the neutron N and proton Z numbers, known as the mass number, and

$$S = \frac{N - Z}{A}$$

is the asymmetry, which describes how neutron-rich/poor the nuclide is. Plots against A help to separate out the features which appear at different masses, while asymmetry provides many useful, channel-specific perspectives. Both are commonly used in functional systematic descriptions of cross sections.

4.1 Global comparisons

Thermal cross sections

The cross section for 0.0253 eV represents a specific differential measurement or a Maxwellian-averaged value for target material which is in room-temperature thermal equilibrium. Nearly one thousand nuclides have such measurements and these are used to set the corresponding low-energy cross sections. The overall distribution of TENDL-2014 calculation (C) to experiment (E) ratios is very tight[1], as can be seen in Figure 2. The only exceptions are the small 'wings' due to various database errors which should be rectified in future evaluations. A summary of all the thermal cross sections contained within the database and compared with TENDL-2014 values extracted using `inter` is provided in Table 3.

The majority of experimental inequalities (*eg* $\sigma_X <$ 1mb) are treated by TENDL-2014 as experimental values to be reproduced (*ie* $\sigma_X =$ 1mb). A few have suspicious value which suggest typos within the input database, including:

- ^{7}Be(n,α) $\sigma_E <$ 100 mb in the *Atlas* and $\sigma_C =$ 100 μb in TENDL-2014
- ^{127}Xe(n,α)$\sigma_E <$ 10 mb in the *Atlas* and $\sigma_C =$ 10 μb in TENDL-2014
- ^{132}Cs(n,α) $\sigma_E <$ 150 mb in the *Atlas* and $\sigma_C =$ 150 μb in TENDL-2014
- ^{210}Po(n,γ)m $\sigma_E <$ 500 μb in the *Atlas* and effectively closed with $\sigma_C =$ 1.72E-17 b in TENDL-2014

[1] As should be expected when a library is generated using the experimental data as inputs

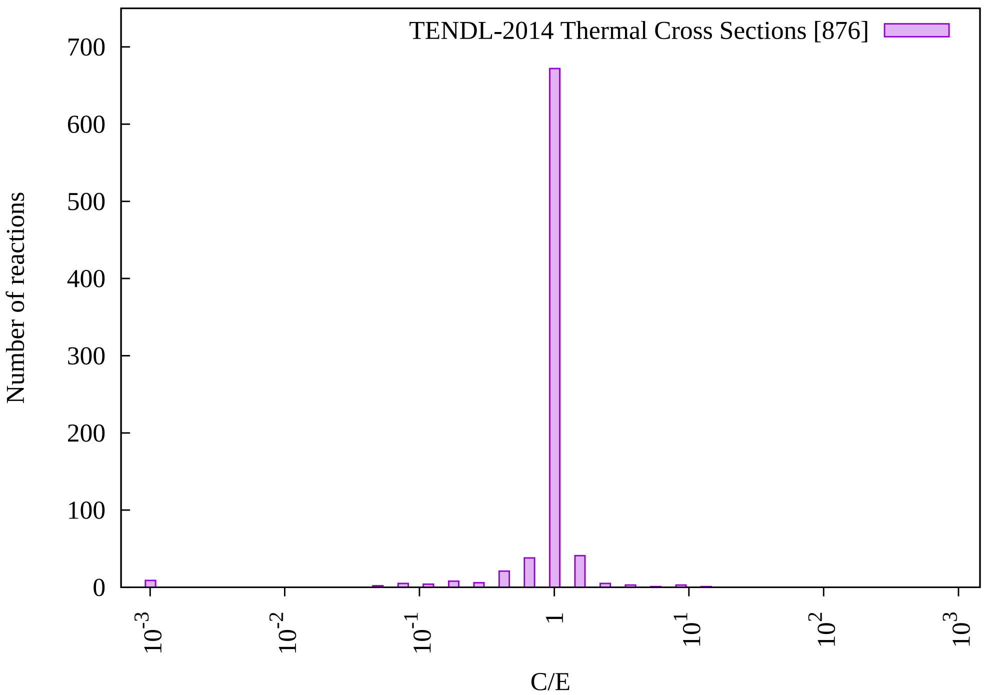

Figure 2: Distribution of TENDL-2014 thermal cross section C/E values.

Integral resonance values

As with the thermal data, the resonance integrals provide an opportunity to correct errors in previous databases, but also provide an integral value which assists in validating the resonance region of the TENDL files. It should be stressed that the resonances used in the construction of TENDL are based upon a combination of databases and extension using the high-fidelity statistical resonances generated by CALENDF [21]. In contrast with the thermal cross sections, these integral values do not reflect one number which is set within the file evaluation, but an integral cross section which crudely summarises the complex concert of evaluation methodologies employed by the TARES module. Given the more nuanced nature of these values, the distribution of C/E values has greater variation than those for thermal cross sections as can be seen in Figure 3. A summary for all experimental and TENDL-2014 values is provided in Table 4.

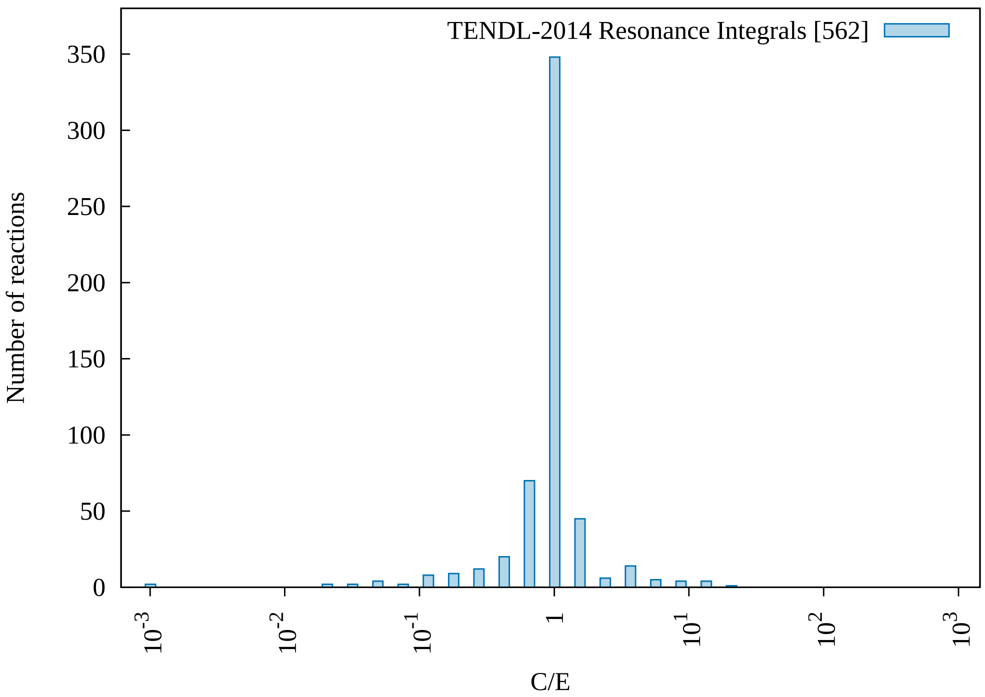

Figure 3: Distribution of TENDL-2014 integral resonance cross section C/E values.

4.2 Channel-specific comparison

4.2.1 Analysis of (n,γ) cross sections

With the majority of the thermal and resonance integral measurements, neutron capture is one of the most well-studied non-threshold reactions outside fission. The thermal cross sections are used as inputs for nuclear data evaluations and as such whatever value found in the *Atlas* is likely to be quite similar to all library values. As a result, the thermal values are almost always very similar to those of the thermal database, as shown in Figures 4 and 5. The resonance integrals show greater C/E variation, as expected due to the complex nature of building the resonance parameter files and potential for selecting data from multiple sources. These are shown in Figures 6 and 7.

A few reactions which lie at the most extreme C/E values are identified within the figures for reference. These are predominantly isomeric production values, which are not handled through the introduction of library values into the TALYS system, but through model calculations employing the most recent RIPL-3 input data [22]. For the isomeric productions which were modified to match with evaluated EXFOR data the agreement is typically quite good, but a few are still in disagreement with experimental results quoted in the *Atlas*.

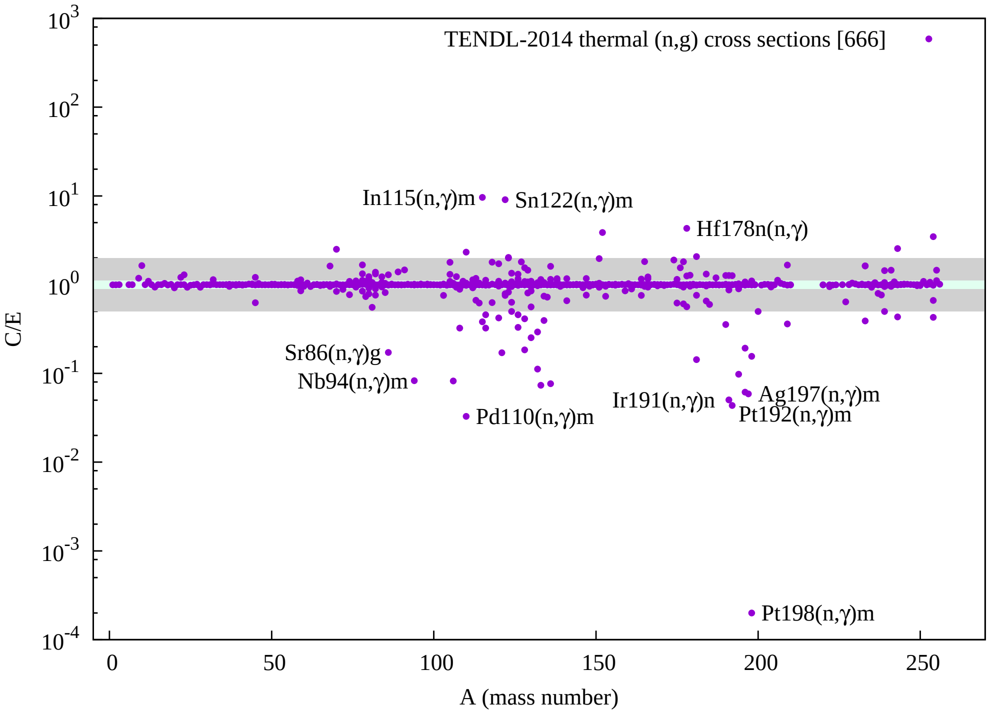

Figure 4: Distribution of TENDL-2014 (n,γ) thermal cross section C/E values against number of nucleons A. The bands represent regions of $\frac{1}{2}$<C/E<2 and |C-E|/E <10%.

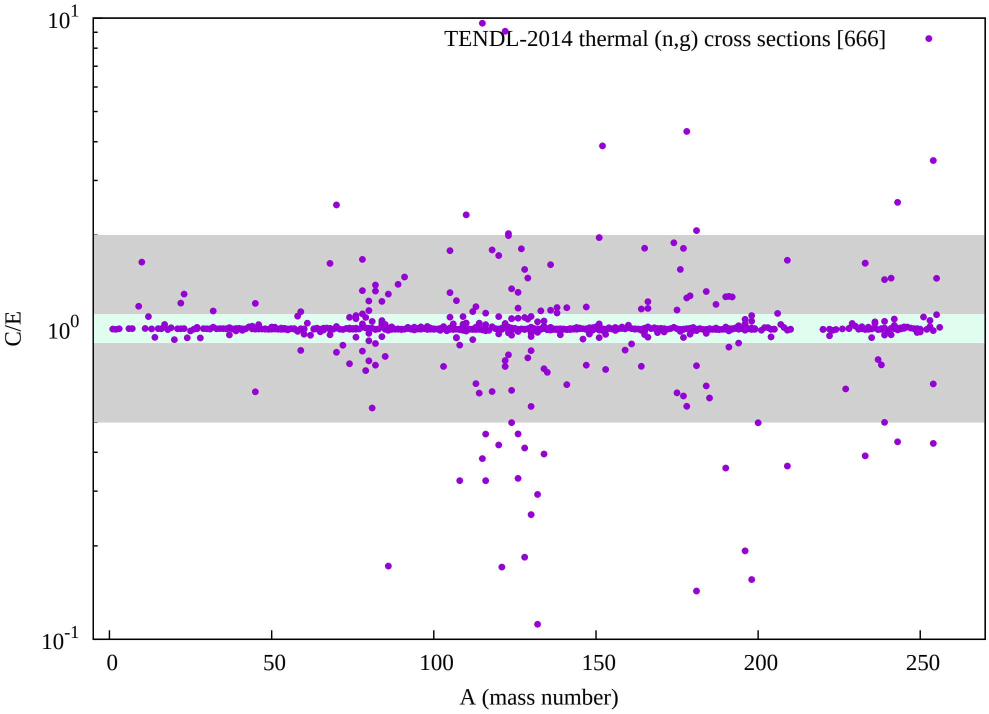

Figure 5: Distribution of TENDL-2014 (n,γ) thermal cross section C/E values against number of nucleons A zoomed into the region of C/E $\in$ [0.1,10]. The bands represent regions of $\frac{1}{2}$<C/E<2 and |C-E|/E <10%.

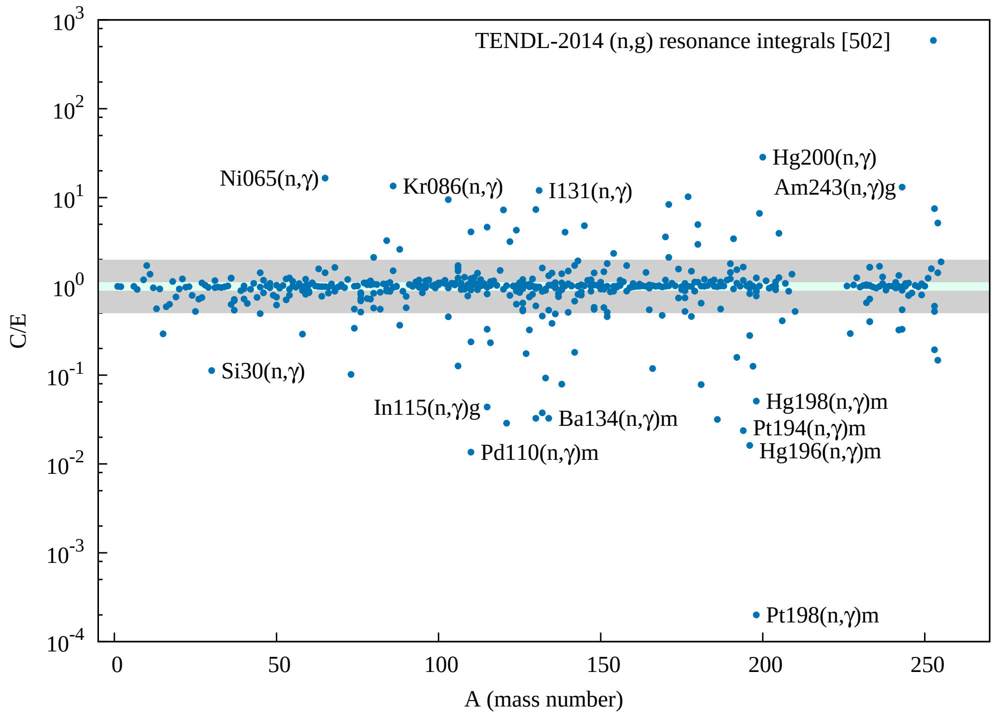

Figure 6: Distribution of TENDL-2014 (n,γ) integral resonance cross section C/E values against number of nucleons A. The bands represent regions of $\frac{1}{2}$<C/E<2 and |C-E|/E <10%.

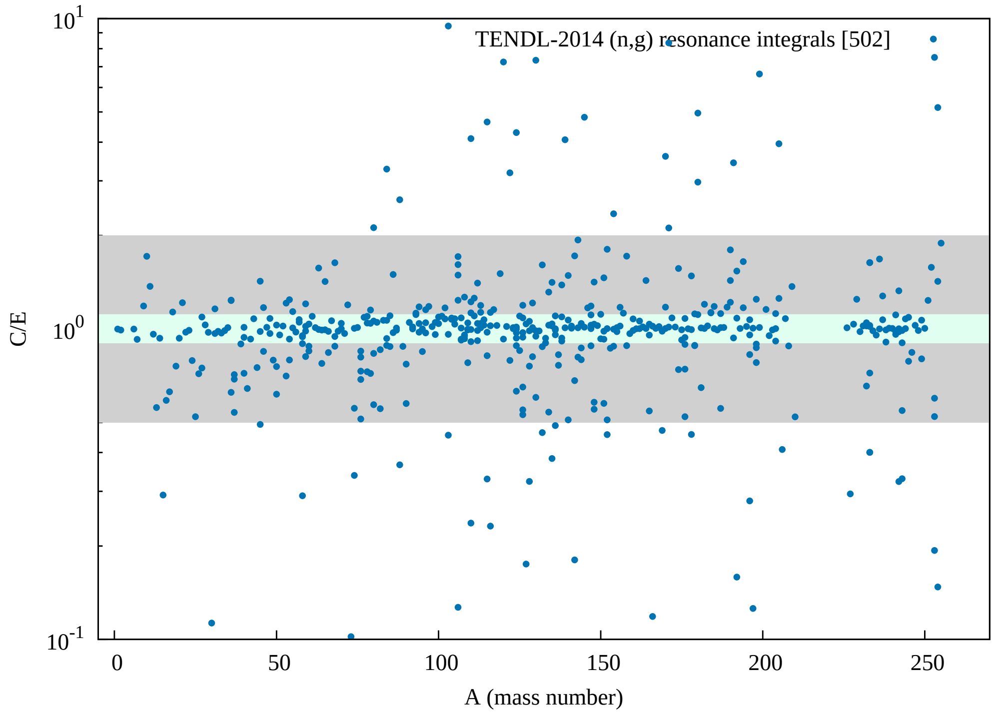

Figure 7: Distribution of TENDL-2014 integral resonance cross section C/E values against number of nucleons A zoomed into the region of C/E $\in$ [0.1,10]. The bands represent regions of $\frac{1}{2}$<C/E<2 and |C-E|/E <10%.

As an additional effective resonance integral, the 30 keV cross section from KADoNiS is used as the standard and is provided with an uncertainty. These provide a second integral value with which to benchmark the complex resonance regions. While simulations with all temperatures are shown in the complete report [8] by isolating the 30 keV an indicative distribution against the experimental data can be obtained. This distribution is similar to that for the resonance integrals and still has a few outliers with more than an order-of-magnitude difference. The summary for all experimental and TENDL-2014 cross sections is provided in Table 5, while the distribution of C/E values for all KADoNiS data is shown in Figures 8 and 9. Following the comparisons experimental data is Figure 10 which shows the global trends in 30 keV capture MACS for all 2632 target nuclides.

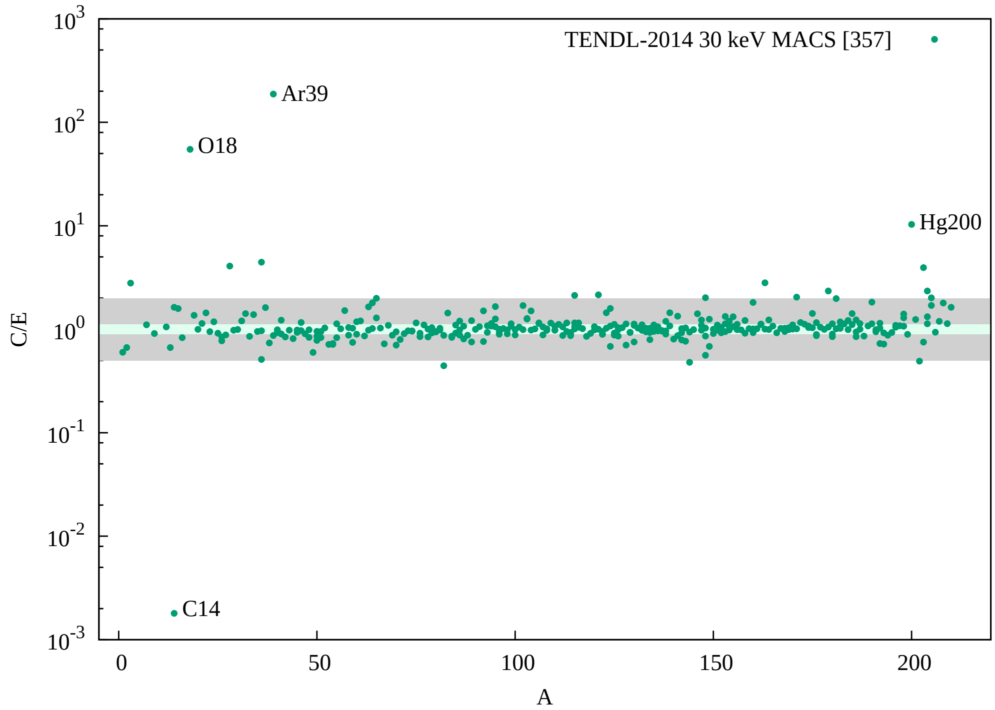

Figure 8: Comparison of all 357 KADoNiS 30 keV cross sections with TENDL-2014 values calculated with maxwav. A few nuclides are isolated which require an adjustment of over one order of magnitude. The bands represent regions of $\frac{1}{2}$<C/E<2 and |C-E|/E <10%.

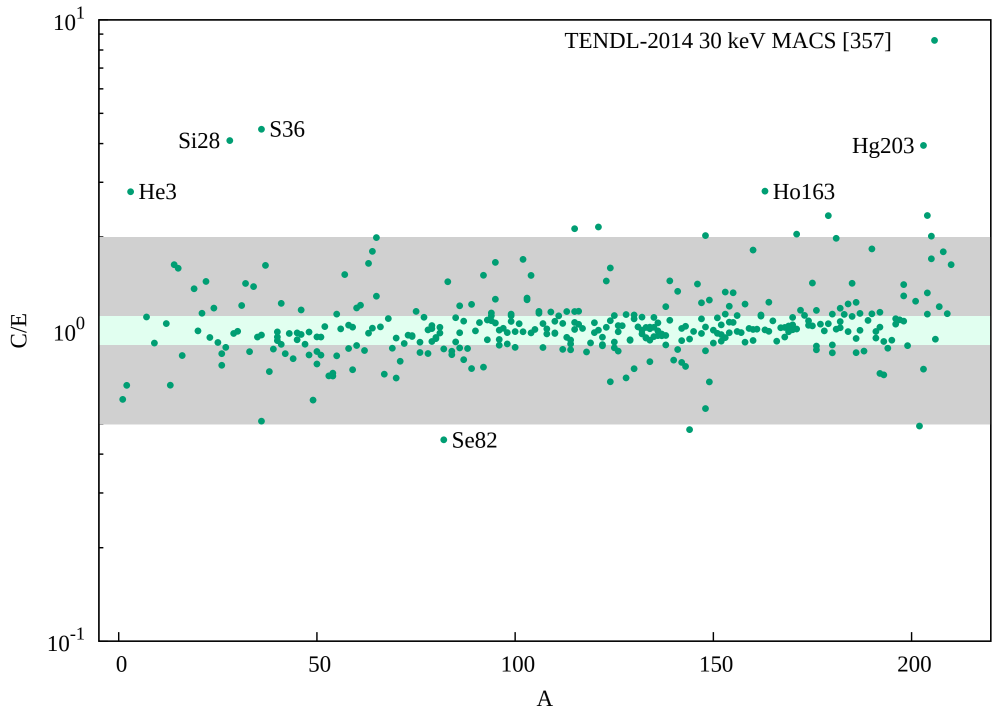

Figure 9: Comparison of all 357 KADoNiS 30 keV cross sections with TENDL-2014 values calculated with maxwav where nuclides with more than one order of magnitude difference are removed. The bands represent regions of $\frac{1}{2}$<C/E<2 and |C-E|/E <10%.

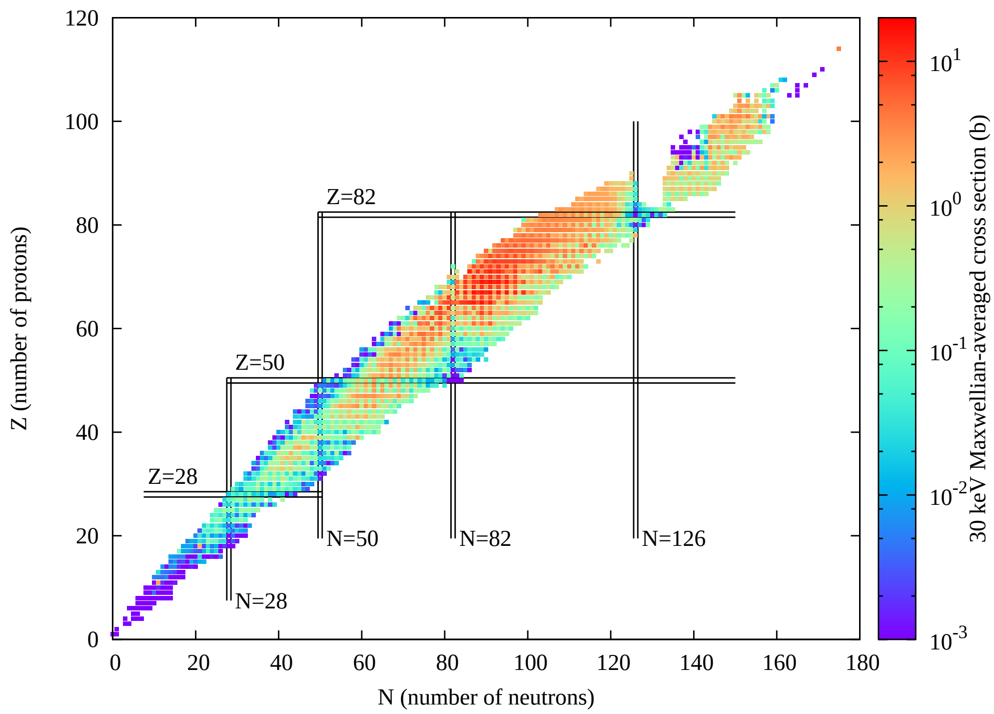

Figure 10: 30 keV (n,γ) MACS for all nuclides in TENDL-2014. Magic numbers are identified by lines to help interpret some lower cross sections. MACS lower than 1 mb are given as the lower plot cutoff of 1 mb.

4.2.2 Analysis of (n,α) cross sections

While there are no resonance integrals for the (n,α) channel, the set of thermal cross sections covers some 52 target nuclides. Six of these contain three order-of-magnitude errors within TENDL-2014 which are most likely attributable to b$\leftrightarrow$mb typos. The following nuclides are affected:

- ^{22}Na, ^{26}Al, ^{37}Ar, ^{59}Ni, ^{65}Zn and ^{109}Cd

The ^{153,155}Gd (n,α) channels are also significantly under-predicted by TENDL-2014, although they are one millionth and one billionth of their capture cross sections, respectively.

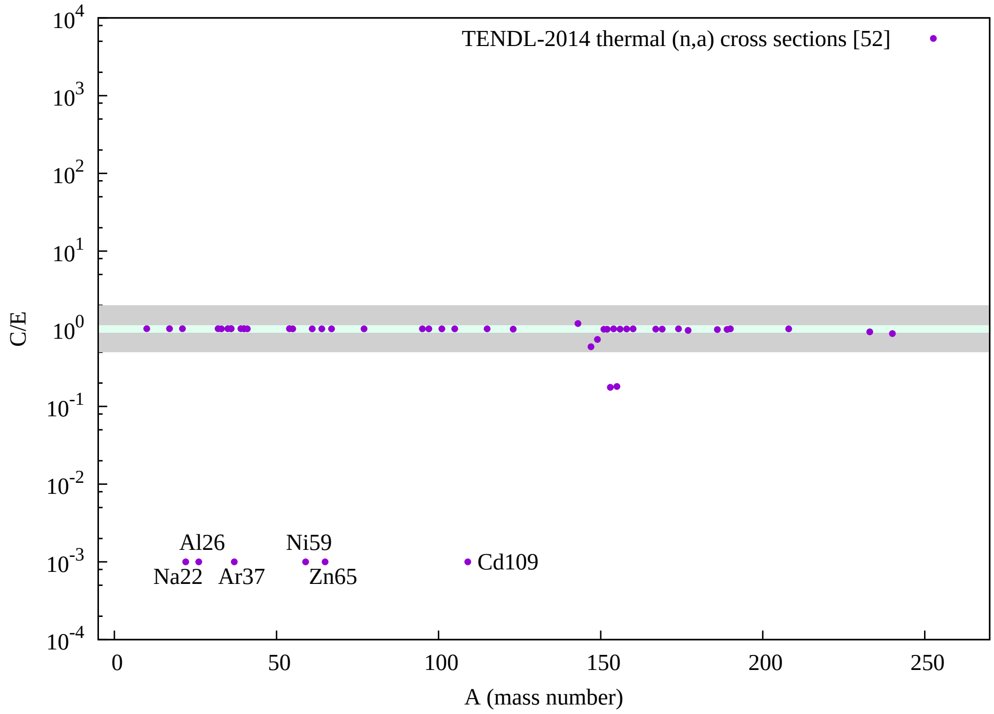

Figure 11: Distribution of TENDL-2014 (n,α) thermal cross section C/E values against number of nucleons A. The bands represent regions of $\frac{1}{2}$<C/E<2 and |C-E|/E <10%.

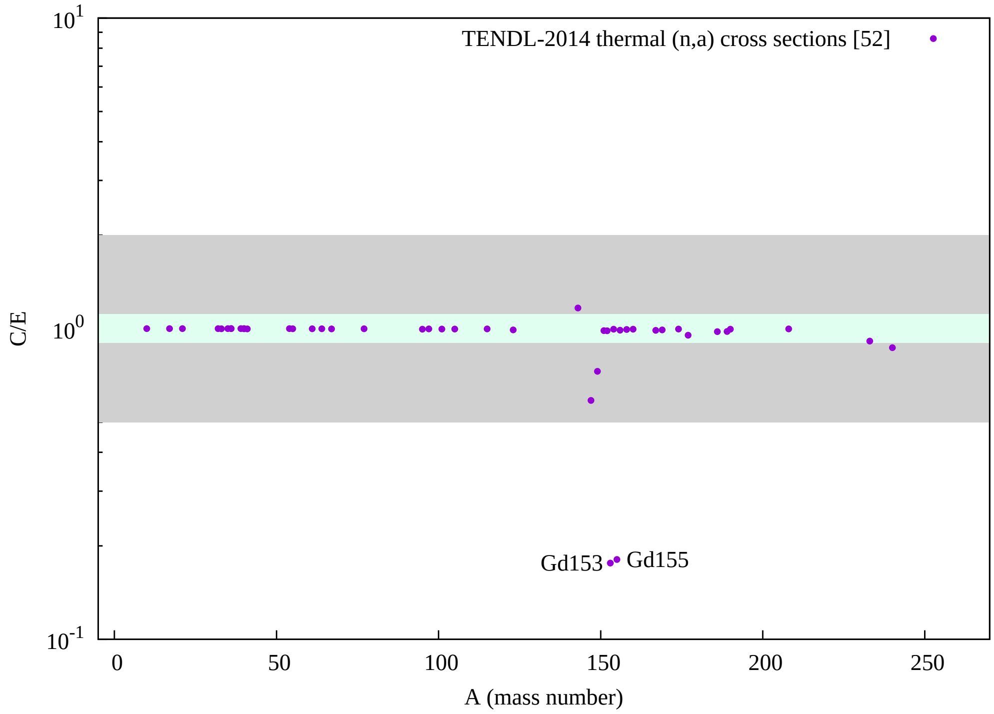

Figure 12: Distribution of TENDL-2014 (n,α) thermal cross section C/E values against number of nucleons A zoomed into the region of C/E $\in$ [0.1,10]. The bands represent regions of $\frac{1}{2}$<C/E<2 and |C-E|/E <10%.

4.2.3 Analysis of (n,p) cross sections

All but one (^{59}Ni C/E=0.822) of the 17 thermal (n,p) cross sections agree within 10% between the experimental values and TENDL-2014. The summary is shown in Figure 13. Of the seven (n,p) resonance integrals, four lie within 5% of the TENDL-2014 predictions, while the remaining have significant differences:

^{22}Na C/E=0.091, ^{35}Cl C/E=0.377, ^{36}Cl C/E=16.8,

as seen in Figure 14. All of these nuclides have thermal cross section measurements which perfectly agree with TENDL-2014, but the (n,p) channel does not possess a proper `MF=2` file for resonance treatment with `LRF=7`. The chlorine nuclides have been the subject of detailed ToF measurements but this information has not been transferred into the nuclear data file. This is a well-known issue for all nuclear data libraries which should be addressed for non-threshold absorption channels.

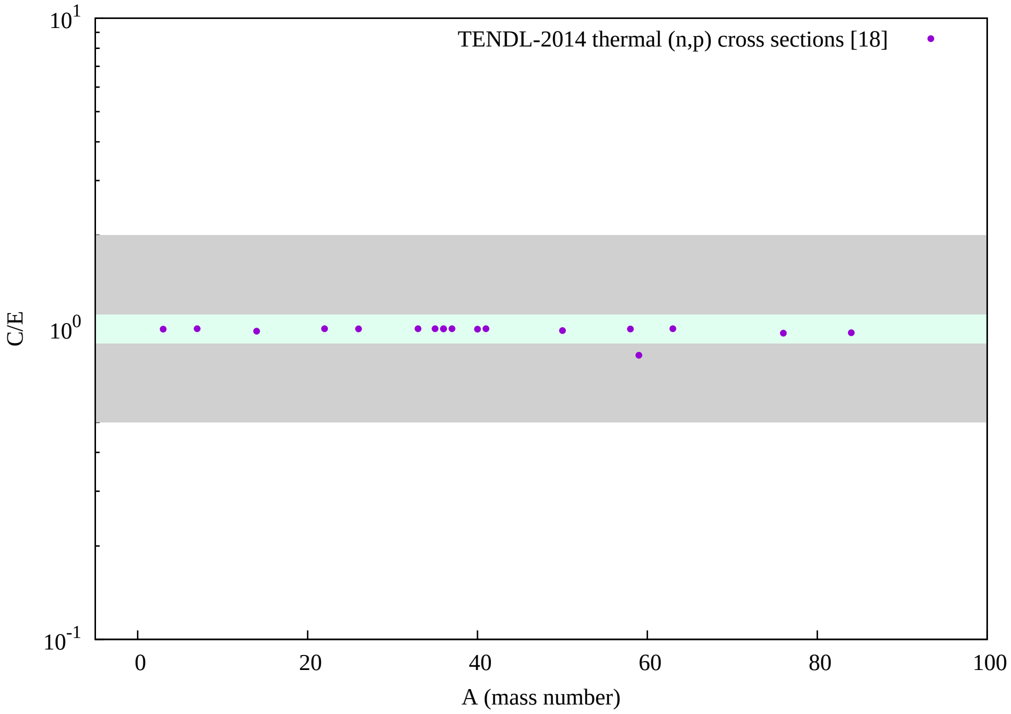

Figure 13: Distribution of TENDL-2014 (n,p) thermal cross section C/E values against number of nucleons A zoomed into the region of C/E $\in$ [0.1,10]. The bands represent regions of $\frac{1}{2}$<C/E<2 and |C-E|/E <10%.

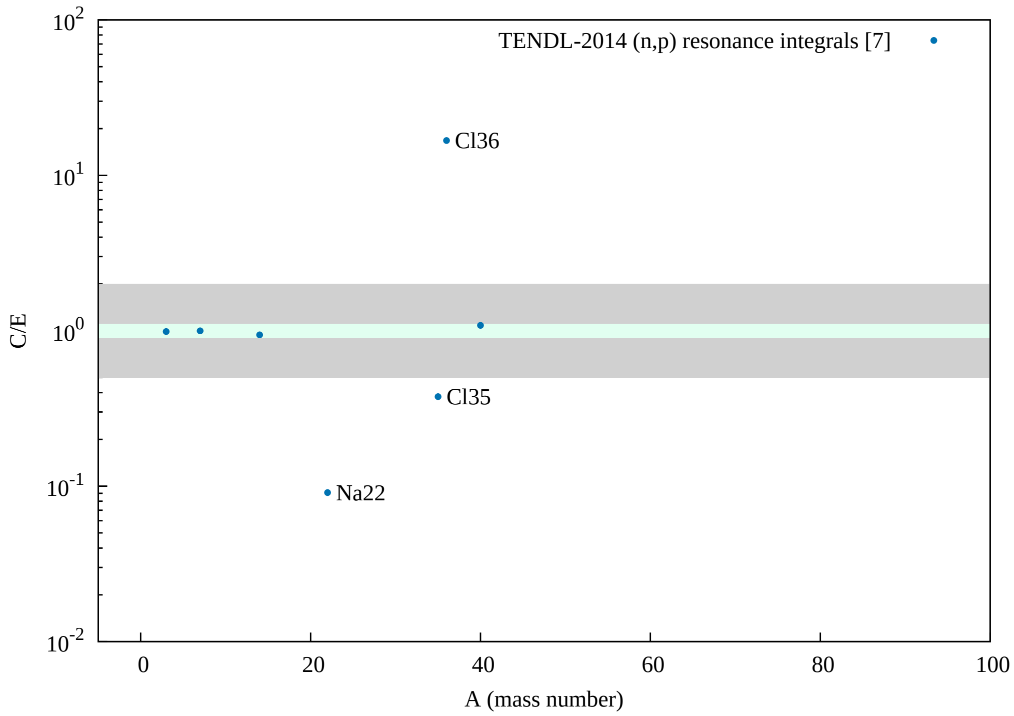

Figure 14: Distribution of TENDL-2014 (n,p) resonance integral cross section C/E values against number of nucleons A. The bands represent regions of $\frac{1}{2}$<C/E<2 and |C-E|/E <10%.

4.2.4 Analysis of (n,f) cross sections

The 83 thermal fission cross sections contain many exotic nuclides from ^{224}Th to ^{254m}Es. The agreement between the experimental values and TENDL-2014 is generally quite good, as seen in Figure 15 with a few notable exceptions including:

- ^{232}Th: The *Atlas* value (52 μb, C/E=13.7) is used for comparison, although the thermal cross sections vary substantially. The evaluated EXFOR value of 187 μb could give a C/E=3.82.
- ^{232}U: TENDL-2014 over-predicts both the *Atlas* and evaluated EXFOR values by 60-70%.
- ^{242m}Am: TENDL-2014 differs from *Atlas* by 10%, although evaluated EXFOR differs by factor of 3.

For many of the other very minor nuclides only limited and less precise[2] data is available. A fair spread in results for these should not be surprising. The resonance integrals follow a similar pattern, in Figure 16, with very precise values for well-known fissiles and a larger spread for the more exotic. A few more notable differences exist for

- ^{232}Th: While the thermal over-predicts, the resonance integral *under*-predicts by nearly an order-of-magnitude.

[2]For example, the *Atlas* and CRC list some cross sections as 'about' X barns.

- ^{238}U: The *Atlas* calculated value of 1.63 mb gives C/E=1.44
- ^{241,242m}Am: Both are under-predicted by 50 and 75%, respectively. ^{241}Am from the *Atlas* is experimental while the ^{242m}Am is calculated.

For nuclides of importance many more measurements exist than can be summarised by one thermal and/or resonance integral. General agreement with the larger experimental dataset is essential and, although not shown here, has been demonstrated for the most important fissiles [23].

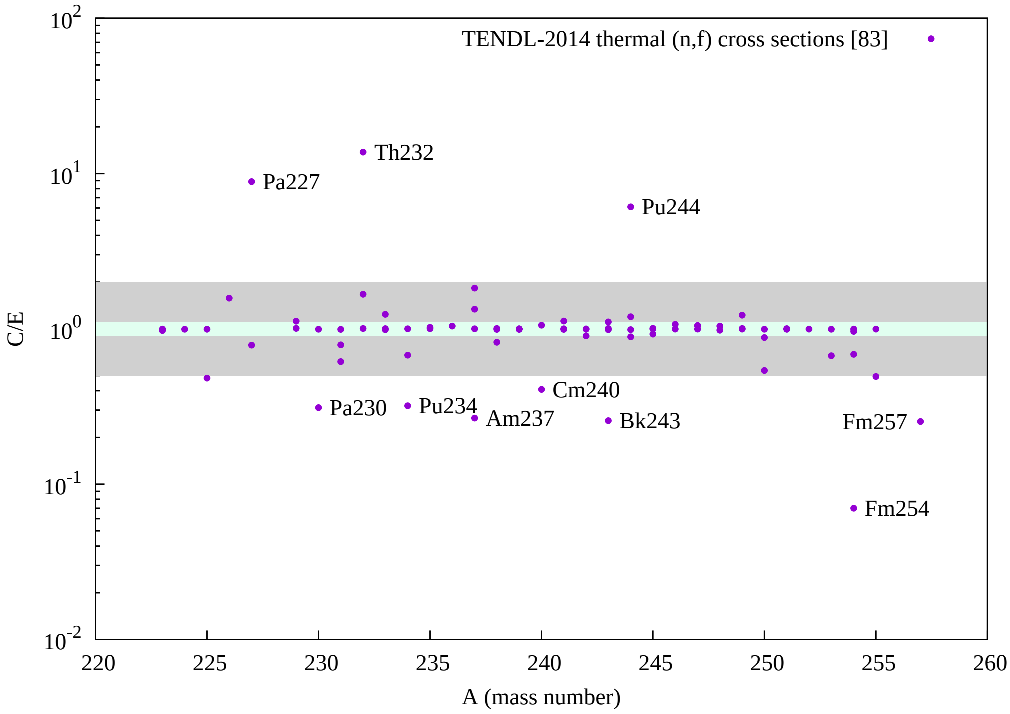

Figure 15: Distribution of TENDL-2014 (n,f) thermal cross section C/E values against number of nucleons A zoomed into the region of C/E $\in$ [0.1,10]. The bands represent regions of $\frac{1}{2}$<C/E<2 and |C-E|/E <10%.

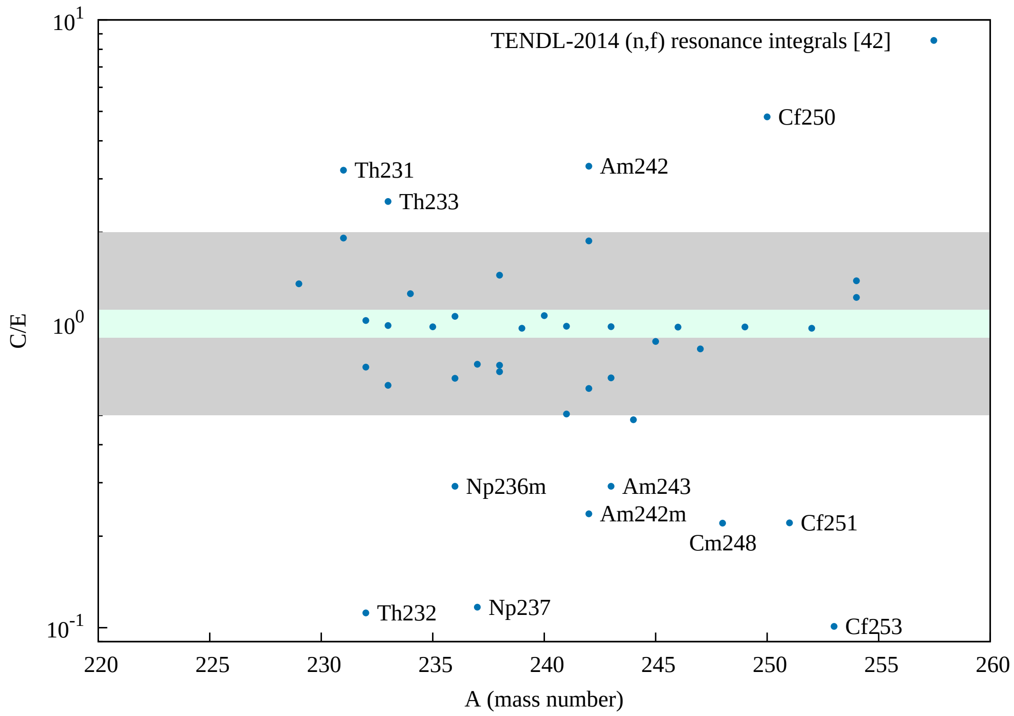

Figure 16: Distribution of TENDL-2014 fission integral resonance cross section C/E values against number of nucleons A zoomed into the region of C/E $\in$ [0.1,10]. The bands represent regions of $\frac{1}{2}$<C/E<2 and |C-E|/E <10%.

This page has been intentionally left blank.

5 Systematics and global verification

Of the 2632 target nuclides for neutron-induced reactions, the majority have no experimental measurements for any reaction channels. While it is not possible to validate these reactions, some efforts must be made to verify that the very large number of files do not contain inconsistencies. Many issues may be detected automatically by nuclear data processing codes, but serious errors may be more subtle – for example a dubious extrapolation of a level density model beyond known and/or stable nuclei. The following subsections include comparisons of TENDL-2014 against the systematics summarised in Appendix B and graphs which cover a variety of quantities for all nuclides within TENDL-2014. The latter are used to identify “suspicious” trends and outliers which may be worthy of re-evaluation or to highlight the complexity which models must account for.

The systematics are grouped by incident neutron energy, as either 30 keV, 3 MeV, 14.5 MeV or 20 MeV. Depending on the energy, different channels should be considered, and depending on which channels/targets some of the systematics are not applicable – for example when considering nuclides far from the line of stability. These systematics have been drawn largely from the EAF-2007 documentation [24], but for all systematics included in this report the original references have been re-examined.

All of the equations describing the systematics used are included in Appendix B.

5.1 Global comparisons

The legacy EAF-2010 nuclear data contains an 816 nuclide subset of TENDL-2014 which is generally clustered around the line of stability, as shown in Figure 17. Even this restricted nuclide set still contains mostly reactions for which no experimental measurements have been made. To address this issue, functional systematics were employed to either renormalise cross sections or validate the predictions from other codes. This methodology may be valid for nuclides near the line of stability and many were fit directly using statistical analysis against (the limited) experimental data. Extrapolation of these relatively simple functions to nuclides far from stability is not valid and of course was not done for the EAF libraries. Because the TENDL files include so many of these nuclides, the systematics cannot be applied except to the subset of nuclides near stability.

The previous sections gave the overview of the agreement between the TENDL-2014 data and experimental values. To better probe the quality of the files, we must examine individual channels over the whole nuclide set. Most target nuclides within TENDL have no experimental data and most of those with *some* data still only have a handful of measurements. The number of measurements per reaction channel is summarised in Table 2, where the columns represent measurement types or data origin. The first three columns are applicable only to non-threshold reactions, which form a subset of the TENDL-2014 total reaction number, while the fourth references another UKAEA validation report which uses integral measurements from fusion and accelerator-driven neutron sources [7].

While the T6 codes contain their own internal consistency checks, human verification of the data is necessary to find unusual behaviour and correct errors. By processing the

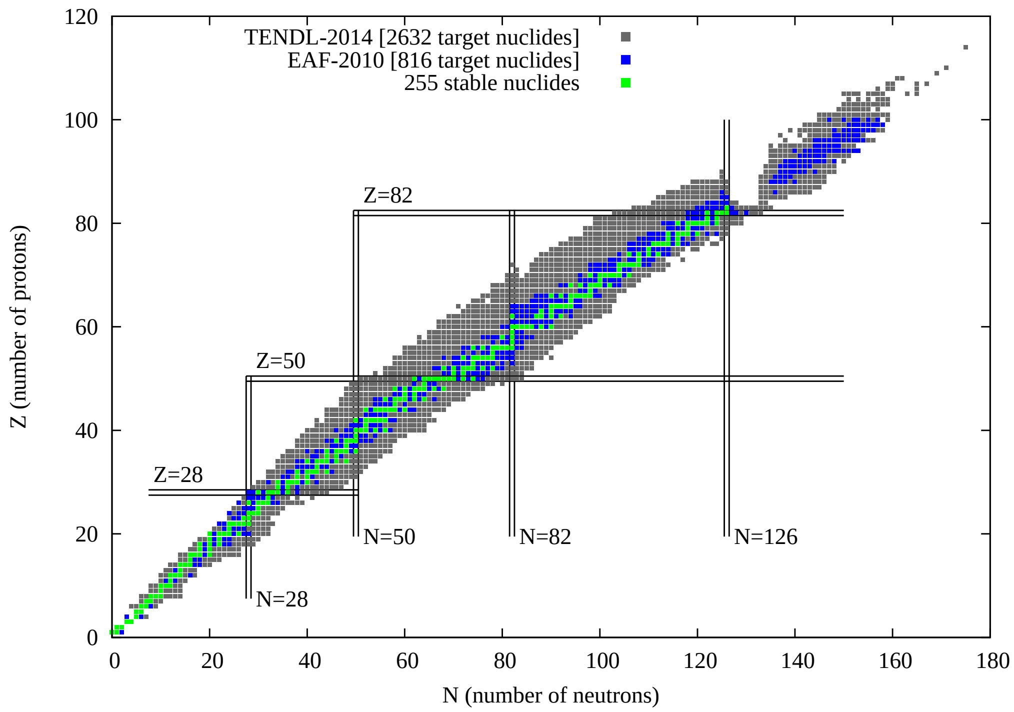

Figure 17: Set of nuclides included in TENDL-2014. The stable nuclides and nuclides included in EAF-2010 are identified with blue and green, respectively.

Reaction	Thermal	Res. Integral	MACS (30)	CCFE-R(15)27	TENDL-14
(n,γ)	691	512	357	42	2629
(n,α)	70	-	-	50	2621
(n,p)	22	7	-	86	2614
(n,f)	92	43	-	12	626
(n,2n)	-	-	-	105	2581
(n,d+np)	-	-	-	7	2111
(n,na)	-	-	-	8	2610
(n,t)	-	-	-	48	2109
(n,abs)	-	11	-	-	-
Total	875	573	357	358	17901

Table 2: Break-down of measurements considered in this report by reaction. The CCFE-R(15)27 column refers to the report with that identifier [7] and TENDL-14 refers to the number of those reactions within the full neutron library.

cross sections and visualising their nominal values at some energy, as well as against systematics where they exist, confidence can be generated in the quality of the library. For example, the total cross section at 2 MeV can be easily extracted by `inter` and displayed, as in Figure 18. While trends are very clear for most nuclides, a few stray off significantly and a selection of those have been identified as examples. Quite importantly, these are often *not* errors, but nuclides with unique features - for example ^{40}Ar has measured resolved resonances up to and above 2 MeV [25] and extraction of a differential cross section is not reasonable. The average over this region is in better agreement with the global trend. ^{48}Ca is an example where the resolved resonance range has been extended using the High-Fidelity Resonance method [26] beyond 2 MeV and the differential again does not give adequate information.

A useful complement to Figure 18 is shown in Figure 19, which shows the same values on the chart of the nuclides. A few interesting, although subtle patterns are discernible from this simple plot. These are ultimately derived from the global optical and global/local level density models within TALYS [27, 28]. As has been previously demonstrated [26], these produce similar trends in various physical parameters which are generally in good agreement with the available experimental data.

This same analysis on the 14 MeV total cross sections is shown in Figures 20 and 21. Again, a few outliers are identified. Although the use of color as the cross section parameter allows us to visualise the three dimensions simultaneously, the cost is our ability to quantify the cross section differences. However, the location in the overall chart gives more information; for example that four of the selected nuclides lie along the neutron-rich frontier of the TENDL target set. Some of these have total cross section measurements, such as the ^{115}In, which has a 14.2 MeV measurement of 4.54(2) b [29], compared with the TENDL-2014 value of 4.876 b. These uncommon and relatively small discrepancies may be due to automatic normalisations within the T6 system which are under examination.

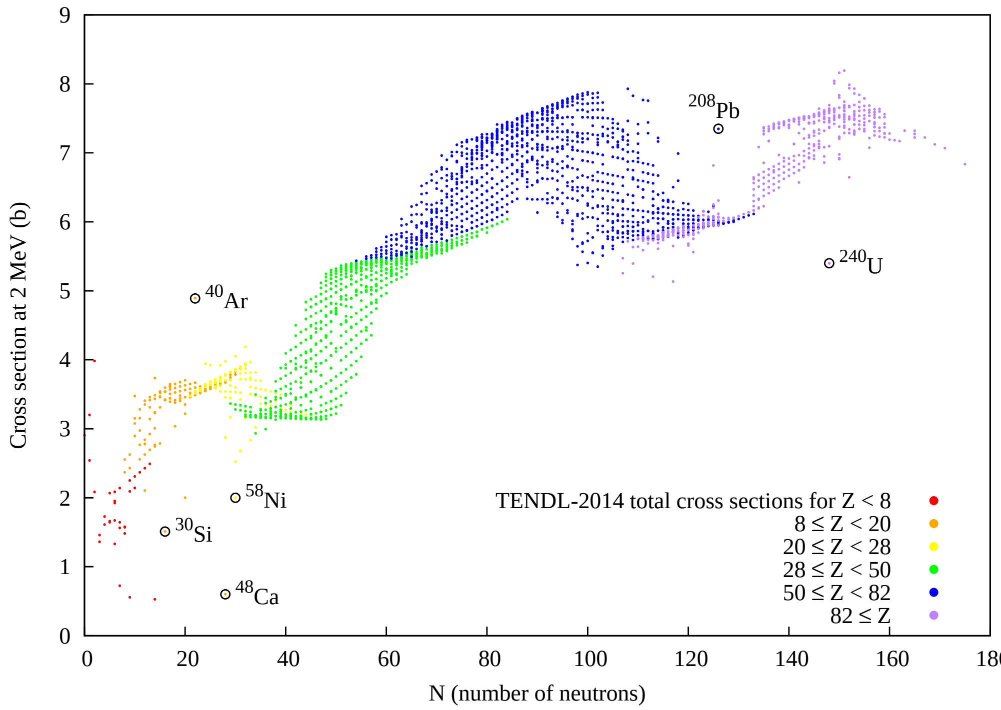

Figure 18: Total cross sections for all TENDL-2014 at 2 MeV, plotted against N and with Z broken down by magic number boundaries. Some potential outliers are highlighted.

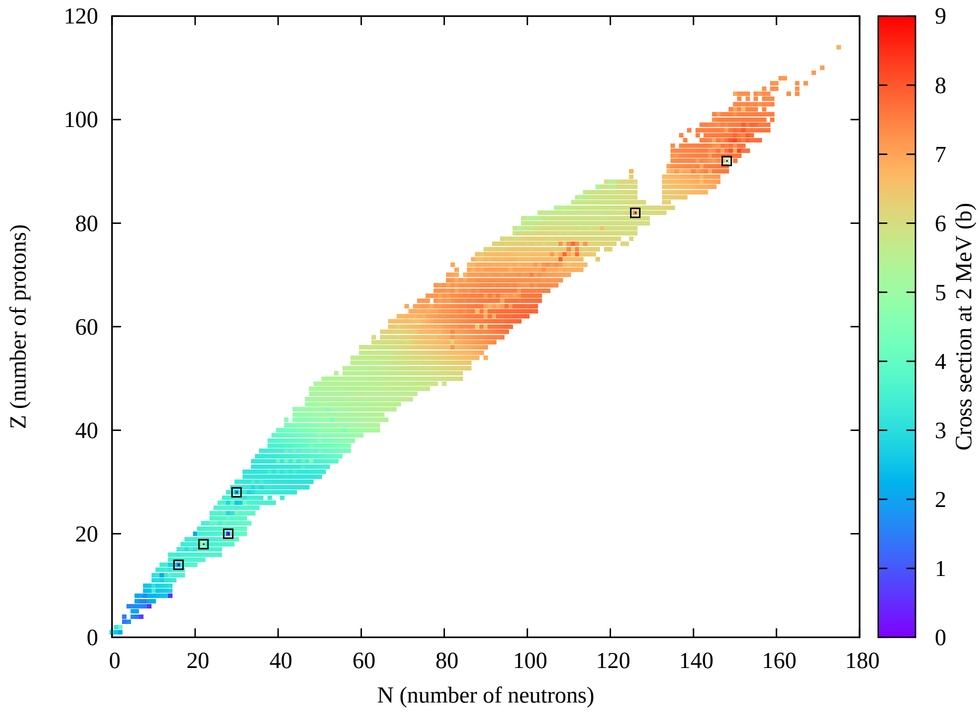

Figure 19: Total cross sections for all TENDL-2014 at 2 MeV, plotted in the chart of the nuclides with those identified in Figure 18 highlighted.

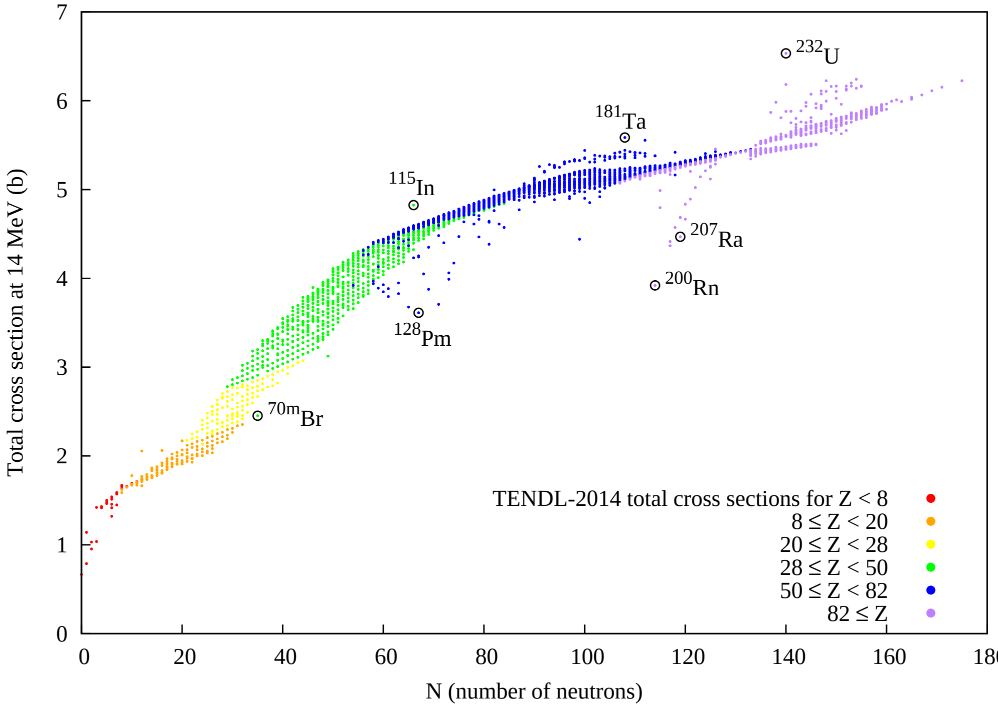

Figure 20: Total cross sections for all TENDL-2014 at 14 MeV, plotted against N and with Z broken down by magic number boundaries. Some potential outliers are highlighted.

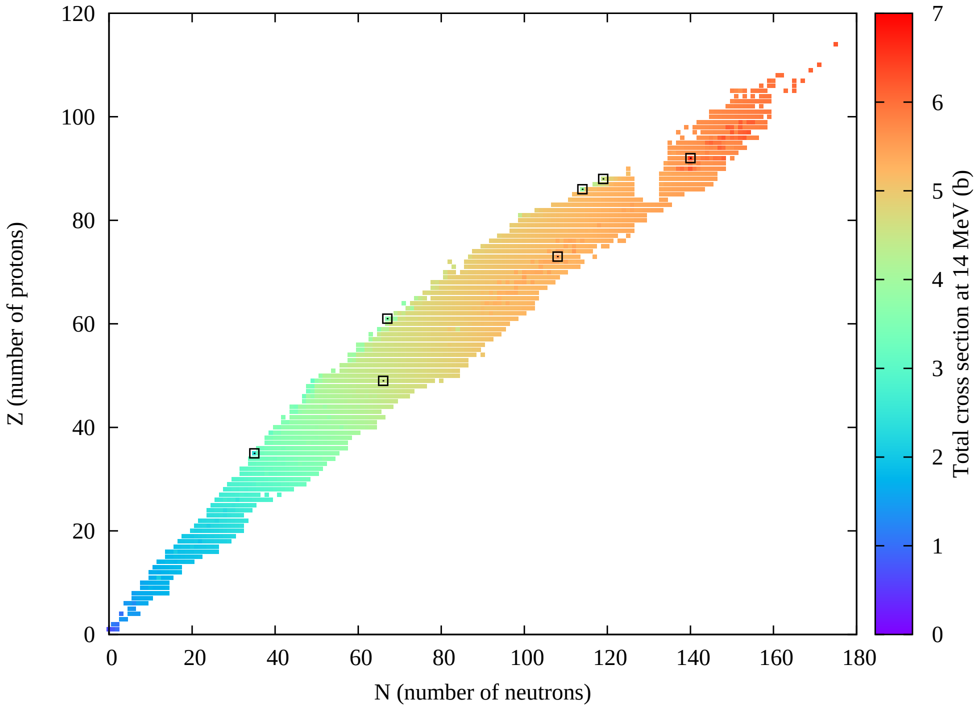

Figure 21: Total cross sections for all TENDL-2014 at 14 MeV, plotted in the chart of the nuclides with those identified in Figure 20 highlighted.

5.1.1 Analysis of (n,γ) cross sections

The (n,γ) systematic used [30] is a relatively simple exponential over the nuclide mass,

$$\sigma_{(n,\gamma)} = 1.18 - 1.13 \exp\{-0.01338A\}\,, \tag{4}$$

which gives a microscopic cross section of 0.9-1.15 mb for all nuclides with A>100. It has been demonstrated that this systematic describes the general, global trend for nuclides with measurements and has been used for previous EAF validations [24]. The TENDL target nuclide set is much larger than that of any EAF library and it extends further away from stability. The global ratios to the systematic (C/S), as shown in Figure23, show that (aside from issues with the low-Z) significant differences develop with the nuclides leading up to A=200, as well as some heavy actinides.

From Figure 24 it is clear that the neutron-poor nuclides above A=80 show the specific trend, with the α-emitters possessing a significantly larger capture cross section. A few other features, such as the low cross sections for the extreme neutron-poor Z<60 nuclides and some heavy, neutron-poor actinides are worth additional investigation. The cross section values are shown for reference in Figure 25.

Note that *all* of these nuclides lie outside the EAF nuclide sets, where the systematic cannot interpolate between regions of agreement with experiment. Disagreement with the systematic does not suggest any error in the TENDL data, but identifies regions where some additional attention could be placed.

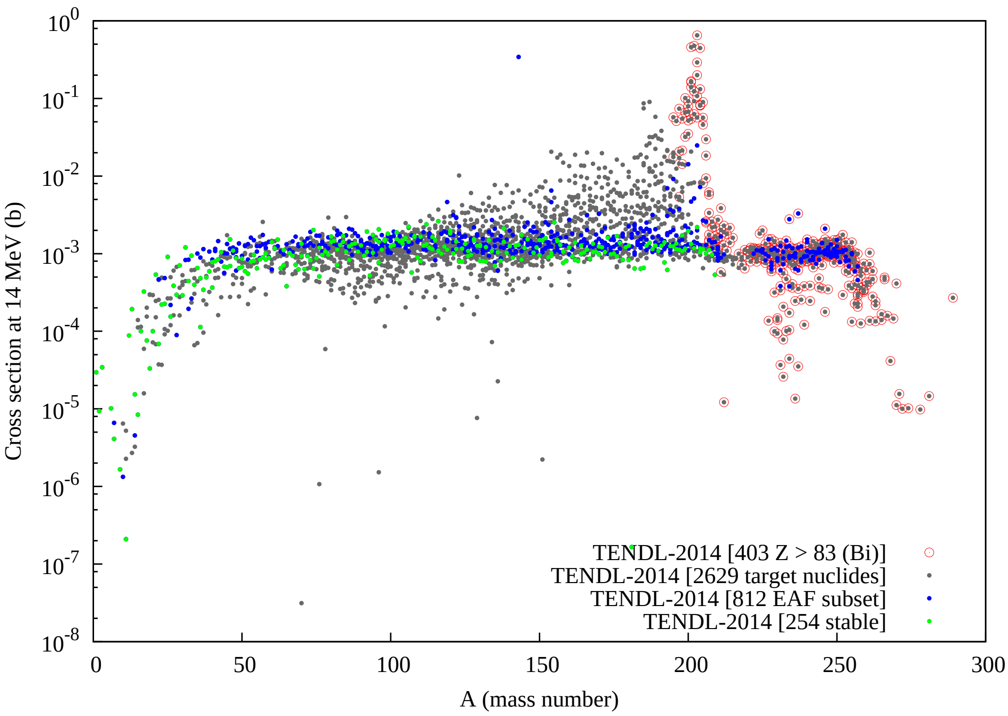

Figure 22: TENDL-2014 (n,γ) 14 MeV cross section values against number of nucleons. Nuclides within the EAF subset and stable nuclides are identified with blue and green, respectively. Those with Z>83 are circled in red.

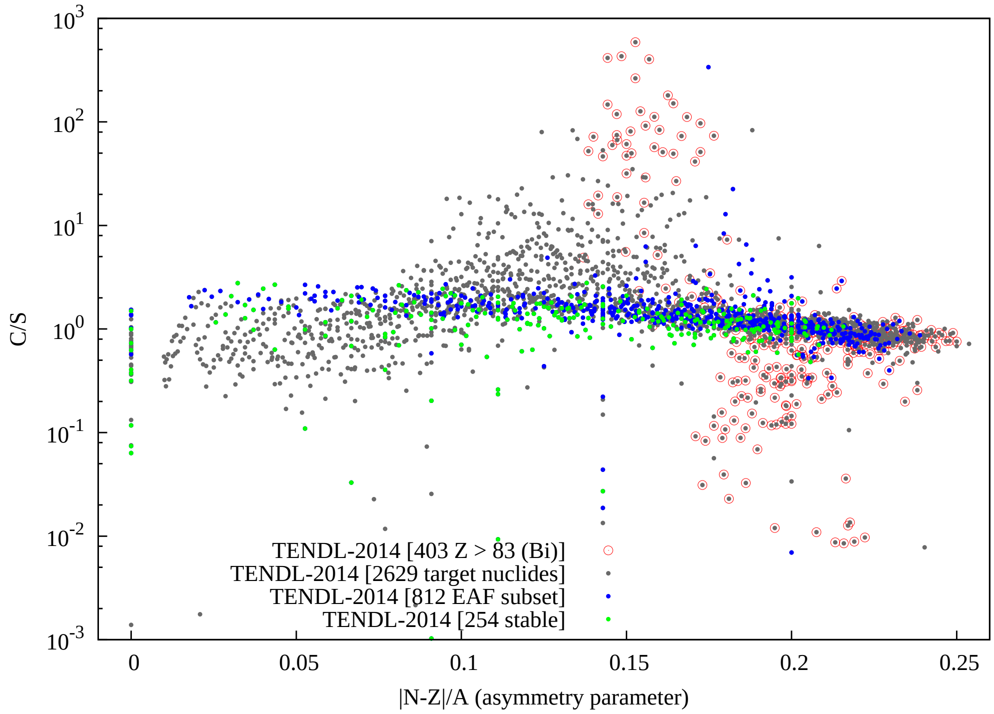

Figure 23: C/S values for all TENDL-2014 14 MeV (n,γ) reactions against asymmetry. Nuclides within the EAF subset and stable nuclides are identified with blue and green, respectively. Those with Z>83 are circled in red.

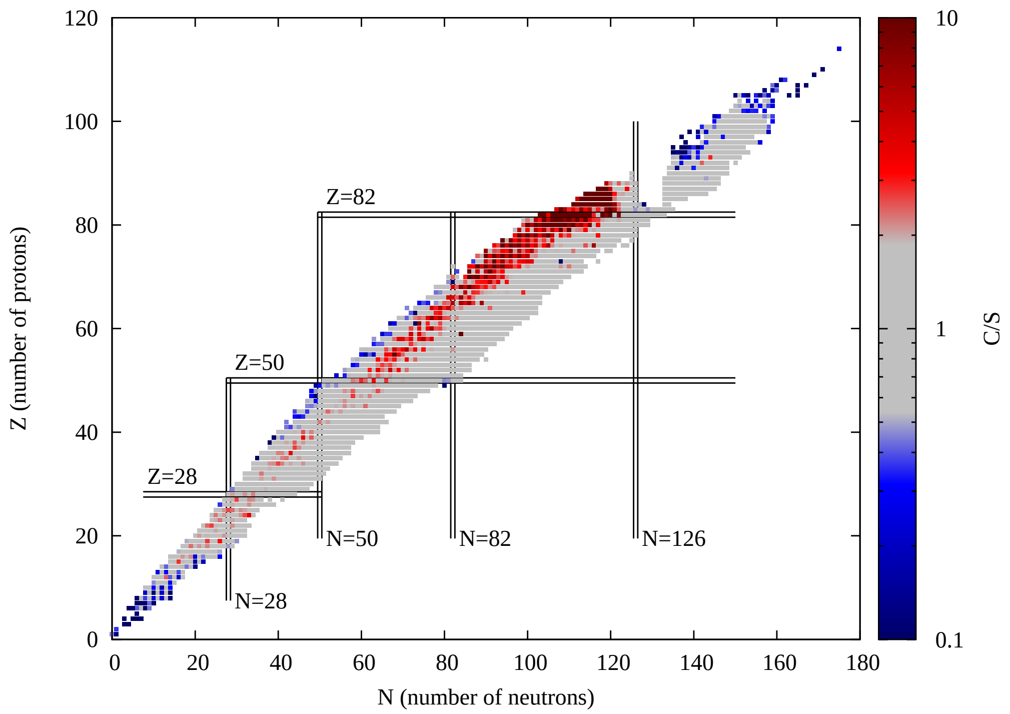

Figure 24: C/S values for all TENDL-2014 14 MeV (n,γ) reactions. Magic numbers are identified by marked lines. Note the top region where C/S>10 which are the unstable α-emitting nuclides.

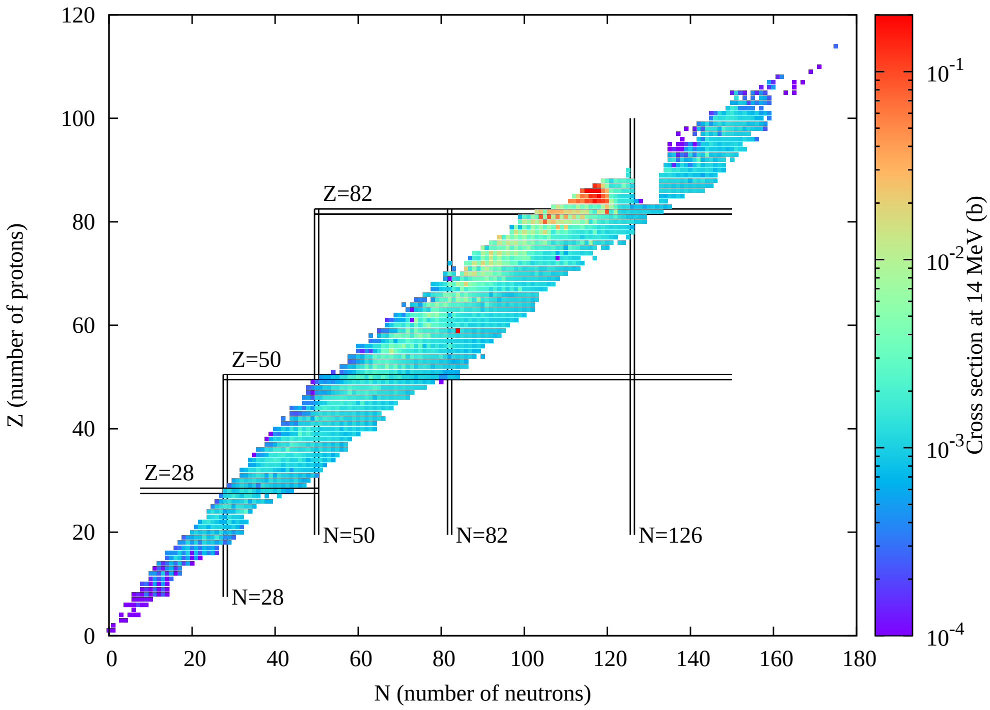

Figure 25: The 14 MeV cross sections for all TENDL-2014 14 MeV (n,γ) reactions.

5.1.2 Analysis of (n,α) cross sections

The (n,α) systematic used [31]

$$\sigma_{(n,\alpha)} = 15.0678 \left(A^{1/3} + 1\right)^2 \exp\left\{-27.55\left(S + S^2\right)\right\}$$

contains an exponential polynomial in asymmetry which drops the prediction for neutron-rich nuclides and increases them for the neutron-poor. As shown in Figure 26, this reasonably agrees with the TENDL-2014 values from the EAF nuclide subset, but fails for nuclides outside it.

The global trends are generally in agreement with the systematic for 14 MeV (n,α) within the EAF 816 nuclide subset, although outside these nuclides the agreement is generally poor, as seen in Figure 27. Looking at the C/S values as a function of N and Z, shown in Figure 28, the general pattern is that the asymmetry biasing is not sufficient for the nuclides which lie further from the line of stability. In particular, the very neutron-rich, where the TENDL-2014 values drop substantially – a trend not matched with the systematic. This is matched on the neutron-poor side with the clear branch above Z>50. The neutron-poor nuclides with 30<Z<60 show a curiously low (n,α), which indicates competition from other reaction channels. For example, the ^{101}Sn In this case, reactions such as the (n,2p)

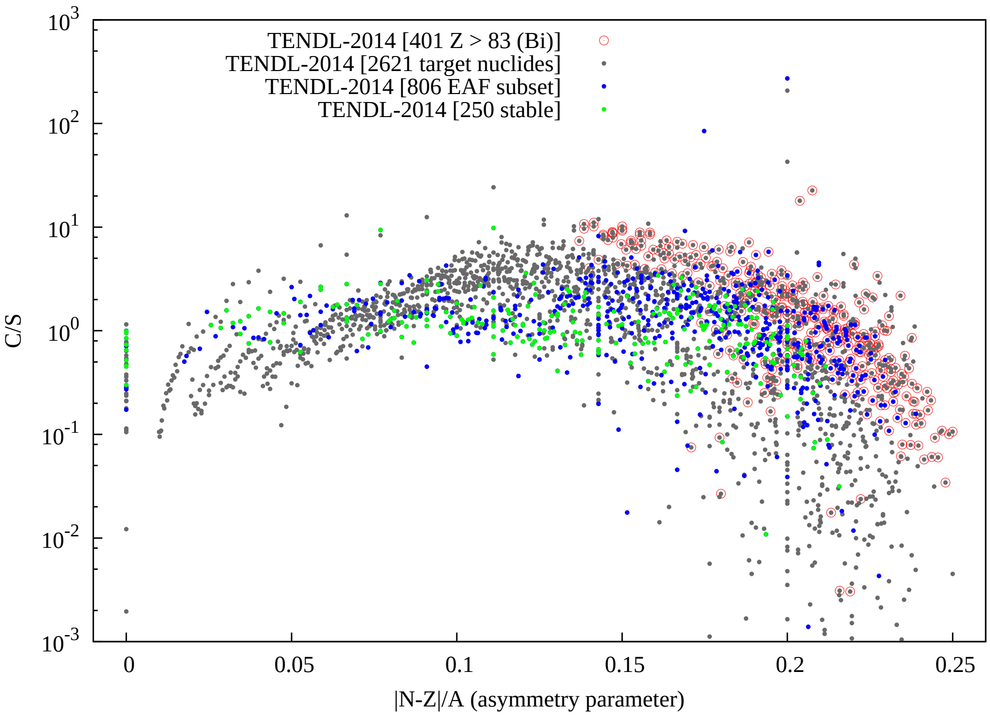

Figure 26: C/S values for all TENDL-2014 14 MeV (n,α) reactions. Nuclides within the EAF subset and stable nuclides are identified with blue and green, respectively. Those with Z>83 are circled in red.

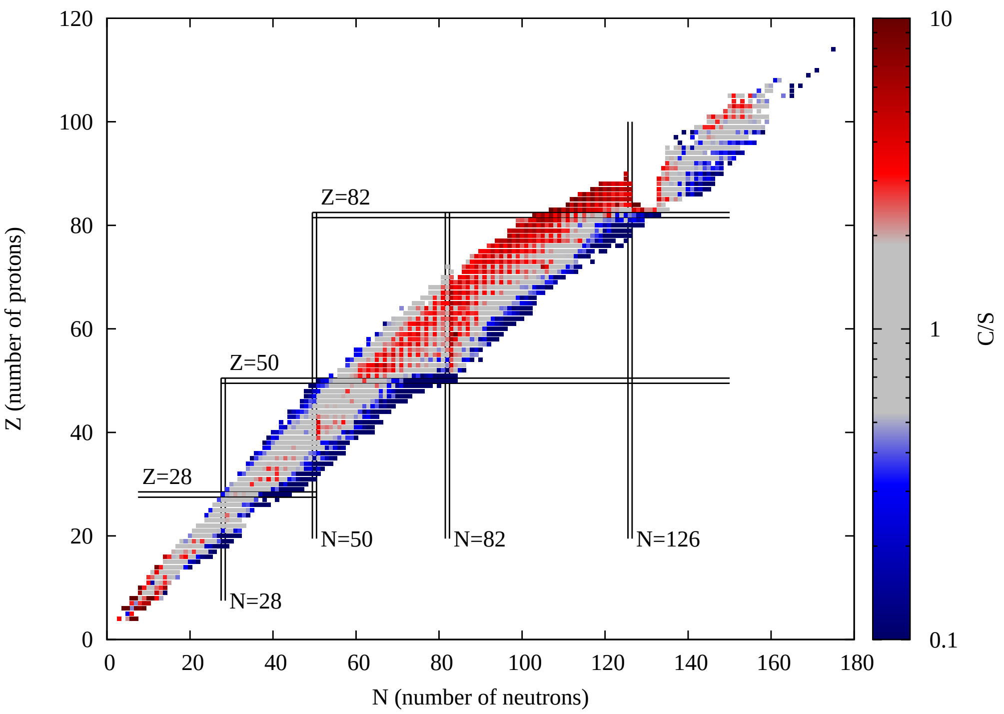

Figure 27: C/S values for all TENDL-2014 14 MeV (n,α) reactions. Magic numbers are identified by marked lines. Note the top region where C/S>10 which are the unstable α-emitting nuclides and the intriguing 2 order-of-magnitude jump in cross section on the neutron-rich edge.

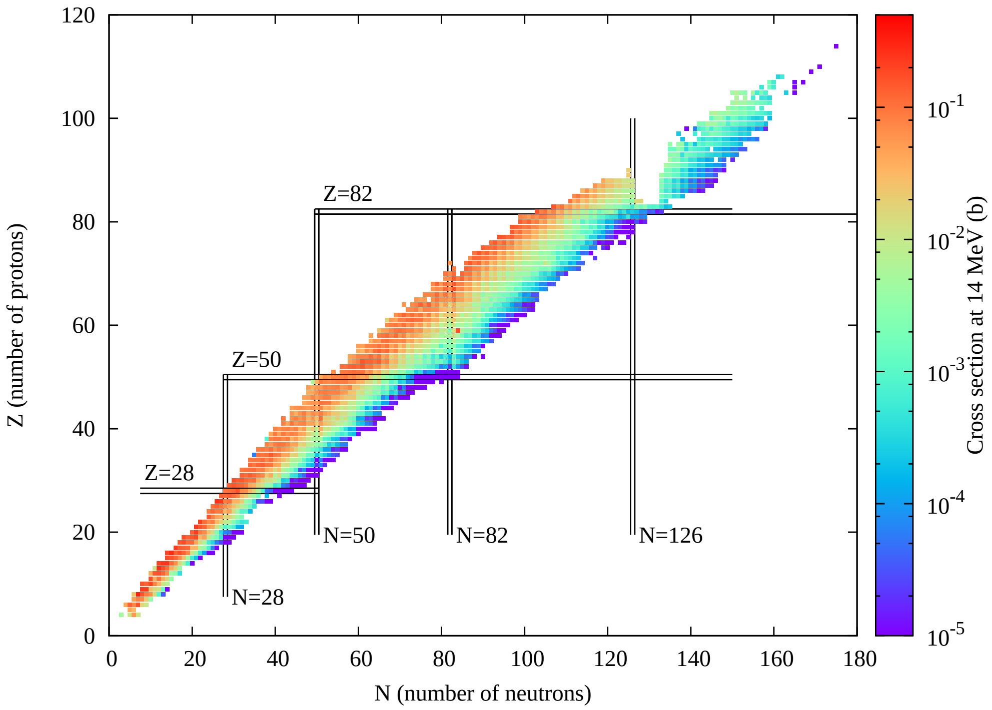

Figure 28: The 14 MeV cross sections for all TENDL-2014 14 MeV (n,α) reactions. Note the trends over the magic numbers and even/odd effects which are absent from the systematic. The neutron-rich frontier possesses a curious jump in cross section.

5.1.3 Analysis of (n,p) cross sections

There are two (n,p) systematics for Z<40 and Z≥40 [32, 33]:

$$\sigma_{(n,p)} = 7.657\left(A^{1/3}+1\right)^2 \exp\left\{-28.80S - 59.24S^2 + 0.2365A^{1/2}\right\} \qquad Z \geq 40$$

$$\sigma_{(n,p)} = 23.659\left(A^{1/3}+1\right)^2 \exp\left\{-23.041\left(S+S^2\right)\right\} \qquad Z<40$$

These have been placed together in the following plots, although distinct differences between the patterns can be seen in Figure 30. While the systematics do account for the general neutron-rich/poor bias, they do not account for even-odd effects and general differences in proton separation energies. As a result, the local trends which can easily been seen in Figure 31 demonstrate clear deficiencies in the systematics.

The cross section generally increases with decreasing asymmetry, but when the nuclei are sufficiently away from stability new reaction channels are opened up which will compete with the (n,p), for example the (n,2p). The ratio of (n,2p)/(n,p) cross sections at 14 MeV is shown in Figure 33, which shows that the apparent under-prediction along the neutron-poor extreme edge of the TENDL nuclides is due to the opened and dominant (n,2p) channel.

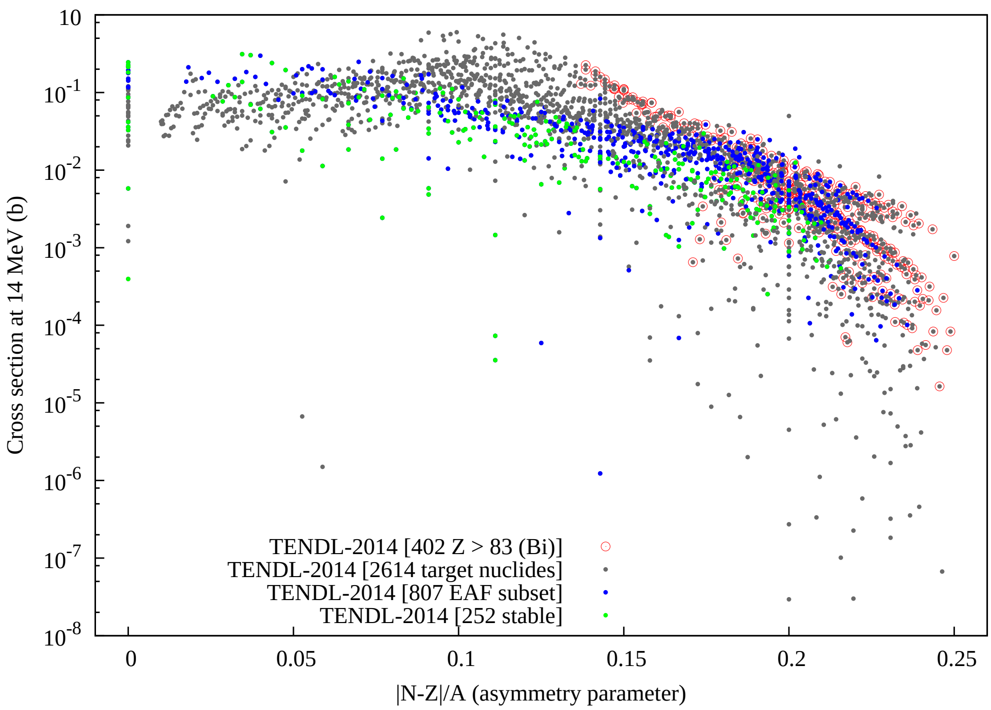

Figure 29: TENDL-2014 (n,p) 14 MeV cross section values against nuclide asymmetry. Nuclides within the EAF subset and stable nuclides are identified with blue and green, respectively. Those with Z>83 are circled in red.

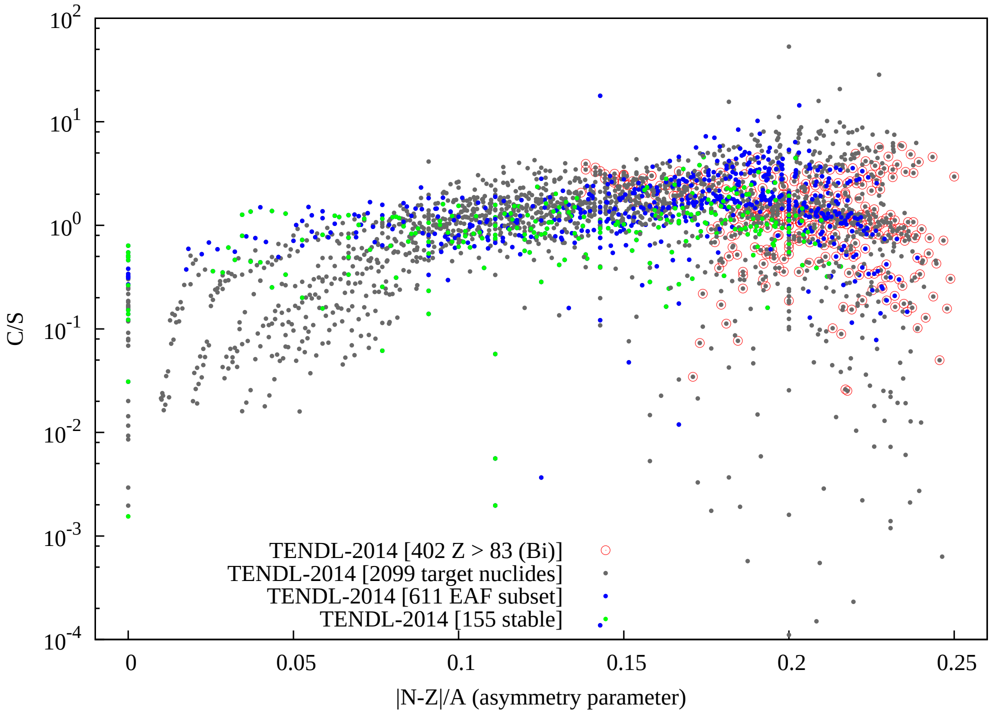

Figure 30: C/S values for all TENDL-2014 14 MeV (n,p) reactions. Nuclides within the EAF subset and stable nuclides are identified with blue and green, respectively. Those with Z>83 are circled in red.

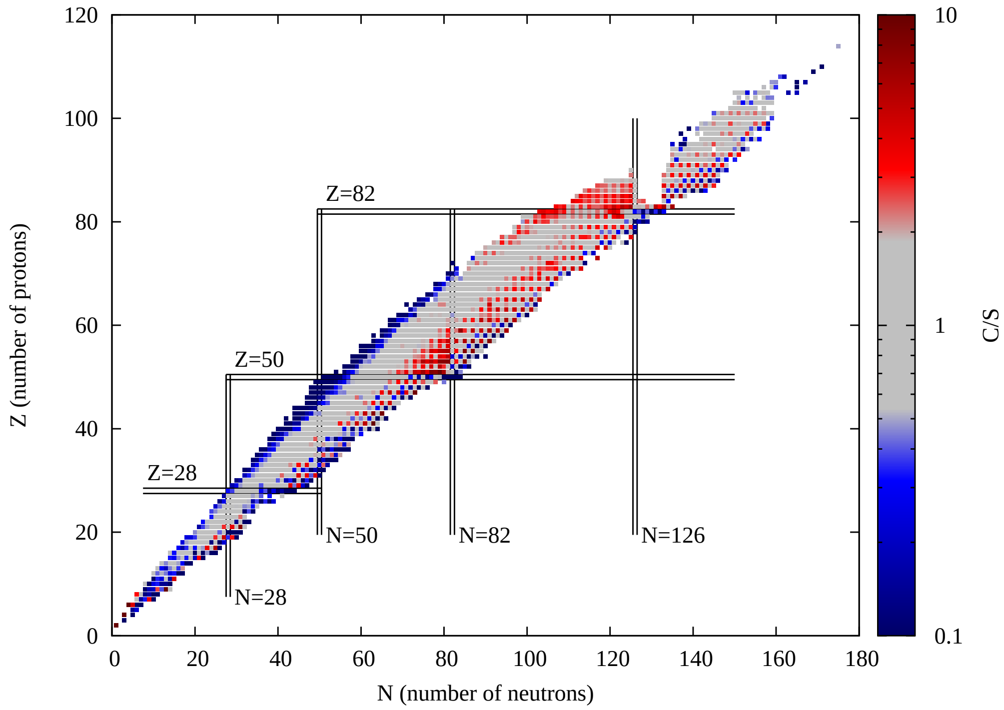

Figure 31: C/S values for all TENDL-2014 14 MeV (n,p) reactions. Magic numbers are identified by marked lines. Note the proton-rich region where C/S<10, where new channels are opened. Also note the strong even-odd effects along the neutron-rich edge.

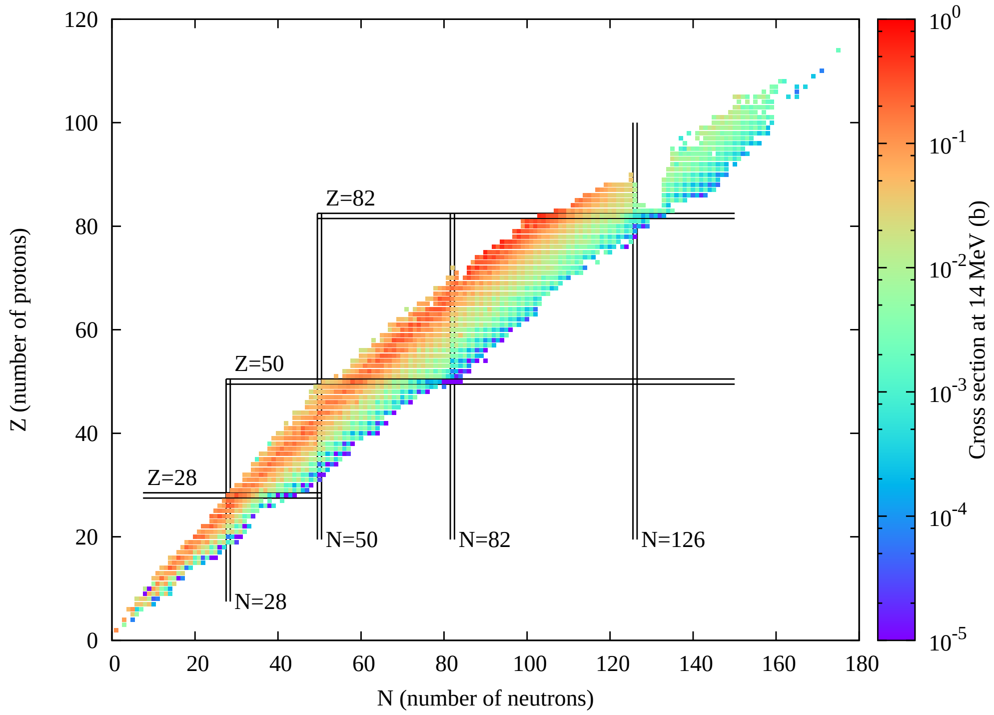

Figure 32: The 14 MeV cross sections for all TENDL-2014 14 MeV (n,p) reactions.

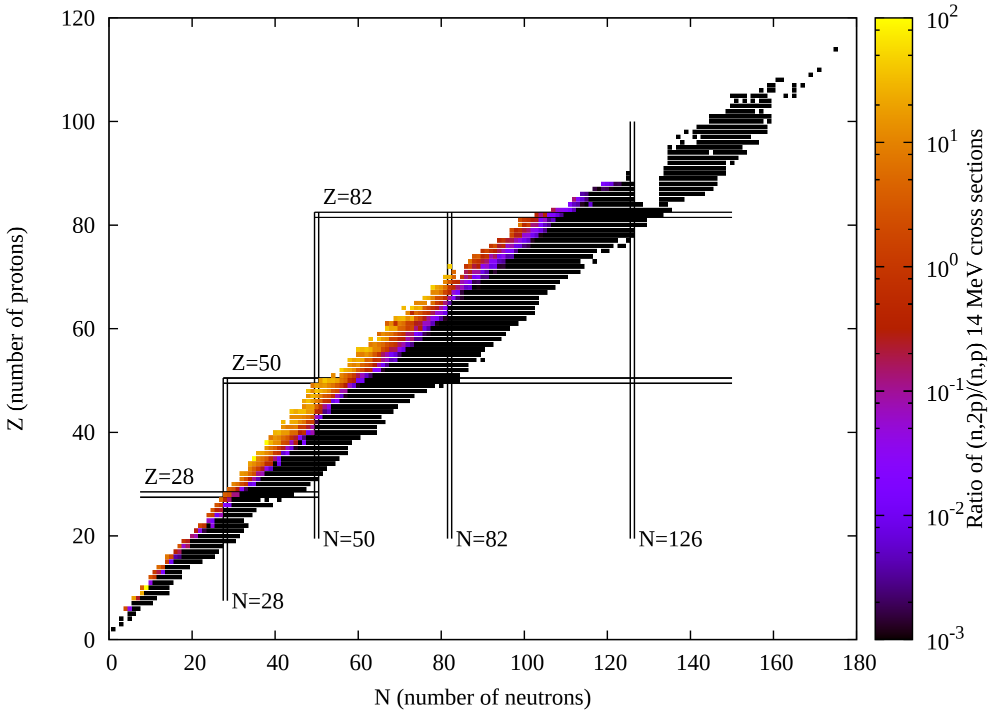

Figure 33: Ratio of TENDL-2014 14 MeV (n,2p)/(n,p) cross sections. Those in black do not have an open (n,2p). The nuclides with strong (n,2p) channels match with the neutron-poor low-C/S from Figure 31.

5.1.4 Analysis of (n,f) and (n,2n) cross sections

Reactions with neutron multiplication compete and must be considered together, as with the (n,2n) and (n,f) addressed in this section. The (n,2n) systematic used [34],

$$\sigma_{(n,2n)} = 47.015 \left(A^{1/3} + 1\right)^2 (1 - 3.9777 \exp\{-24.116S\}), \tag{5}$$

gives some weight to the asymmetry of the nuclides, but cannot account for competing pathways such as fission, which will draw from this channel. Surveying the C/S values in Figures 34 and 35, the EAF restricted set generally has good agreement with the systematic, but disagrees far from stability and for many actinides. The latter is due to the lack of a fission compensation, while the former has two different causes: (1) insufficient bias for extremely neutron-poor nuclides within the asymmetry terms and (2) lack of compensation for alternative neutron-multiplication channels (such as (n,3n)) for the neutron-rich above N=82.

When the fission channel is added to the (n,2n), the trend is improved considerably for the actinides. As shown in Figure 36, when this channel is added the actinides follow the same trends as with the other nuclides. Those which are very neutron-poor drop off rapidly while the neutron-rich have a slight dip due to competing pathways.

Figure 37 shows the ratio between (n,3n) and (n,2n) cross sections, to demonstrate where the competing reaction channels become significant. Many other channels will become open at different energies, masses, asymmetries, *etc*, but this gives an excellent illustration of how the apparently missing cross section has been drawn into a newly opened channel. In legacy libraries where only those nuclides around stability are considered, these are exotic channels which are not significant or even observed, but they are essential for TENDL.

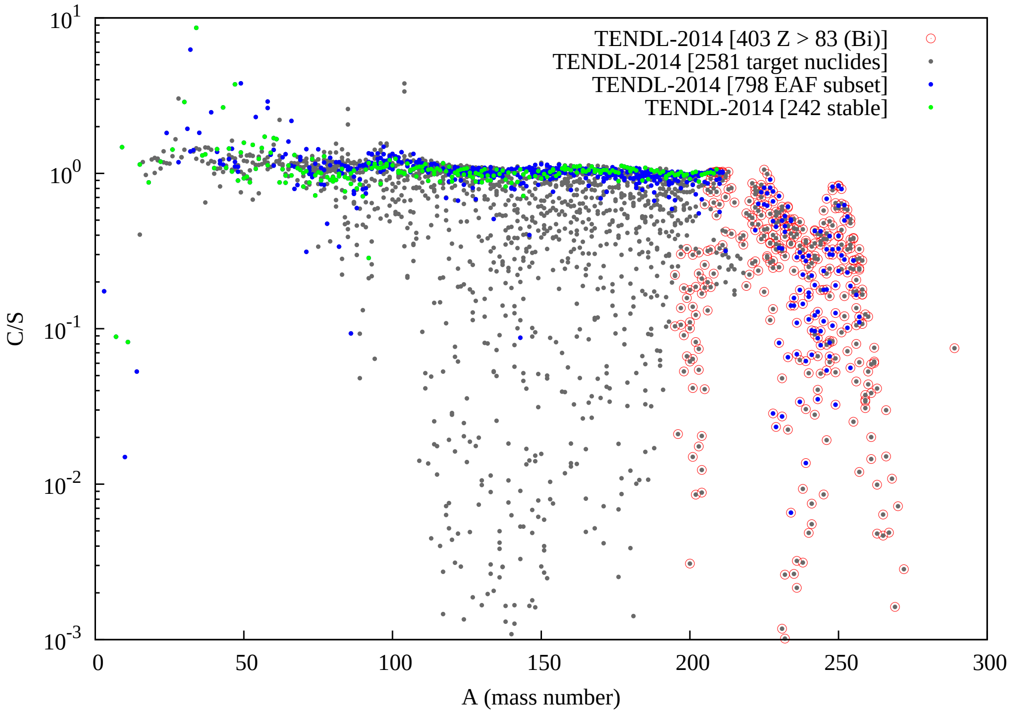

Figure 34: C/S values for all TENDL-2014 14 MeV (n,2n) reactions against mass number A. Nuclides within the EAF subset and stable nuclides are identified with blue and green, respectively. Those with Z>83 are circled in red. Note that the fissionable actinides are under-predicted by the systematic.

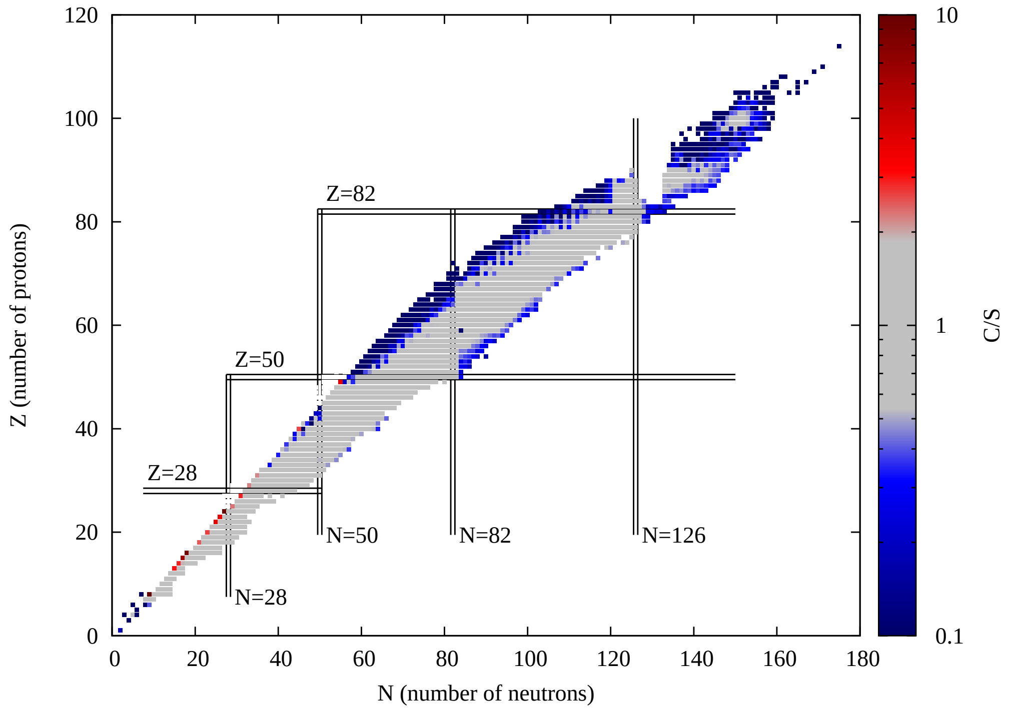

Figure 35: C/S values for all TENDL-2014 14 MeV (n,2n) reactions. Magic numbers are identified by marked lines. The actinides are missing the (n,f) contributions and are inaccurate with this systematic.

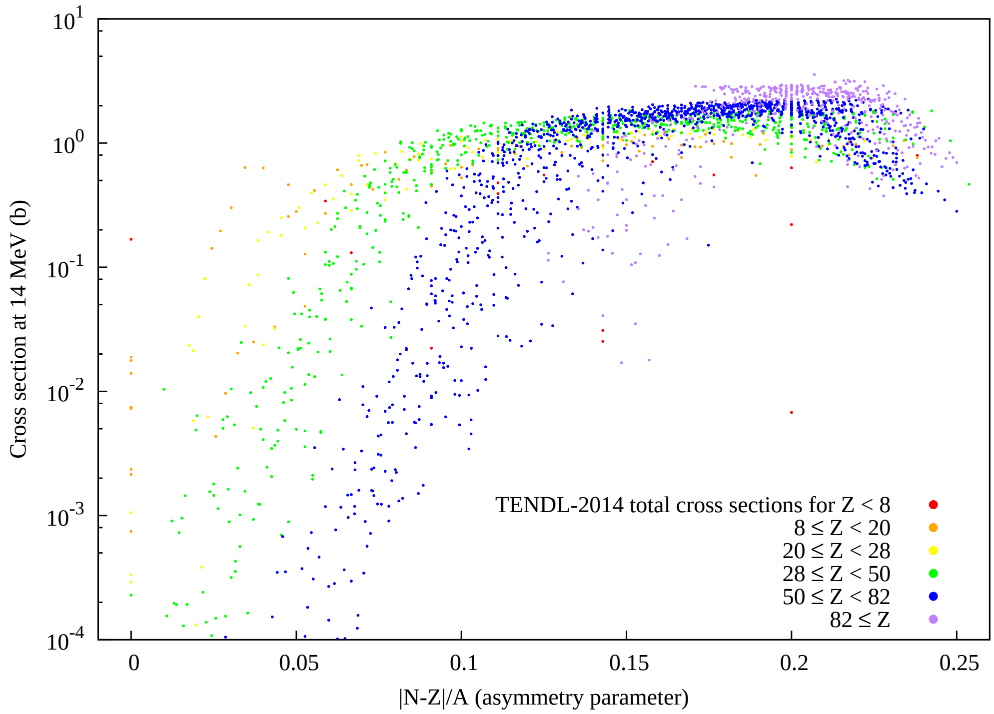

Figure 36: TENDL-2014 14 MeV (n,2n+f) cross sections against asymmetry, broken down by magic numbers in Z. Note the clear decrease for neutron-poor nuclides and the higher values for the actinides. Without the (n,f) these would be significantly lower and not follow the general trends.

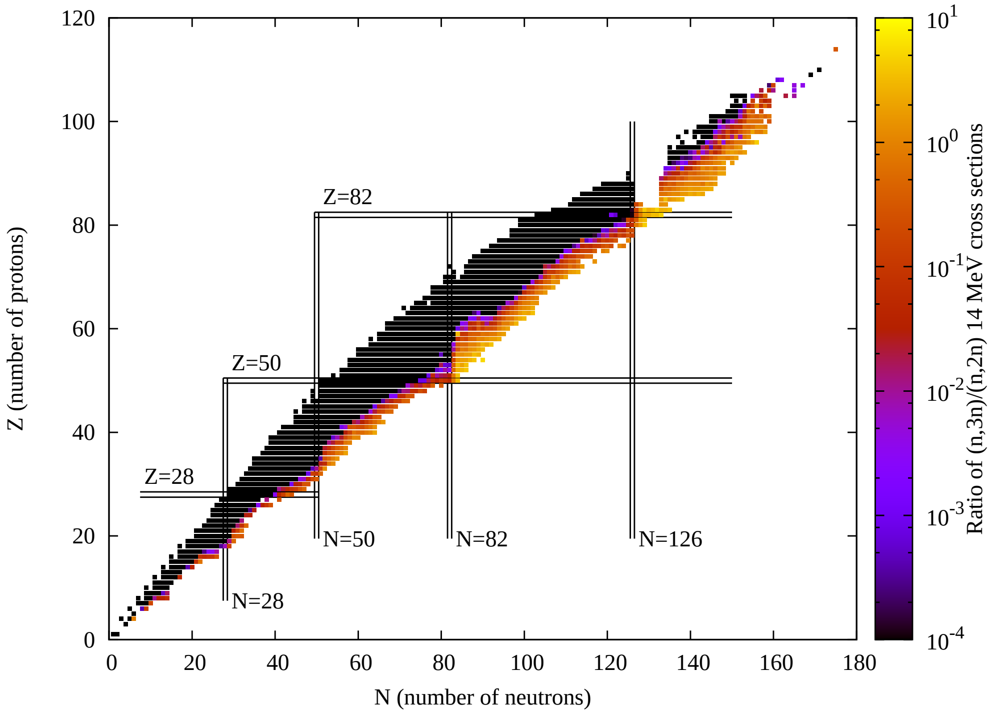

Figure 37: Ratio of TENDL-2014 14 MeV (n,3n)/(n,2n) cross sections. Those in black do not have an open (n,3n). The nuclides with strong (n,3n) channels match with the neutron-rich low-C/S from Figure 35.

5.1.5 Analysis of (n,nα) cross sections

The (n,nα) systematic used for comparison is a simple exponential over asymmetry [35]:

$$\sigma_{(n,n\alpha)} = 17.48 \exp\{-24.2S\} \tag{6}$$

which does not capture virtually any of the global features of this more exotic (but, for many applications, still quite relevant) channel, as demonstrated in Figure 38. Clear trends such as those seen at Z two above magic numbers or the opening of new channels at large asymmetry simply are not possible to approximate with a one parameter fit. More physical knowledge must be incorporated to provide a more useful tool to compare with TENDL and help identify any outliers.

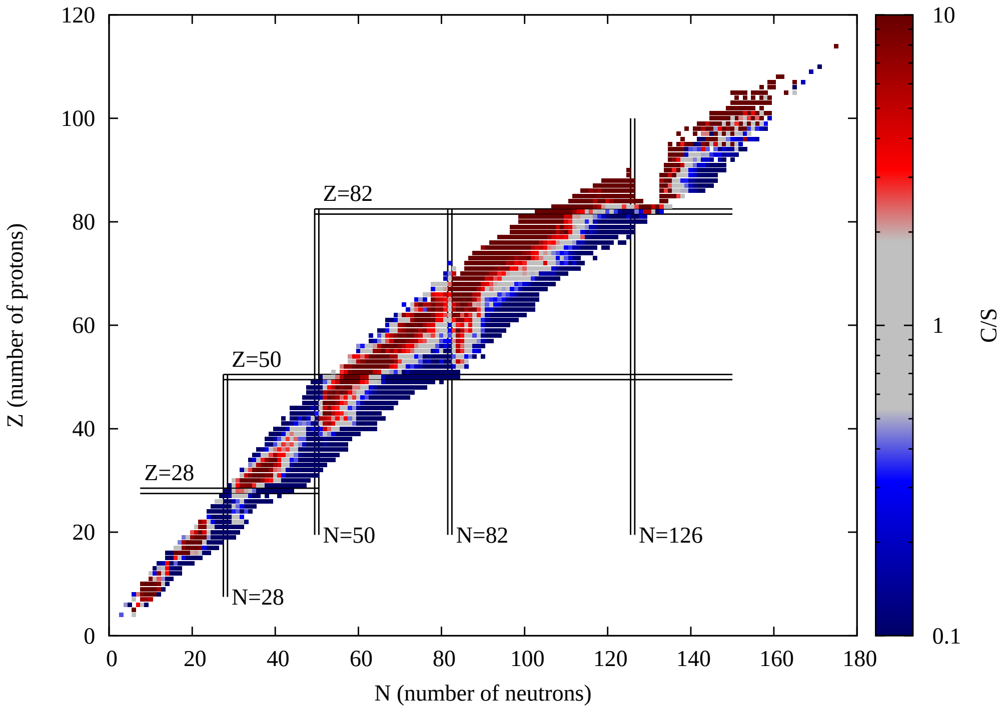

Figure 38: C/S values for all TENDL-2014 14 MeV (n,nα) reactions. Magic numbers are identified by marked lines. Most regions are very poorly approximated by the simply exponential over asymmetry.

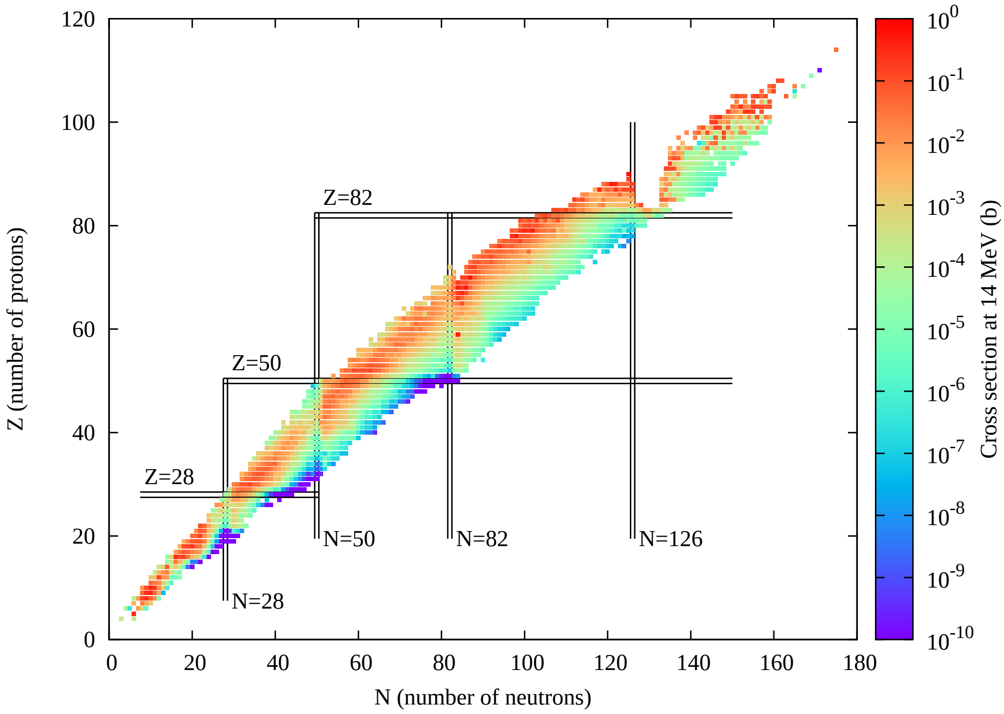

Figure 39: 14 MeV cross sections for all TENDL-2014 (n,nα) reactions. Note the strong discontinuities near magic nuclides and in particular the neutron-rich double magic.

5.1.6 Analysis of (n,np) and (n,d) cross sections

The 14.5 MeV systematics for (n,d) reactions used in previous EAF reports included two parameter exponentials of asymmetry and, for those with S>0.125, a one parameter fit to nuclear surface area. The (n,np+d) used alongside these would occasionally produce negative cross sections for the (n,np) away from stability (but still in the EAF subset, which is considerably more restricted than TENDL), underlining how unsuitable they are for the majority of nuclides in TENDL-2014.

For these channels a more recent, six and three parameter systematics are used [36] for comparison:

$$\begin{aligned}\sigma_{(n,np)} =&53.066\left(A^{1/3}+1\right)^2\left(A^{-1/3}\Big(-2.7098\big(S+1.5A^{-1}\big)+0.67115\Big)^2\right.\\ &\left.+\ \exp\left\{-496.74\left(S+1.5A^{-1}\right)^2+48.162\left(S+1.5A^{-1}\right)-1.6714\right\}\right)\end{aligned}$$

$$\sigma_{(n,d)} = 53.066\left(A^{1/3}+1\right)^2 A^{-1/3}\left(-1.3107S+0.0019167ZA^{-1/3}+0.48491\right)^3 \qquad (7)$$

These were originally created for higher-energy applications at 20 MeV. It can be used in the same manner to identify trends and outliers within the TENDL data. As seen in Figures 40 and 42, the agreement across the line of stability, and a fair region surrounding it, is quite good. The combination of these two, as shown in Figure 44 yields some better agreement in the neutron-rich nuclides which indicates a mis-match between the TENDL-2014 and systematic apportionment between the two similar channels. The C/S disagreements in the neutron-poor nuclides shown in Figure 40 remain in the combined channel, with the under-prediction likely due to competition with additional channels.

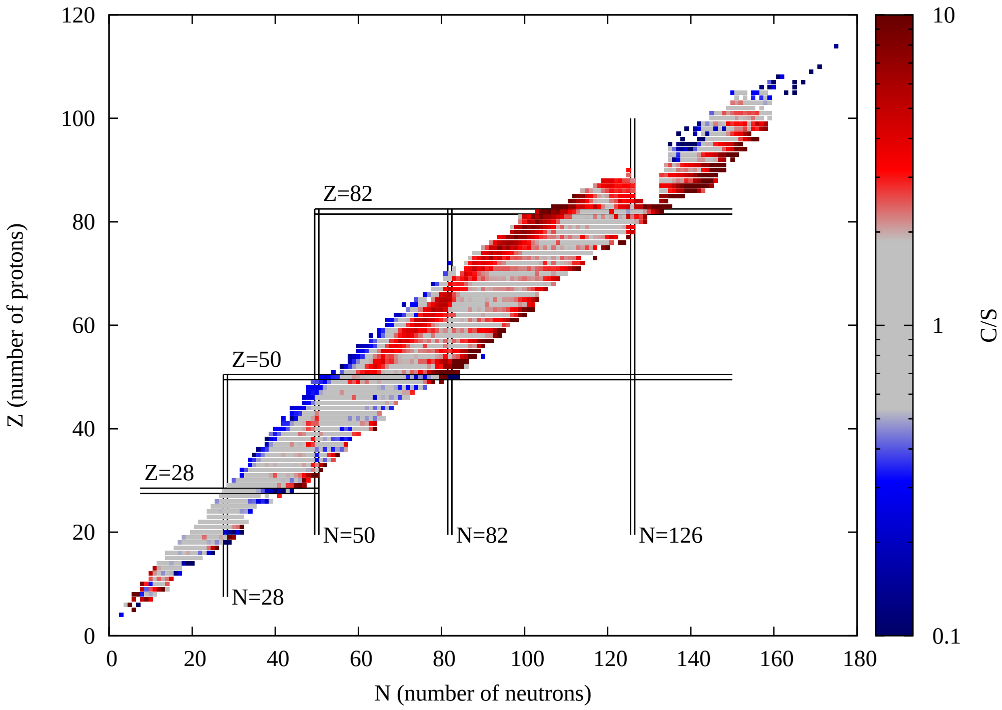

Figure 40: C/S values for all TENDL-2014 20 MeV (n,np) reactions.

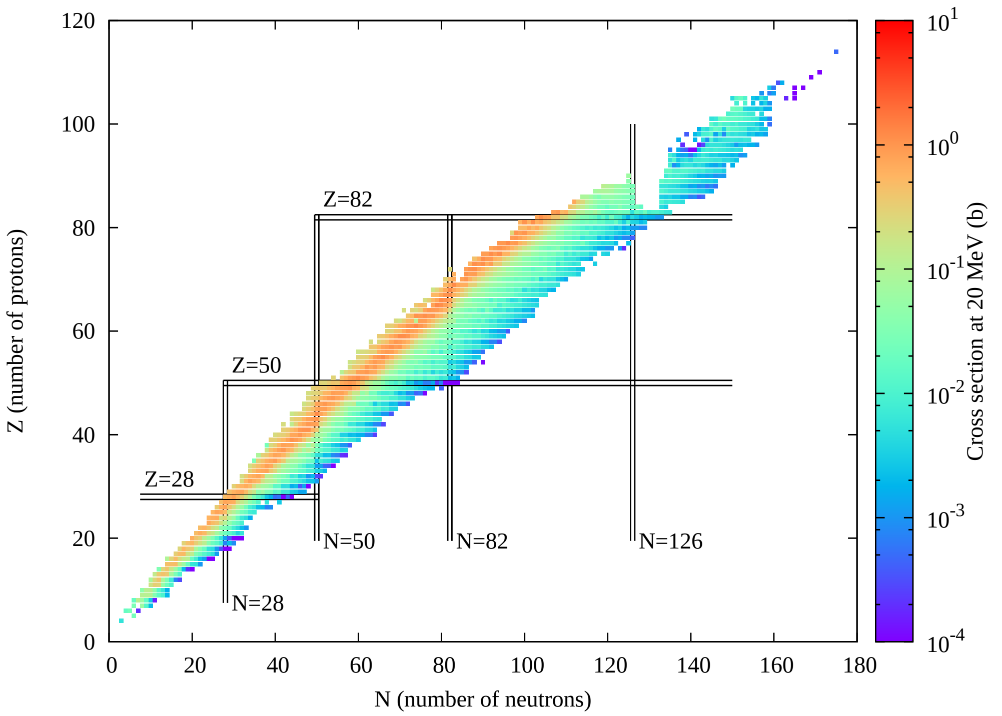

Figure 41: 20 MeV cross sections for all TENDL-2014 (n,np) reactions.

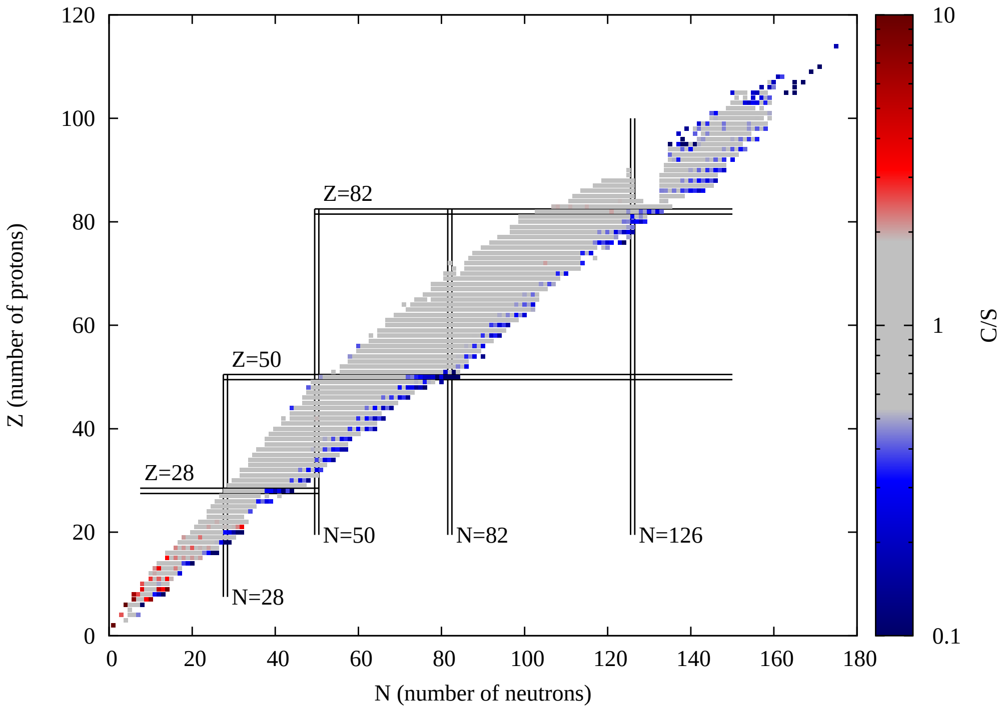

Figure 42: C/S values for all TENDL-2014 20 MeV (n,d) reactions.

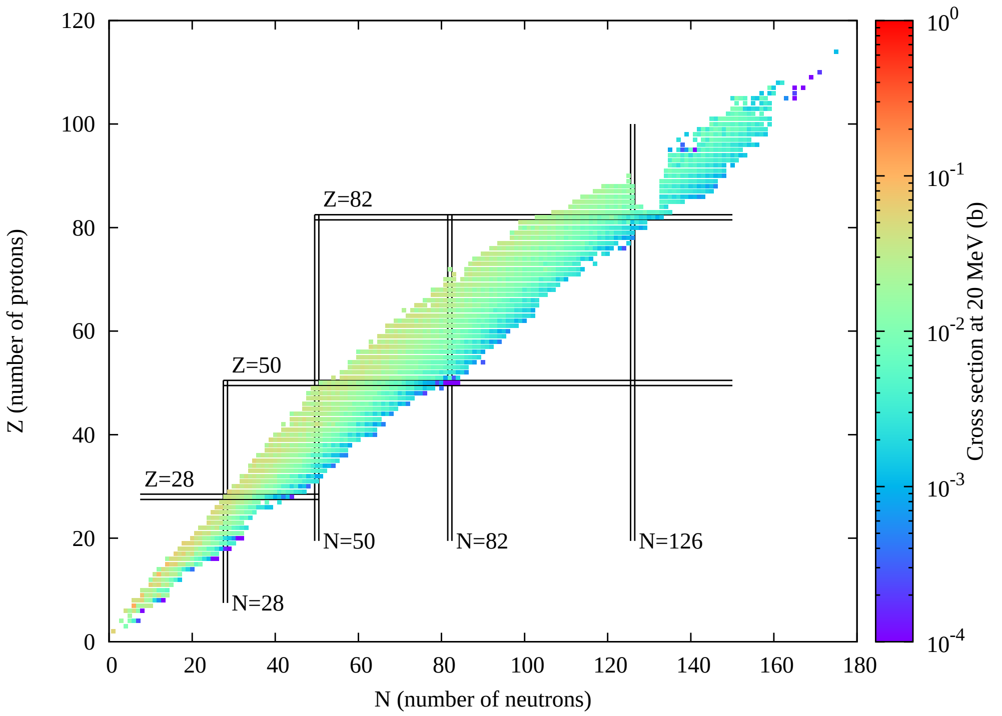

Figure 43: 20 MeV cross sections for all TENDL-2014 (n,d) reactions.

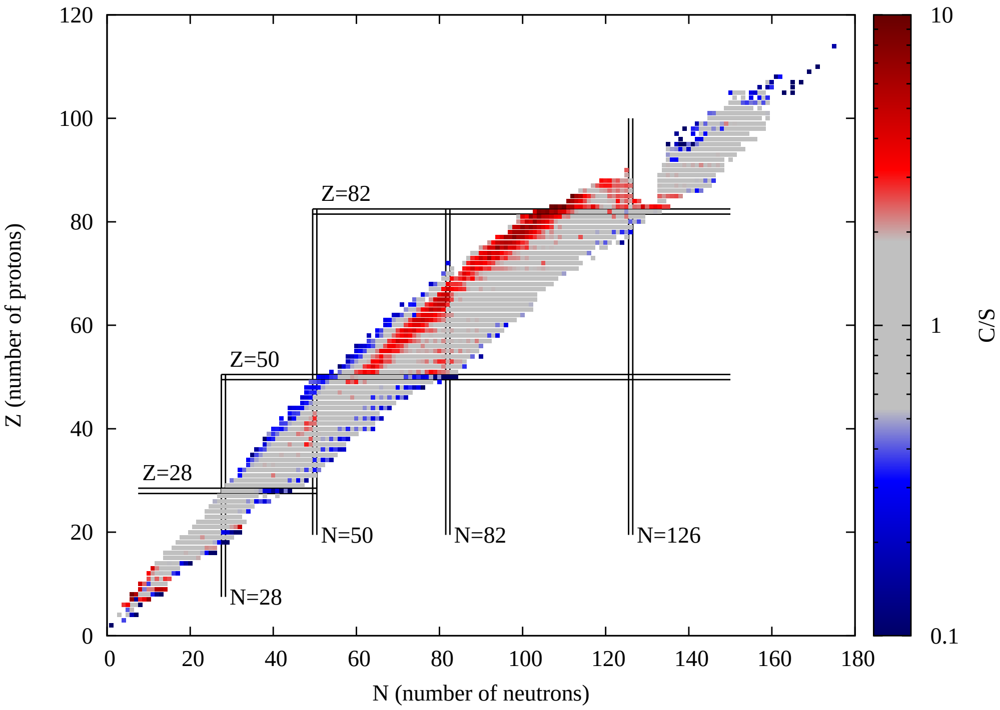

Figure 44: C/S values for all TENDL-2014 20 MeV (n,np+d) reactions.

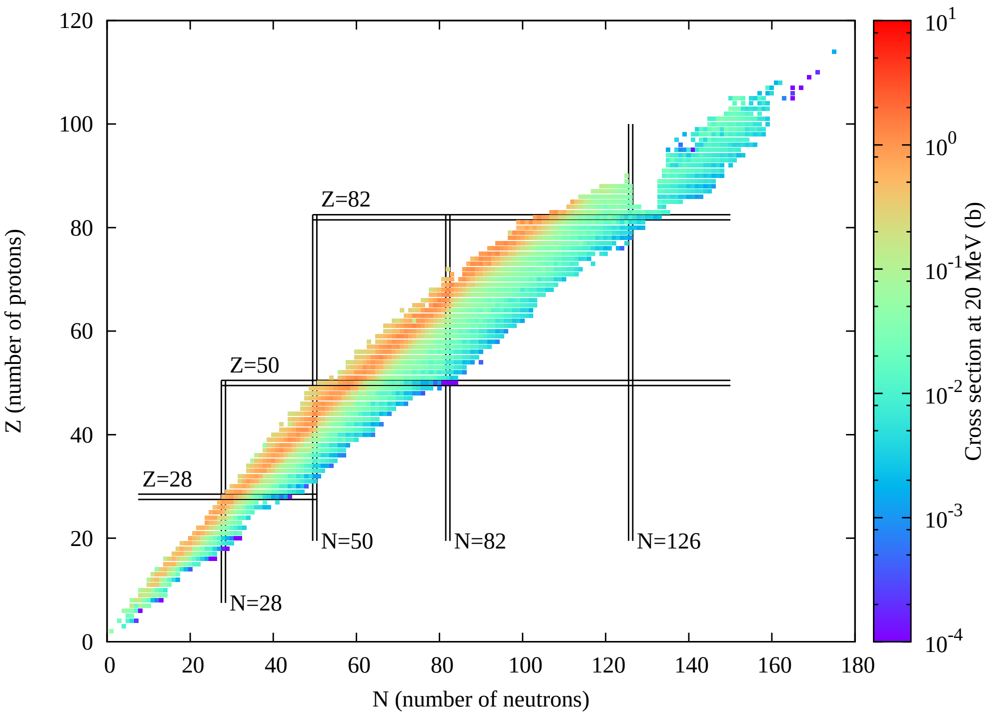

Figure 45: 20 MeV cross sections for all TENDL-2014 (n,np+d) reactions.

6 Conclusion

Except for the few errors identified in the report, primarily due to typos and misattribution of reaction channels, TENDL-2014 generally shows excellent agreement with the experimental data used in this report. Note that the resonance integrals are mostly effectively comparisons with another 'library' of resonance parameters within the *Atlas* [4] and that some of the thermal cross sections are inputs for the TALYS codes. The 30 keV Maxwellian-averaged, integral cross sections only consider a subset of the astrophysical quantities and the TENDL-2014 values have generally better agreement with the available experimental data than for any other major neutron-induced nuclear data library [8].

The extrapolation of nuclear data outside the stable nuclides is a complicated and invariably speculative affair. The approach of fitting some systematic function of a few nuclear parameters (such as mass, charge, separation energies, combinations of these, *etc*) has been successful in the **interpolation** between nuclides with experimental data, but this approach cannot be used to extrapolate far from stability. This is highlighted by the introduction of addition reaction channels which are not the primary focus for most nuclear data evaluations, such as the (n,2p) which competes with the (n,p) in neutron-poor nuclides.

The completeness of TENDL-2014 rather overwhelms the legacy systematic approach. The TENDL cross sections are, in effect, another systematic employing considerably more physics than a polynomial function of a few parameters. To probe the global cross section trends in TENDL-2014 individual reaction channels cannot be isolated and explored, but viewed in the wider context with their competitors.

While it is not possible to validate the global predictions of TENDL-2014 against experiments, the comparisons with legacy systematics (which have been fit to experimental databases) show good agreement where the systematics could be valid. Trends outside these regions are typically intuitive with some few patterns, such as the increased capture around neutron-poor Pb, which may be worth additional exploration. In all of these cases the lack of experimental data suggests the use of cross-model comparisons (*e.g.* with EMPIRE [37] or GNASH [38]) to identify regions with non-negligible variation amongst 'mature' nuclear model code predictions.

A Summary of C/E Values

Tables containing all of the UKAEA thermal and resonance integral cross sections, as well as the calculated TENDL-2014 values are provided in the following sections. Note that values which specify bounds (*ie* <X barns) have no C/E values. The isomeric identification of targets is in keeping with the TENDL-2014 values, but the product isomers are kept in a simple notation rather than including the spin-parity or RIPL level (as is done within the TENDL files). For example, the ^{176}Lu (n,γ) reaction can produce isomers of ^{177}Lu including [9/2-], [1/2+] and [23/2-] with half-lives of 130 ns, 0.16 ns and 160 days, respectively. Only the latter two are identified in the *Atlas* and only the third isomer is included in TENDL-2014, so it has been identified as ^{177m}Lu. Since TENDL contains specific identifiers for the level taken from RIPL, the interested reader can always find the specific channel in question.

Thermal cross sections

The data in Table 3 presents all of the thermal cross sections for reaction channels within the new UKAEA database. The experimental and TENDL-2014 cross sections are provided in barns, with C/E values in the last column. Reactions marked with **(M)** are thermal cross-sections from a maxwellian spectrum with first moment of 0.0253 eV. Note that all values which are given as inequalities have no C/E value or uncertainty and are not included in the statistical analysis of this dataset. The total absorption reaction channels are the sum of (n,γ), (n,p) and (n,α) channels.

Table 3: Summary of thermal cross section comparison.

Reaction	σ_E(b)	$\Delta\sigma_E$(b)	σ_{T14}(b)	C/E
H1(n,g)	3.33E-01	0.2 %	3.32E-01	1.00
H2(n,g) (M)	5.08E-04	3.0 %	5.06E-04	1.00
He3(n,g) (M)	5.50E-05	5.5 %	5.50E-05	1.00
He3(n,p)	5.33E+03	0.1 %	5.32E+03	1.00
Li6(n,t)	9.40E+02	0.4 %	9.38E+02	1.00
Li6(n,g) (M)	3.85E-02	7.8 %	3.85E-02	1.00
Li7(n,g) (M)	4.54E-02	5.9 %	4.54E-02	1.00
Be7(n,a)	<1.00E-01	-	1.00E-04	-
Be7(n,p)	3.88E+04	2.1 %	3.88E+04	1.00
Be9(n,g) (M)	8.49E-03	4.0 %	1.00E-02	1.18
Be10(n,g) (M)	<1.00E-03	-	2.44E-04	-
B10(n,a)	3.84E+03	0.2 %	3.84E+03	1.00
B10(n,g) (M)	3.05E-01	5.2 %	5.00E-01	1.64
B11(n,g) (M)	5.50E-03	60.0 %	5.51E-03	1.00
C12(n,g)	3.53E-03	2.0 %	3.86E-03	1.09
C13(n,g) (M)	1.37E-03	2.9 %	1.37E-03	1.00
C14(n,g) (M)	<1.00E-06	-	8.11E-07	-

Reaction	σ_E(b)	$\Delta\sigma_E$(b)	σ_{T14}(b)	C/E
N14(n,g) (M)	8.00E-02	0.8 %	7.50E-02	0.94
N14(n,p)	1.86E+00	1.6 %	1.83E+00	0.98
N15(n,g) (M)	2.40E-05	33.3 %	2.40E-05	1.00
O16(n,g) (M)	1.90E-04	10.0 %	1.90E-04	1.00
O17(n,a)	2.35E-01	4.3 %	2.35E-01	1.00
O17(n,g) (M)	5.38E-04	12.1 %	5.55E-04	1.03
O18(n,g) (M)	1.60E-04	6.2 %	1.59E-04	0.99
F19(n,g) (M)	9.51E-03	0.9 %	9.58E-03	1.01
Ne20(n,g) (M)	4.00E-02	10.0 %	3.69E-02	0.92
Ne21(n,a)	1.80E-04	38.9 %	1.80E-04	1.00
Ne21(n,g) (M)	6.66E-01	16.5 %	6.66E-01	1.00
Ne22(n,g) (M)	4.55E-02	13.2 %	4.55E-02	1.00
Na22(n,p)	2.78E+04	8.6 %	2.78E+04	1.00
Na22(n,a)	2.62E+02	19.1 %	2.62E-01	0.00
Na22(n,g)	2.83E+04	2.1 %	3.42E+04	1.21
Na23(n,g) (M)	4.00E-01	7.5 %	5.17E-01	1.29
Na23(n,g)	5.17E-01	0.8 %	5.17E-01	1.00
Mg24(n,g)	5.38E-02	2.4 %	5.03E-02	0.93
Mg25(n,g) (M)	1.99E-01	1.5 %	1.96E-01	0.98
Mg26(n,g)	3.84E-02	1.6 %	3.83E-02	1.00
Mg27(n,g) (M)	7.00E-02	28.6 %	7.00E-02	1.00
Al26(n,p)	1.97E+00	5.1 %	1.97E+00	1.00
Al26(n,a)	3.35E-01	4.2 %	3.35E-04	0.00
Al27(n,g)	2.31E-01	1.3 %	2.33E-01	1.01
Si28(n,g) (M)	1.77E-01	2.3 %	1.65E-01	0.93
Si29(n,g) (M)	1.19E-01	2.5 %	1.19E-01	1.00
Si30(n,g) (M)	1.07E-01	1.9 %	1.07E-01	1.00
Si31(n,g) (M)	7.30E-02	8.2 %	7.30E-02	1.00
Si32(n,g) (M)	5.00E-01	-	5.70E-01	1.14
P31(n,g)	1.65E-01	1.8 %	1.64E-01	1.00
S32(n,a)	7.00E-03	57.1 %	7.00E-03	1.00
S32(n,g) (M)	5.18E-01	2.7 %	5.24E-01	1.01
S33(n,p)	2.00E-03	50.0 %	2.00E-03	1.00
S33(n,a)	1.15E-01	8.7 %	1.15E-01	1.00
S33(n,g) (M)	4.54E-01	5.5 %	4.54E-01	1.00
S34(n,g) (M)	2.56E-01	3.5 %	2.56E-01	1.00
S36(n,g) (M)	2.36E-01	2.5 %	2.36E-01	1.00
Cl35(n,a)	8.00E-05	50.0 %	8.00E-05	1.00
Cl35(n,g) (M)	4.36E+01	0.9 %	4.36E+01	1.00
Cl35(n,p)	4.89E-01	2.9 %	4.89E-01	1.00
Cl36(n,p)	4.62E-02	8.7 %	4.62E-02	1.00
Cl36(n,a)	5.90E-04	11.9 %	5.90E-04	1.00
Cl36(n,g) (M)	<1.00E+01	-	9.99E+00	-
Cl37(n,g) (M)	4.33E-01	1.4 %	4.34E-01	1.00

Reaction	σ_E(b)	$\Delta\sigma_E$(b)	σ_{T14}(b)	C/E
Cl37(n,g)m	4.70E-02	21.3 %	4.49E-02	0.95
Cl37(n,g)g	3.86E-01	-	3.89E-01	1.01
Ar36(n,a)	5.50E-03	1.8 %	5.50E-03	1.00
Ar36(n,g) (M)	5.20E+00	9.6 %	5.19E+00	1.00
Ar36(n,p)	1.50E-03	-	1.50E-03	1.00
Ar37(n,a)	1.97E+03	16.8 %	1.97E+00	0.00
Ar37(n,p)	6.90E+01	0.2 %	6.90E+01	1.00
Ar38(n,g) (M)	8.00E-01	25.0 %	7.99E-01	1.00
Ar39(n,g) (M)	6.00E+02	50.0 %	5.90E+02	0.98
Ar40(n,g) (M)	6.60E-01	1.5 %	6.60E-01	1.00
Ar41(n,g) (M)	5.00E-01	20.0 %	4.98E-01	1.00
K39(n,a)	4.30E-03	11.6 %	4.30E-03	1.00
K39(n,g) (M)	2.10E+00	9.5 %	2.10E+00	1.00
K40(n,g) (M)	3.00E+01	26.7 %	3.00E+01	1.00
K40(n,p)	4.40E+00	6.8 %	4.39E+00	1.00
K40(n,a)	3.90E-01	7.7 %	3.90E-01	1.00
K41(n,g) (M)	1.46E+00	2.1 %	1.44E+00	0.99
Ca40(n,a)	2.50E-03	44.0 %	2.50E-03	1.00
Ca40(n,g)	4.10E-01	4.9 %	4.11E-01	1.00
Ca41(n,a)	1.00E-02	20.0 %	9.98E-03	1.00
Ca41(n,g) (M)	4.00E+00	-	3.99E+00	1.00
Ca41(n,p)	7.00E-03	28.6 %	7.00E-03	1.00
Ca42(n,g) (M)	6.80E-01	10.3 %	6.80E-01	1.00
Ca43(n,g) (M)	6.20E+00	9.7 %	6.28E+00	1.01
Ca44(n,g)	8.80E-01	5.7 %	8.96E-01	1.02
Ca45(n,g) (M)	1.50E+01	-	1.50E+01	1.00
Ca46(n,g) (M)	7.40E-01	9.5 %	7.39E-01	1.00
Ca48(n,g) (M)	1.09E+00	12.8 %	1.09E+00	1.00
Sc45(n,g) (M)	2.72E+01	4.0 %	2.71E+01	1.00
Sc45(n,g)	2.72E+01	0.7 %	2.71E+01	1.00
Sc45(n,g)g	1.74E+01	6.3 %	2.10E+01	1.21
Sc45(n,g)m	9.80E+00	11.2 %	6.14E+00	0.63
Sc46(n,g) (M)	8.00E+00	12.5 %	7.99E+00	1.00
Ti44(n,g)	1.10E+00	18.2 %	1.10E+00	1.00
Ti46(n,g) (M)	5.90E-01	30.5 %	6.08E-01	1.03
Ti47(n,g) (M)	1.63E+00	2.5 %	1.63E+00	1.00
Ti48(n,g) (M)	8.32E+00	1.9 %	8.32E+00	1.00
Ti49(n,g) (M)	1.87E+00	2.1 %	1.86E+00	0.99
Ti50(n,g)	1.79E-01	1.7 %	1.81E-01	1.01
V50(n,p)	4.00E-04	-	3.95E-04	0.99
V50(n,g)	4.50E+01	8.9 %	4.48E+01	1.00
V51(n,g)	4.94E+00	0.8 %	4.99E+00	1.01
Cr50(n,g) (M)	1.54E+01	1.3 %	1.54E+01	1.00
Cr51(n,g)	1.00E+01	-	9.97E+00	1.00

Reaction	σ_E(b)	$\Delta\sigma_E$(b)	σ_{T14}(b)	C/E
Cr52(n,g) (M)	8.60E-01	2.3 %	8.56E-01	1.00
Cr53(n,g) (M)	1.86E+01	3.2 %	1.87E+01	1.00
Cr54(n,g) (M)	4.10E-01	9.8 %	4.11E-01	1.00
Mn52(n,g)	6.00E+01	11.7 %	5.98E+01	1.00
Mn53(n,g) (M)	7.00E+01	14.3 %	6.96E+01	0.99
Mn54(n,g) (M)	3.80E+01	-	3.79E+01	1.00
Mn55(n,g)	1.34E+01	0.4 %	1.33E+01	0.99
Fe54(n,a)	1.00E-05	-	1.00E-05	1.00
Fe54(n,g) (M)	2.25E+00	8.0 %	2.25E+00	1.00
Fe55(n,g)	1.30E+01	15.4 %	1.30E+01	1.00
Fe56(n,g) (M)	2.59E+00	5.4 %	2.59E+00	1.00
Fe57(n,g) (M)	2.48E+00	12.1 %	2.48E+00	1.00
Fe58(n,g)	1.32E+00	2.3 %	1.30E+00	0.98
Fe59(n,g)	1.30E+01	23.1 %	1.30E+01	1.00
Co57(n,g) (M)	5.10E+01	9.8 %	5.08E+01	1.00
Co58(n,g) (M)	1.90E+03	10.5 %	1.86E+03	0.98
Co58(n,p)	1.71E+03	11.7 %	1.71E+03	1.00
Co58m(n,g) (M)	1.40E+05	7.1 %	1.38E+05	0.98
Co59(n,g)	3.72E+01	0.2 %	3.72E+01	1.00
Co59(n,g)g	1.65E+01	-	1.40E+01	0.85
Co59(n,g)m	2.04E+01	3.9 %	2.31E+01	1.13
Co60(n,g) (M)	2.00E+00	10.0 %	1.99E+00	1.00
Co60m(n,g) (M)	5.80E+01	13.8 %	5.78E+01	1.00
Ni58(n,g) (M)	4.37E+00	2.3 %	4.79E+00	1.10
Ni59(n,a)	1.23E+01	4.9 %	1.23E-02	0.00
Ni59(n,g)	7.77E+01	5.3 %	7.74E+01	1.00
Ni59(n,p)	1.63E+00	22.9 %	1.34E+00	0.82
Ni60(n,g) (M)	2.50E+00	2.4 %	2.40E+00	0.96
Ni61(n,a)	3.00E-05	-	3.00E-05	1.00
Ni61(n,g) (M)	2.10E+00	19.0 %	2.19E+00	1.04
Ni62(n,g) (M)	1.49E+01	2.0 %	1.42E+01	0.95
Ni63(n,g) (M)	2.44E+01	12.3 %	2.43E+01	1.00
Ni64(n,g)	1.64E+00	2.4 %	1.64E+00	1.00
Ni65(n,g) (M)	2.24E+01	8.9 %	2.23E+01	1.00
Cu63(n,g)	4.50E+00	0.4 %	4.50E+00	1.00
Cu63(n,p)	4.80E-05	25.0 %	4.80E-05	1.00
Cu64(n,g) (M)	2.70E+02	63.0 %	2.70E+02	1.00
Cu65(n,g)	2.17E+00	1.4 %	2.15E+00	0.99
Cu66(n,g) (M)	1.35E+02	7.4 %	1.34E+02	0.99
Zn64(n,g) (M)	7.90E-01	2.5 %	7.93E-01	1.00
Zn64(n,a)	1.10E-05	27.3 %	1.10E-05	1.00
Zn65(n,a)	2.00E+00	10.0 %	1.99E-03	0.00
Zn65(n,g)	6.60E+01	12.1 %	6.45E+01	0.98
Zn66(n,a)	<2.00E-05	-	2.00E-05	-

Reaction	σ_E(b)	$\Delta\sigma_E$(b)	σ_{T14}(b)	C/E
Zn66(n,g) (M)	6.20E-01	9.7 %	6.22E-01	1.00
Zn67(n,a)	1.59E-04	12.6 %	1.59E-04	1.00
Zn67(n,g) (M)	7.50E+00	13.3 %	7.53E+00	1.00
Zn68(n,g) (M)	1.07E+00	9.3 %	1.07E+00	1.00
Zn68(n,g)g	1.00E+00	10.0 %	9.56E-01	0.96
Zn68(n,g)m	7.20E-02	5.6 %	1.17E-01	1.62
Zn70(n,g) (M)	9.00E-02	5.6 %	9.15E-02	1.02
Zn70(n,g)g	8.30E-02	6.0 %	6.97E-02	0.84
Zn70(n,g)m	8.70E-03	5.7 %	2.18E-02	2.50
Ga69(n,g)	1.75E+00	4.0 %	1.74E+00	1.00
Ga71(n,g)	4.61E+00	3.3 %	4.59E+00	1.00
Ge68(n,g) (M)	1.00E+00	50.0 %	9.97E-01	1.00
Ge70(n,g)	3.05E+00	4.3 %	3.07E+00	1.01
Ge70(n,g)	3.05E+00	4.3 %	3.07E+00	1.01
Ge72(n,g)	8.90E-01	9.0 %	8.85E-01	0.99
Ge72(n,g)m	5.00E-01	2.0 %	4.42E-01	0.88
Ge73(n,g)	1.47E+01	2.7 %	1.47E+01	1.00
Ge74(n,g) (M)	5.20E-01	7.7 %	5.18E-01	1.00
Ge74(n,g)m	1.64E-01	6.1 %	1.27E-01	0.77
Ge74(n,g)g	3.60E-01	11.1 %	3.92E-01	1.09
Ge76(n,g) (M)	1.55E-01	6.5 %	1.54E-01	1.00
Ge76(n,g)g	5.50E-02	36.4 %	6.06E-02	1.10
Ge76(n,g)m	1.00E-01	10.0 %	9.39E-02	0.94
As75(n,g)	4.09E+00	2.0 %	4.10E+00	1.00
Se74(n,g)	5.22E+01	1.5 %	5.24E+01	1.00
Se75(n,g)	3.30E+02	30.3 %	3.29E+02	1.00
Se76(n,g)	8.48E+01	6.1 %	8.48E+01	1.00
Se76(n,g)m	2.00E+01	5.0 %	2.15E+01	1.08
Se76(n,g)g	6.30E+01	-	6.32E+01	1.00
Se77(n,a)	9.70E-04	0.3 %	9.70E-04	1.00
Se77(n,g) (M)	4.15E+01	10.1 %	4.14E+01	1.00
Se78(n,g) (M)	4.23E-01	1.6 %	4.28E-01	1.01
Se78(n,g)g	1.35E-01	64.4 %	1.79E-01	1.33
Se78(n,g)m	2.94E-01	32.7 %	2.49E-01	0.85
Se80(n,g) (M)	5.97E-01	3.2 %	5.77E-01	0.97
Se80(n,g)g	4.63E-01	14.4 %	4.23E-01	0.91
Se80(n,g)m	1.25E-01	61.2 %	1.54E-01	1.23
Se82(n,g) (M)	4.41E-02	6.4 %	4.39E-02	0.99
Se82(n,g)g	1.84E-02	71.7 %	2.43E-02	1.32
Se82(n,g)m	2.56E-02	52.3 %	1.95E-02	0.76
Br76(n,p)	2.24E+02	18.8 %	2.17E+02	0.97
Br79(n,g)	1.03E+01	2.4 %	1.04E+01	1.01
Br79(n,g)g	7.88E+00	3.0 %	8.57E+00	1.09
Br79(n,g)m	2.44E+00	3.3 %	1.79E+00	0.73

Reaction	σ_E(b)	$\Delta\sigma_E$(b)	σ_{T14}(b)	C/E
Br81(n,g)	2.36E+00	2.1 %	2.37E+00	1.00
Br81(n,g)g	2.35E-01	3.4 %	1.31E-01	0.56
Br81(n,g)m	2.12E+00	2.4 %	2.24E+00	1.06
Kr78(n,g) (M)	5.75E+00	11.4 %	6.42E+00	1.12
Kr78(n,g)g	5.02E+00	-	5.20E+00	1.04
Kr78(n,g)m	7.28E-01	79.5 %	1.22E+00	1.67
Kr80(n,g) (M)	1.15E+01	4.3 %	1.15E+01	1.00
Kr80(n,g)g	6.97E+00	-	7.97E+00	1.14
Kr80(n,g)m	4.53E+00	14.3 %	3.57E+00	0.79
Kr82(n,g) (M)	1.90E+01	21.1 %	1.89E+01	1.00
Kr82(n,g)g	3.90E+00	-	5.39E+00	1.38
Kr82(n,g)m	1.51E+01	17.9 %	1.35E+01	0.90
Kr83(n,g) (M)	1.97E+02	5.1 %	1.97E+02	1.00
Kr84(n,g) (M)	1.06E-01	4.5 %	1.11E-01	1.04
Kr84(n,g)g	1.79E-02	13.5 %	2.19E-02	1.22
Kr84(n,g)m	8.36E-02	10.0 %	8.88E-02	1.06
Kr85(n,g) (M)	1.66E+00	12.0 %	1.65E+00	1.00
Kr86(n,g) (M)	3.00E-03	66.7 %	2.96E-03	0.99
Rb84(n,p)	1.20E+01	16.7 %	1.17E+01	0.97
Rb85(n,g) (M)	4.88E-01	1.9 %	4.99E-01	1.02
Rb85(n,g)g	4.52E-01	5.8 %	4.67E-01	1.03
Rb85(n,g)m	3.98E-02	42.7 %	3.24E-02	0.81
Rb86(n,g)	2.00E+01	-	1.99E+01	1.00
Rb87(n,g) (M)	1.22E-01	2.5 %	1.21E-01	1.00
Rb88(n,g) (M)	1.00E+00	30.0 %	9.96E-01	1.00
Sr84(n,g) (M)	8.22E-01	14.6 %	8.33E-01	1.01
Sr84(n,g)g	1.99E-01	50.3 %	1.88E-01	0.94
Sr84(n,g)m	6.23E-01	9.6 %	6.46E-01	1.04
Sr86(n,g) (M)	1.04E+00	6.7 %	1.03E+00	0.99
Sr86(n,g)g	2.30E-01	13.0 %	3.96E-02	0.17
Sr86(n,g)m	7.70E-01	7.8 %	9.95E-01	1.29
Sr87(n,g) (M)	1.70E+01	17.6 %	1.72E+01	1.01
Sr88(n,g) (M)	5.80E-03	6.9 %	5.78E-03	1.00
Sr89(n,g) (M)	4.20E-01	9.5 %	4.19E-01	1.00
Sr90(n,g) (M)	1.04E-02	13.5 %	1.03E-02	1.00
Y89(n,g)	1.28E+00	1.6 %	1.28E+00	1.00
Y89(n,g)g	1.28E+00	-	1.28E+00	1.00
Y89(n,g)m	2.31E-03	56.7 %	3.21E-03	1.39
Y90(n,g) (M)	6.50E+00	-	6.46E+00	0.99
Y91(n,g) (M)	1.40E+00	21.4 %	1.39E+00	1.00
Zr90(n,g) (M)	1.07E-02	62.0 %	1.07E-02	1.00
Zr91(n,g) (M)	8.30E-01	9.6 %	1.22E+00	1.47
Zr92(n,g) (M)	2.60E-01	30.8 %	2.60E-01	1.00
Zr93(n,g) (M)	1.00E+00	-	9.96E-01	1.00

Reaction	σ_E(b)	$\Delta\sigma_E$(b)	σ_{T14}(b)	C/E
Zr94(n,g) (M)	4.94E-02	3.4 %	5.00E-02	1.01
Zr96(n,g) (M)	2.29E-02	4.4 %	2.31E-02	1.01
Nb93(n,g)	1.15E+00	4.3 %	1.15E+00	1.00
Nb94(n,g)	1.49E+01	6.7 %	1.48E+01	0.99
Nb94(n,g)g	1.49E+01	6.7 %	1.48E+01	0.99
Nb94(n,g)m	6.00E-01	16.7 %	4.96E-02	0.08
Nb95(n,g) (M)	7.00E+00	-	6.98E+00	1.00
Mo92(n,g) (M)	8.00E-02	25.0 %	8.08E-02	1.01
Mo94(n,g) (M)	3.40E-01	17.6 %	3.40E-01	1.00
Mo95(n,a)	3.00E-05	-	2.99E-05	1.00
Mo95(n,g) (M)	1.34E+01	2.2 %	1.34E+01	1.00
Mo96(n,g) (M)	5.00E-01	40.0 %	5.06E-01	1.01
Mo97(n,a)	4.00E-07	-	3.99E-07	1.00
Mo97(n,g) (M)	2.20E+00	9.1 %	2.20E+00	1.00
Mo98(n,g)	1.30E-01	4.6 %	1.32E-01	1.02
Mo100(n,g) (M)	1.99E-01	1.5 %	1.99E-01	1.00
Tc98(n,g) (M)	9.30E-01	21.5 %	9.26E-01	1.00
Tc99(n,g)	2.28E+01	5.7 %	2.27E+01	1.00
Ru96(n,g)	2.90E-01	6.9 %	2.89E-01	1.00
Ru98(n,g) (M)	8.00E+00	-	7.97E+00	1.00
Ru99(n,g)	7.24E+00	13.8 %	7.27E+00	1.00
Ru100(n,g)	5.80E+00	6.9 %	5.77E+00	1.00
Ru101(n,a)	1.50E-07	-	1.50E-07	1.00
Ru101(n,g)	5.20E+00	5.8 %	5.19E+00	1.00
Ru102(n,g)	1.27E+00	3.1 %	1.27E+00	1.00
Ru103(n,g) (M)	1.20E+00	-	1.21E+00	1.01
Ru104(n,g)	4.91E-01	2.0 %	4.88E-01	0.99
Ru105(n,g)	3.90E-01	15.4 %	3.88E-01	1.00
Ru106(n,g)	1.46E-01	30.8 %	1.45E-01	1.00
Rh103(n,g)	1.42E+02	2.4 %	1.42E+02	1.00
Rh103(n,g)g	1.35E+02	-	1.37E+02	1.02
Rh103(n,g)m	6.57E+00	66.4 %	4.96E+00	0.76
Rh104(n,g) (M)	4.00E+01	75.0 %	3.94E+01	0.98
Rh104m(n,g) (M)	8.00E+02	12.5 %	7.90E+02	0.99
Rh105(n,g)	1.60E+04	-	2.09E+04	1.31
Rh105(n,g)g	1.10E+04	27.3 %	1.20E+04	1.09
Rh105(n,g)m	5.00E+03	20.0 %	8.92E+03	1.78
Pd102(n,g) (M)	1.82E+00	11.0 %	1.80E+00	0.99
Pd104(n,g) (M)	6.50E-01	46.2 %	6.48E-01	1.00
Pd105(n,a)	5.00E-07	-	4.99E-07	1.00
Pd105(n,g) (M)	2.10E+01	7.1 %	2.11E+01	1.01
Pd106(n,g) (M)	3.05E-01	9.8 %	3.03E-01	0.99
Pd106(n,g)g	2.92E-01	9.9 %	3.03E-01	1.04
Pd106(n,g)m	6.86E-03	94.2 %	5.63E-04	0.08

Reaction	σ_E(b)	$\Delta\sigma_E$(b)	σ_{T14}(b)	C/E
Pd107(n,g) (M)	2.54E+00	7.9 %	2.53E+00	1.00
Pd108(n,g) (M)	7.60E+00	6.6 %	7.58E+00	1.00
Pd108(n,g)g	8.48E+00	5.9 %	7.51E+00	0.89
Pd108(n,g)m	1.85E-01	5.4 %	6.00E-02	0.32
Pd110(n,g) (M)	7.30E-01	23.3 %	7.31E-01	1.00
Pd110(n,g)g	7.00E-01	24.3 %	7.30E-01	1.04
Pd110(n,g)m	3.30E-02	9.1 %	1.08E-03	0.03
Ag107(n,g)	3.76E+01	3.2 %	3.52E+01	0.94
Ag107(n,g)g	3.73E+01	-	3.48E+01	0.93
Ag107(n,g)m	3.30E-01	24.2 %	4.06E-01	1.23
Ag109(n,g)	9.10E+01	1.1 %	9.02E+01	0.99
Ag109(n,g)g	8.70E+01	3.4 %	8.59E+01	0.99
Ag109(n,g)m	3.95E+00	1.3 %	4.32E+00	1.09
Ag110m(n,g)	8.20E+01	13.4 %	8.21E+01	1.00
Ag111(n,g) (M)	3.00E+00	66.7 %	2.99E+00	1.00
Cd106(n,g) (M)	1.00E+00	-	9.96E-01	1.00
Cd108(n,g) (M)	7.20E-01	18.1 %	7.15E-01	0.99
Cd109(n,a)	5.00E-02	-	4.96E-05	0.00
Cd109(n,g) (M)	7.00E+02	14.3 %	7.24E+02	1.03
Cd110(n,g) (M)	1.10E+01	9.1 %	1.10E+01	1.00
Cd110(n,g)g	1.10E+01	-	1.08E+01	0.98
Cd110(n,g)m	1.07E-01	67.9 %	2.49E-01	2.33
Cd111(n,g)	6.90E+00	11.6 %	6.87E+00	1.00
Cd112(n,g) (M)	2.20E+00	22.7 %	2.20E+00	1.00
Cd113(n,a)	3.90E+00	10.3 %	9.99E-07	0.00
Cd113(n,g)	2.06E+04	1.9 %	2.05E+04	0.99
Cd114(n,g) (M)	3.30E-01	5.5 %	3.29E-01	1.00
Cd114(n,g)g	2.94E-01	5.4 %	3.06E-01	1.04
Cd114(n,g)m	3.60E-02	19.4 %	2.23E-02	0.62
Cd116(n,g) (M)	7.57E-02	1.3 %	7.46E-02	0.98
Cd116(n,g)g	6.01E-02	16.8 %	6.74E-02	1.12
Cd116(n,g)m	1.56E-02	64.1 %	7.14E-03	0.46
In113(n,g)	1.20E+01	9.2 %	1.21E+01	1.01
In113(n,g)g	3.90E+00	10.3 %	2.60E+00	0.67
In113(n,g)m	8.10E+00	9.9 %	9.54E+00	1.18
In115(n,g)	2.02E+02	1.0 %	2.02E+02	1.00
In115(n,g)g	4.00E+01	5.0 %	5.05E-20	0.00
In115(n,g)m	8.10E+01	9.9 %	7.80E+02	9.63
In115(n,g)n	8.10E+01	9.9 %	3.09E+01	0.38
Sn112(n,g) (M)	8.50E-01	4.7 %	8.45E-01	0.99
Sn112(n,g)g	5.60E-01	3.6 %	5.16E-01	0.92
Sn112(n,g)m	2.90E-01	10.3 %	3.29E-01	1.14
Sn113(n,g) (M)	8.80E+00	13.6 %	8.79E+00	1.00
Sn114(n,g) (M)	1.25E-01	24.0 %	1.24E-01	1.00

Reaction	σ_E(b)	$\Delta\sigma_E$(b)	σ_{T14}(b)	C/E
Sn115(n,a)	6.00E-05	-	5.99E-05	1.00
Sn115(n,g) (M)	5.80E+01	13.8 %	5.75E+01	0.99
Sn116(n,g) (M)	1.30E-01	30.8 %	1.29E-01	0.99
Sn116(n,g)g	1.24E-01	-	1.28E-01	1.03
Sn116(n,g)m	3.50E-03	14.3 %	1.13E-03	0.32
Sn117(n,g) (M)	1.07E+00	4.7 %	1.06E+00	0.99
Sn118(n,g) (M)	2.20E-01	22.7 %	2.23E-01	1.01
Sn118(n,g)g	1.21E-01	-	2.17E-01	1.79
Sn118(n,g)m	1.00E-02	60.0 %	6.28E-03	0.63
Sn119(n,g)	2.19E+00	2.7 %	2.19E+00	1.00
Sn120(n,g) (M)	1.40E-01	21.4 %	1.40E-01	1.00
Sn120(n,g)g	1.38E-01	-	1.33E-01	0.96
Sn120(n,g)m	3.96E-03	73.0 %	6.81E-03	1.72
Sn122(n,g) (M)	1.42E-01	-	1.46E-01	1.03
Sn122(n,g)g	4.10E-03	29.3 %	3.72E-02	9.07
Sn122(n,g)m	1.38E-01	7.2 %	1.09E-01	0.79
Sn124(n,g) (M)	1.30E-01	3.8 %	1.30E-01	1.00
Sn124(n,g)g	4.20E-03	31.0 %	5.64E-03	1.34
Sn124(n,g)m	1.30E-01	3.8 %	1.24E-01	0.95
Sb121(n,g)	5.77E+00	1.9 %	5.74E+00	0.99
Sb121(n,g)g	5.71E+00	-	5.73E+00	1.00
Sb121(n,g)m	6.00E-02	16.7 %	1.02E-02	0.17
Sb123(n,g)	4.07E+00	3.8 %	3.94E+00	0.97
Sb123(n,g)g	3.46E+00	15.6 %	2.85E+00	0.82
Sb123(n,g)m	4.53E-01	91.8 %	9.16E-01	2.02
Sb123(n,g)n	8.93E-02	78.7 %	1.78E-01	1.99
Sb124(n,g) (M)	1.74E+01	16.1 %	1.73E+01	0.99
Te120(n,g)	2.34E+00	15.4 %	2.33E+00	1.00
Te120(n,g)g	2.00E+00	15.0 %	2.19E+00	1.09
Te120(n,g)m	3.40E-01	17.6 %	1.44E-01	0.42
Te122(n,g) (M)	3.90E+00	10.3 %	3.92E+00	1.00
Te122(n,g)g	3.41E+00	-	3.55E+00	1.04
Te122(n,g)m	4.90E-01	16.3 %	3.70E-01	0.76
Te123(n,g) (M)	4.18E+02	7.2 %	4.23E+02	1.01
Te123(n,a)	4.60E-05	13.0 %	4.56E-05	0.99
Te124(n,g) (M)	6.30E+00	11.1 %	6.33E+00	1.00
Te124(n,g)g	5.49E+00	-	5.91E+00	1.08
Te124(n,g)m	8.51E-01	7.2 %	4.24E-01	0.50
Te125(n,g) (M)	1.29E+00	12.4 %	1.29E+00	1.00
Te126(n,g) (M)	3.81E-01	-	4.44E-01	1.16
Te126(n,g)g (M)	3.25E-01	4.3 %	4.25E-01	1.31
Te126(n,g)m (M)	5.60E-02	5.4 %	1.85E-02	0.33
Te127m(n,g)	3.38E+03	15.1 %	6.11E+03	1.81
Te128(n,g) (M)	2.00E-01	4.0 %	1.99E-01	1.00

Reaction	σ_E(b)	$\Delta\sigma_E$(b)	σ_{T14}(b)	C/E
Te128(n,g)g	1.80E-01	4.4 %	1.96E-01	1.09
Te128(n,g)m	2.00E-02	10.0 %	3.68E-03	0.18
Te130(n,g) (M)	1.95E-01	5.1 %	1.95E-01	1.00
Te130(n,g)g	1.85E-01	5.4 %	1.87E-01	1.01
Te130(n,g)m	1.00E-02	30.0 %	8.50E-03	0.85
I125(n,g)	8.94E+02	10.1 %	8.96E+02	1.00
I126(n,g) (M)	5.96E+03	-	5.84E+03	0.98
I127(n,g)	6.15E+00	1.0 %	6.14E+00	1.00
I128(n,g)	2.20E+01	18.2 %	2.19E+01	0.99
I129(n,g)	3.03E+01	4.0 %	3.25E+01	1.07
I129(n,g)m	1.78E+01	3.9 %	1.43E+01	0.81
I129(n,g)g	1.25E+01	4.0 %	1.82E+01	1.46
I130(n,g) (M)	1.80E+01	16.7 %	1.82E+01	1.01
I131(n,g) (M)	8.00E+01	62.5 %	7.97E+01	1.00
Xe124(n,g)	1.50E+02	13.3 %	1.49E+02	0.99
Xe124(n,g)g	1.22E+02	-	1.31E+02	1.08
Xe124(n,g)m	2.80E+01	17.9 %	1.77E+01	0.63
Xe125(n,a)	<3.00E-05	-	2.93E-05	-
Xe126(n,g)	3.50E+00	22.9 %	3.48E+00	1.00
Xe126(n,g)g	3.02E+00	-	3.26E+00	1.08
Xe126(n,g)m	4.80E-01	20.8 %	2.20E-01	0.46
Xe127(n,a)	<1.00E-02	-	9.88E-06	-
Xe128(n,g)	5.23E+00	24.9 %	5.20E+00	0.99
Xe128(n,g)g	3.30E+00	-	5.12E+00	1.55
Xe128(n,g)m	1.93E-01	148.7 %	7.97E-02	0.41
Xe129(n,g)	2.10E+01	14.3 %	2.10E+01	1.00
Xe130(n,g)	5.07E+00	5.8 %	4.79E+00	0.94
Xe130(n,g)g	4.77E+00	-	4.62E+00	0.97
Xe130(n,g)m	2.99E-01	71.2 %	1.68E-01	0.56
Xe131(n,g)	8.70E+01	11.5 %	8.71E+01	1.00
Xe132(n,g)	4.49E-01	13.4 %	4.48E-01	1.00
Xe132(n,g)g	4.23E-01	-	4.45E-01	1.05
Xe132(n,g)m	2.63E-02	90.5 %	2.94E-03	0.11
Xe133(n,g) (M)	1.90E+02	47.4 %	1.90E+02	1.00
Xe134(n,g)	2.65E-01	7.5 %	2.69E-01	1.02
Xe134(n,g)g	2.63E-01	-	2.68E-01	1.02
Xe134(n,g)m	2.16E-03	39.6 %	1.61E-03	0.74
Xe135(n,g)	2.65E+06	4.2 %	2.65E+06	1.00
Xe136(n,g)	2.60E-01	7.7 %	2.60E-01	1.00
Cs132(n,a)	<1.50E-01	-	1.49E-04	-
Cs133(n,g)	3.03E+01	3.6 %	3.02E+01	1.00
Cs133(n,g)g	2.63E+01	3.8 %	3.00E+01	1.14
Cs133(n,g)m	2.70E+00	4.8 %	1.98E-01	0.07
Cs134(n,g) (M)	1.40E+02	8.6 %	1.40E+02	1.00

Reaction	σ_E(b)	$\Delta\sigma_E$(b)	σ_{T14}(b)	C/E
Cs135(n,g) (M)	8.30E+00	3.6 %	8.23E+00	0.99
Cs137(n,g) (M)	2.70E-01	11.1 %	2.69E-01	0.99
Ba130(n,g) (M)	8.70E+00	10.3 %	8.66E+00	1.00
Ba130(n,g)g	7.70E+00	11.7 %	8.43E+00	1.09
Ba130(n,g)m	9.80E-01	5.1 %	2.47E-01	0.25
Ba132(n,g) (M)	6.50E+00	12.3 %	6.47E+00	1.00
Ba132(n,g)g	6.50E+00	12.3 %	6.33E+00	0.97
Ba132(n,g)m	5.00E-01	-	1.46E-01	0.29
Ba133(n,g) (M)	4.20E+00	35.7 %	4.18E+00	0.99
Ba134(n,g) (M)	1.50E+00	20.0 %	1.50E+00	1.00
Ba134(n,g)g	1.37E+00	-	1.45E+00	1.06
Ba134(n,g)m	1.34E-01	17.9 %	5.29E-02	0.39
Ba135(n,g) (M)	5.80E+00	15.5 %	5.79E+00	1.00
Ba135(n,g)g	5.79E+00	-	5.78E+00	1.00
Ba135(n,g)m	1.39E-02	5.0 %	1.01E-02	0.72
Ba136(n,g) (M)	6.80E-01	25.0 %	6.79E-01	1.00
Ba136(n,g)g	6.70E-01	25.4 %	6.64E-01	0.99
Ba136(n,g)m	1.00E-02	10.0 %	1.61E-02	1.61
Ba137(n,g) (M)	3.60E+00	5.6 %	3.60E+00	1.00
Ba138(n,g) (M)	4.04E-01	9.9 %	4.02E-01	0.99
Ba139(n,g) (M)	6.20E+00	25.8 %	6.17E+00	1.00
Ba140(n,g) (M)	1.60E+00	18.8 %	1.59E+00	1.00
La138(n,g)	5.72E+01	10.0 %	5.71E+01	1.00
La139(n,g)	9.04E+00	0.4 %	9.04E+00	1.00
La140(n,g) (M)	2.70E+00	11.1 %	2.69E+00	1.00
Ce136(n,g) (M)	7.45E+00	13.4 %	7.53E+00	1.01
Ce136(n,g)g	6.50E+00	15.4 %	7.45E+00	1.15
Ce136(n,g)m	9.50E-01	26.3 %	7.27E-02	0.08
Ce138(n,g) (M)	1.22E+00	20.1 %	1.21E+00	0.99
Ce138(n,g)g	1.02E+00	23.5 %	1.19E+00	1.17
Ce138(n,g)m	1.50E-02	33.3 %	1.69E-02	1.12
Ce139(n,g) (M)	4.80E+02	-	4.59E+02	0.96
Ce140(n,g) (M)	5.80E-01	3.4 %	5.78E-01	1.00
Ce141(n,g) (M)	2.90E+01	10.3 %	2.88E+01	0.99
Ce142(n,g) (M)	9.70E-01	2.1 %	9.71E-01	1.00
Ce143(n,g) (M)	4.50E+00	15.6 %	4.48E+00	1.00
Ce144(n,g) (M)	1.00E+00	10.0 %	9.96E-01	1.00
Pr141(n,g)	1.15E+01	2.6 %	1.15E+01	1.00
Pr141(n,g)g	7.60E+00	-	8.88E+00	1.17
Pr141(n,g)m	3.90E+00	7.7 %	2.57E+00	0.66
Pr142(n,g)	2.00E+01	15.0 %	1.99E+01	0.99
Pr143(n,g)	9.00E+01	11.1 %	9.00E+01	1.00
Nd142(n,g) (M)	1.87E+01	3.7 %	1.87E+01	1.00
Nd143(n,g)	3.25E+02	3.1 %	3.25E+02	1.00

Reaction	σ_E(b)	$\Delta\sigma_E$(b)	σ_{T14}(b)	C/E
Nd143(n,a)	1.74E-02	9.2 %	2.03E-02	1.17
Nd144(n,g) (M)	3.60E+00	8.3 %	3.63E+00	1.01
Nd145(n,a)	<1.00E-04	-	9.70E-05	-
Nd145(n,g)	5.00E+01	2.0 %	5.00E+01	1.00
Nd146(n,g)	1.49E+00	4.0 %	1.49E+00	1.00
Nd147(n,g) (M)	4.40E+02	34.1 %	4.39E+02	1.00
Nd148(n,g)	2.58E+00	2.7 %	2.60E+00	1.01
Nd150(n,g)	1.04E+00	3.8 %	1.05E+00	1.01
Pm146(n,g) (M)	8.90E+03	18.9 %	8.24E+03	0.93
Pm147(n,g)	1.68E+02	2.1 %	1.68E+02	1.00
Pm147(n,g)g	9.60E+01	1.9 %	1.13E+02	1.17
Pm147(n,g)m	7.24E+01	4.1 %	5.52E+01	0.76
Pm148(n,g) (M)	2.00E+03	50.0 %	1.94E+03	0.97
Pm148m(n,g)	1.06E+04	9.4 %	1.07E+04	1.01
Pm149(n,g) (M)	1.40E+03	21.4 %	1.38E+03	0.99
Pm151(n,g) (M)	5.00E+02	-	4.95E+02	0.99
Sm144(n,g) (M)	1.64E+00	6.1 %	1.63E+00	1.00
Sm145(n,g) (M)	2.80E+02	7.5 %	2.81E+02	1.00
Sm147(n,g)	5.70E+01	5.3 %	5.67E+01	0.99
Sm147(n,a)	5.80E-04	10.3 %	3.41E-04	0.59
Sm148(n,g) (M)	2.40E+00	25.0 %	2.39E+00	0.99
Sm149(n,a)	3.07E-02	6.8 %	2.24E-02	0.73
Sm149(n,g)	4.01E+04	1.5 %	4.04E+04	1.01
Sm150(n,g)	1.00E+02	4.0 %	1.00E+02	1.00
Sm151(n,g)	1.52E+04	2.0 %	1.52E+04	1.00
Sm152(n,g)	2.06E+02	2.9 %	2.06E+02	1.00
Sm153(n,g)	4.20E+02	42.9 %	4.18E+02	1.00
Sm154(n,g) (M)	8.30E+00	6.0 %	8.31E+00	1.00
Eu151(n,a)	8.90E-06	20.2 %	8.77E-06	0.99
Eu151(n,g)	9.17E+03	1.1 %	9.19E+03	1.00
Eu151(n,g)g	6.03E+03	2.2 %	6.25E+03	1.04
Eu151(n,g)m	3.12E+03	0.6 %	2.92E+03	0.94
Eu151(n,g)n	1.36E+01	70.5 %	2.67E+01	1.96
Eu152(n,g)	1.28E+04	4.7 %	1.26E+04	0.99
Eu152m(n,g)	1.84E+04	21.7 %	7.13E+04	3.88
Eu153(n,a)	<1.00E-06	-	9.99E-07	-
Eu153(n,g)	3.12E+02	2.2 %	2.99E+02	0.96
Eu154(n,g)	1.34E+03	9.7 %	1.35E+03	1.01
Eu155(n,g)	3.95E+03	3.2 %	3.94E+03	1.00
Gd148(n,g) (M)	1.40E+04	10.0 %	1.34E+04	0.96
Gd152(n,g) (M)	7.35E+02	2.7 %	7.32E+02	1.00
Gd152(n,a)	7.00E-03	-	6.89E-03	0.98
Gd153(n,a)	2.10E-02	-	3.69E-03	0.18
Gd153(n,g) (M)	2.23E+04	13.5 %	1.65E+04	0.74

Reaction	σ_E(b)	$\Delta\sigma_E$(b)	σ_{T14}(b)	C/E
Gd154(n,a)	6.00E-04	-	5.98E-04	1.00
Gd154(n,g)	8.50E+01	14.1 %	8.51E+01	1.00
Gd155(n,g)	6.09E+04	0.8 %	6.09E+04	1.00
Gd155(n,a)	8.20E-05	13.4 %	1.48E-05	0.18
Gd156(n,g) (M)	1.80E+00	38.9 %	1.78E+00	0.99
Gd157(n,a)	<5.00E-04	-	4.97E-05	-
Gd157(n,g)	2.54E+05	0.3 %	2.54E+05	1.00
Gd158(n,g)	2.20E+00	9.1 %	2.20E+00	1.00
Gd160(n,g) (M)	1.40E+00	21.4 %	1.41E+00	1.01
Gd161(n,g) (M)	1.90E+04	31.6 %	1.70E+04	0.89
Tb159(n,g)	2.34E+01	1.7 %	2.34E+01	1.00
Tb160(n,g) (M)	3.34E+02	19.2 %	3.43E+02	1.03
Dy156(n,g)	3.30E+01	9.1 %	3.33E+01	1.01
Dy156(n,a)	9.00E-03	-	8.91E-03	0.99
Dy158(n,g)	4.30E+01	14.0 %	4.35E+01	1.01
Dy158(n,a)	6.00E-03	-	5.97E-03	0.99
Dy159(n,g)	8.00E+03	25.0 %	6.82E+03	0.85
Dy160(n,g)	5.50E+01	5.5 %	5.54E+01	1.01
Dy160(n,a)	3.00E-04	-	2.99E-04	1.00
Dy161(n,a)	<3.00E-05	-	2.96E-05	-
Dy161(n,g)	6.00E+02	4.2 %	6.00E+02	1.00
Dy162(n,g)	1.94E+02	5.2 %	1.94E+02	1.00
Dy163(n,g)	1.34E+02	5.2 %	1.34E+02	1.00
Dy163(n,a)	<2.00E-05	-	1.99E-05	-
Dy164(n,g) (M)	2.65E+03	2.6 %	2.62E+03	0.99
Dy164(n,g)g	1.04E+03	13.5 %	7.87E+02	0.76
Dy164(n,g)m	1.61E+03	14.9 %	1.86E+03	1.16
Dy165(n,g) (M)	3.60E+03	8.3 %	3.53E+03	0.98
Dy165m(n,g) (M)	2.00E+03	30.0 %	1.97E+03	0.98
Ho165(n,g)	6.47E+01	1.9 %	6.49E+01	1.00
Ho165(n,g)g	6.12E+01	1.8 %	5.85E+01	0.96
Ho165(n,g)m	3.50E+00	11.4 %	6.36E+00	1.82
Ho165(n,a)	<2.00E-05	-	1.99E-05	-
Ho166m(n,g) (M)	3.60E+03	16.7 %	4.18E+03	1.16
Er162(n,a)	<1.10E-02	-	1.08E-02	-
Er162(n,g) (M)	1.90E+01	10.5 %	1.89E+01	1.00
Er164(n,a)	<1.20E-03	-	1.19E-03	-
Er164(n,g) (M)	1.30E+01	15.4 %	1.29E+01	1.00
Er166(n,g) (M)	1.69E+01	9.5 %	1.71E+01	1.01
Er166(n,g)g	4.50E+00	57.8 %	5.50E+00	1.22
Er166(n,g)m	1.24E+01	21.0 %	1.16E+01	0.94
Er166(n,a)	<7.00E-05	-	6.97E-05	-
Er167(n,g)	6.49E+02	1.2 %	6.49E+02	1.00
Er167(n,a)	7.00E-05	-	6.92E-05	0.99

Reaction	σ_E(b)	$\Delta\sigma_E$(b)	σ_{T14}(b)	C/E
Er168(n,g)	2.74E+00	2.9 %	2.76E+00	1.01
Er168(n,a)	<9.00E-05	-	8.98E-05	-
Er169(n,a)	1.00E-05	-	9.91E-06	0.99
Er170(n,g) (M)	8.85E+00	3.4 %	8.86E+00	1.00
Er171(n,g) (M)	2.80E+02	10.7 %	2.74E+02	0.98
Tm169(n,g)	1.05E+02	1.9 %	1.05E+02	1.00
Tm169(n,a)	<1.00E-05	-	9.95E-06	-
Tm170(n,g) (M)	9.20E+01	4.3 %	9.18E+01	1.00
Tm171(n,g) (M)	<1.90E+02	-	1.89E+02	-
Yb168(n,g)	2.30E+03	7.4 %	2.31E+03	1.00
Yb168(n,a)	<1.00E-04	-	9.81E-05	-
Yb169(n,g) (M)	3.60E+03	8.3 %	3.50E+03	0.97
Yb170(n,g)	9.90E+00	18.2 %	9.92E+00	1.00
Yb170(n,a)	<1.00E-05	-	9.89E-06	-
Yb171(n,g)	5.83E+01	6.5 %	5.83E+01	1.00
Yb171(n,a)	<1.50E-06	-	1.46E-06	-
Yb172(n,g)	1.30E+00	61.5 %	1.29E+00	1.00
Yb172(n,a)	<1.00E-06	-	9.95E-07	-
Yb173(n,g) (M)	1.55E+01	9.7 %	1.55E+01	1.00
Yb173(n,a)	<1.00E-06	-	9.86E-07	-
Yb174(n,g)	6.32E+01	2.4 %	1.20E+02	1.89
Yb174(n,a)	2.00E-05	-	1.99E-05	1.00
Yb176(n,a)	<1.00E-06	-	9.99E-07	-
Yb176(n,g)	2.85E+00	1.8 %	2.83E+00	0.99
Lu175(n,g)	2.33E+01	4.7 %	2.33E+01	1.00
Lu175(n,g)g	6.60E+00	4.5 %	4.10E+00	0.62
Lu175(n,g)m	1.67E+01	7.8 %	1.92E+01	1.15
Lu175(n,a)	<6.00E-05	-	5.95E-05	-
Lu176(n,a)	<2.00E-03	-	1.96E-03	-
Lu176(n,g)	2.06E+03	2.1 %	2.02E+03	0.98
Lu176(n,g)g	2.05E+03	-	2.01E+03	0.98
Lu176(n,g)m	6.75E+00	73.0 %	1.05E+01	1.55
Lu177(n,g)	1.20E+03	25.0 %	1.20E+03	1.00
Lu177m(n,g) (M)	3.18E+00	9.4 %	2.98E+00	0.94
Hf174(n,g)	6.48E+02	10.8 %	6.55E+02	1.01
Hf176(n,g)	1.68E+01	18.5 %	1.67E+01	1.00
Hf177(n,g)	3.75E+02	2.7 %	3.73E+02	1.00
Hf177(n,g)g	3.74E+02	-	3.72E+02	0.99
Hf177(n,g)m	9.60E-01	5.2 %	1.74E+00	1.81
Hf177(n,g)n	2.60E-06	-	1.58E-06	0.61
Hf177(n,a)	2.00E-05	-	1.91E-05	0.95
Hf178(n,g)	8.40E+01	4.8 %	8.40E+01	1.00
Hf178(n,g)g	3.10E+01	-	1.74E+01	0.56
Hf178(n,g)m	5.30E+01	11.3 %	6.66E+01	1.26

Reaction	σ_E(b)	$\Delta\sigma_E$(b)	σ_{T14}(b)	C/E
Hf178n(n,g)	4.40E+02	-	1.90E+03	4.32
Hf179(n,g)	4.10E+01	7.3 %	4.11E+01	1.00
Hf179(n,g)g	4.06E+01	-	4.05E+01	1.00
Hf179(n,g)m	4.45E-01	0.7 %	5.68E-01	1.28
Hf180(n,g)	1.30E+01	0.5 %	1.31E+01	1.01
Hf180(n,a)	<1.30E-05	-	1.29E-05	-
Hf181(n,g) (M)	4.00E+01	75.0 %	3.98E+01	1.00
Ta179(n,g) (M)	9.32E+02	6.7 %	8.95E+02	0.96
Ta180(n,g)	5.63E+02	10.7 %	5.56E+02	0.99
Ta180m(n,g)	5.63E+02	10.7 %	5.63E+02	1.00
Ta181(n,g)	2.08E+01	2.4 %	2.05E+01	0.99
Ta181(n,g)g	1.72E+01	22.7 %	1.31E+01	0.76
Ta181(n,g)m	3.59E+00	-	7.43E+00	2.07
Ta181(n,g)n	6.84E-03	90.1 %	9.78E-04	0.14
Ta181(n,a)	<1.00E-06	-	9.93E-07	-
Ta182(n,g)	8.20E+03	7.3 %	8.20E+03	1.00
W180(n,g) (M)	<1.50E+02	-	1.49E+02	-
W182(n,g)	1.99E+01	1.5 %	1.99E+01	1.00
W183(n,g)	1.04E+01	1.9 %	1.03E+01	0.99
W184(n,g)	1.70E+00	5.9 %	1.69E+00	1.00
W184(n,g)g	1.70E+00	-	1.69E+00	0.99
W184(n,g)m	2.00E-03	50.0 %	2.64E-03	1.32
W185(n,g) (M)	2.10E+00	14.3 %	2.09E+00	0.99
W186(n,g)	3.81E+01	1.3 %	3.79E+01	0.99
W187(n,g) (M)	6.40E+01	15.6 %	6.39E+01	1.00
W188(n,g)	1.20E+01	20.8 %	1.19E+01	1.00
Re184(n,g) (M)	9.90E+03	-	9.56E+03	0.97
Re185(n,g)	1.12E+02	1.8 %	1.12E+02	1.00
Re185(n,g)g	1.12E+02	-	1.12E+02	1.00
Re185(n,g)m	3.40E-01	29.4 %	2.03E-01	0.60
Re187(n,g)	7.64E+01	1.3 %	7.64E+01	1.00
Re187(n,g)g	7.44E+01	1.3 %	7.40E+01	0.99
Re187(n,g)m	2.05E+00	4.4 %	2.45E+00	1.20
Re188(n,g) (M)	2.00E+00	-	1.99E+00	0.99
Os184(n,a)	<1.00E-02	-	9.75E-03	-
Os184(n,g) (M)	3.00E+03	5.0 %	1.96E+03	0.65
Os186(n,g)	8.00E+01	16.2 %	7.97E+01	1.00
Os186(n,a)	1.00E-04	-	9.79E-05	0.98
Os187(n,g)	3.20E+02	3.1 %	3.21E+02	1.00
Os187(n,a)	<1.00E-04	-	9.59E-05	-
Os188(n,g)	5.50E+00	20.0 %	5.47E+00	1.00
Os188(n,a)	<3.00E-05	-	2.98E-05	-
Os189(n,g)	2.50E+01	16.0 %	2.49E+01	0.99
Os189(n,a)	1.00E-05	-	9.80E-06	0.98

Reaction	σ_E(b)	$\Delta\sigma_E$(b)	σ_{T14}(b)	C/E
Os190(n,g)	1.31E+01	2.3 %	1.30E+01	1.00
Os190(n,g)g	3.90E+00	2.6 %	1.39E+00	0.36
Os190(n,g)m	9.20E+00	7.6 %	1.16E+01	1.27
Os190(n,a)	2.00E-05	-	1.99E-05	1.00
Os191(n,g) (M)	3.83E+02	14.1 %	3.77E+02	0.98
Os192(n,g)	3.12E+00	5.1 %	3.12E+00	1.00
Os193(n,g) (M)	3.80E+01	26.3 %	3.82E+01	1.01
Ir191(n,g)	9.54E+02	1.0 %	9.55E+02	1.00
Ir191(n,g)g	3.09E+02	9.7 %	3.92E+02	1.27
Ir191(n,g)m	6.45E+02	5.0 %	5.62E+02	0.87
Ir191(n,g)n	3.10E-02	45.2 %	1.56E-03	0.05
Ir192(n,g)	1.59E+03	12.6 %	1.58E+03	1.00
Ir193(n,g)	1.11E+02	4.5 %	1.11E+02	1.00
Ir194(n,g)	1.57E+03	18.5 %	1.41E+03	0.90
Pt190(n,a)	<8.00E-03	-	7.75E-03	-
Pt190(n,g)	1.52E+02	2.6 %	1.54E+02	1.01
Pt192(n,g)	1.00E+01	25.0 %	9.96E+00	1.00
Pt192(n,g)g	7.80E+00	-	9.87E+00	1.26
Pt192(n,g)m	2.20E+00	36.4 %	9.57E-02	0.04
Pt192(n,a)	<2.00E-04	-	1.98E-04	-
Pt194(n,g)	1.44E+00	13.2 %	1.43E+00	1.00
Pt194(n,g)g	1.40E+00	-	1.43E+00	1.02
Pt194(n,g)m	3.60E-02	11.1 %	3.52E-03	0.10
Pt194(n,a)	<5.00E-06	-	4.99E-06	-
Pt195(n,g)	2.75E+01	4.4 %	2.75E+01	1.00
Pt195(n,a)	<5.00E-06	-	4.96E-06	-
Pt196(n,g)	5.80E-01	5.2 %	5.83E-01	1.01
Pt196(n,g)g	5.36E-01	-	5.75E-01	1.07
Pt196(n,g)m	4.40E-02	9.1 %	8.47E-03	0.19
Pt198(n,g)	3.61E+00	3.0 %	3.59E+00	0.99
Pt198(n,g)g	3.26E+00	-	3.59E+00	1.10
Pt198(n,g)m	3.50E-01	11.4 %	7.73E-05	0.00
Pt199(n,g) (M)	1.50E+01	133.3 %	1.49E+01	0.99
Au197(n,g)	9.87E+01	0.1 %	9.87E+01	1.00
Au197(n,g)g	9.86E+01	-	9.87E+01	1.00
Au197(n,g)m	8.00E-03	25.0 %	4.71E-04	0.06
Au198(n,g) (M)	2.51E+04	1.5 %	2.65E+04	1.06
Au199(n,g) (M)	3.00E+01	50.0 %	3.00E+01	1.00
Hg196(n,g) (M)	3.08E+03	5.8 %	3.05E+03	0.99
Hg196(n,g)g	2.97E+03	-	3.08E+03	1.04
Hg196(n,g)m	1.07E+02	1.4 %	6.58E+00	0.06
Hg198(n,g) (M)	2.00E+00	15.0 %	1.99E+00	1.00
Hg198(n,g)g	1.98E+00	-	1.99E+00	1.00
Hg198(n,g)m	1.80E-02	22.2 %	2.80E-03	0.16

Reaction	σ_E(b)	$\Delta\sigma_E$(b)	σ_{T14}(b)	C/E
Hg199(n,g)	2.15E+03	2.2 %	2.15E+03	1.00
Hg200(n,g) (M)	6.00E+01	-	2.99E+01	0.50
Hg201(n,g)	4.90E+00	12.2 %	4.85E+00	0.99
Hg202(n,g)	4.89E+00	1.0 %	4.93E+00	1.01
Hg204(n,g) (M)	4.30E-01	23.3 %	4.28E-01	1.00
Tl203(n,a)	<2.85E-02	-	2.85E-02	-
Tl203(n,g)	1.14E+01	1.8 %	1.15E+01	1.01
Tl204(n,g) (M)	2.16E+01	9.3 %	2.15E+01	1.00
Tl205(n,g) (M)	1.04E-01	16.3 %	1.04E-01	1.00
Pb204(n,g)	7.03E-01	5.0 %	6.61E-01	0.94
Pb205(n,g)	5.00E+00	-	4.98E+00	1.00
Pb206(n,g)	2.66E-02	4.9 %	2.98E-02	1.12
Pb207(n,g)	6.22E-01	2.3 %	6.42E-01	1.03
Pb208(n,g)	2.30E-04	8.7 %	2.32E-04	1.01
Pb208(n,a)	8.00E-06	-	7.98E-06	1.00
Pb210(n,g) (M)	5.00E-01	100.0 %	4.98E-01	1.00
Bi209(n,g)	3.42E-02	2.0 %	3.38E-02	0.99
Bi209(n,g)g	1.65E-02	4.2 %	2.74E-02	1.66
Bi209(n,g)m	1.77E-02	4.0 %	6.39E-03	0.36
Bi210m(n,g) (M)	5.40E-02	9.3 %	5.37E-02	1.00
Po210(n,a)	<2.00E-03	-	5.12E-04	-
Po210(n,g) (M)	<3.50E-02	-	1.49E-02	-
Po210(n,g)g (M)	<3.00E-02	-	1.49E-02	-
Po210(n,g)m (M)	<5.00E-04	-	1.72E-17	-
Rn220(n,g) (M)	2.00E-01	-	1.99E-01	1.00
Rn222(n,g) (M)	7.20E-01	9.7 %	7.18E-01	1.00
Fr220(n,g) (M)	2.00E-01	-	1.99E-01	0.99
Fr222(n,g) (M)	7.20E-01	9.7 %	6.83E-01	0.95
Ra223(n,g) (M)	1.30E+02	15.4 %	1.28E+02	0.99
Ra223(n,f)	7.00E-01	42.9 %	6.83E-01	0.98
Ra224(n,g) (M)	1.20E+01	4.2 %	1.19E+01	0.99
Ra226(n,f)	<5.00E-05	-	4.67E-05	-
Ra226(n,g)	1.28E+01	11.7 %	1.28E+01	1.00
Ra228(n,g) (M)	3.60E+01	13.9 %	3.61E+01	1.00
Ra228(n,f)	<2.00E+00	-	1.99E+00	-
Ac223(n,f)	3.30E-02	-	3.29E-02	1.00
Ac225(n,f)	3.30E-03	-	3.28E-03	0.99
Ac227(n,f)	<2.90E-04	-	2.20E-04	-
Ac227(n,g) (M)	8.90E+02	3.4 %	5.70E+02	0.64
Th224(n,f)	2.20E-01	-	2.19E-01	1.00
Th226(n,f)	1.00E-02	-	1.58E-02	1.58
Th227(n,f)	2.02E+02	6.4 %	1.59E+02	0.79
Th228(n,f)	<3.00E-01	-	3.39E-01	-
Th228(n,g) (M)	1.23E+02	12.2 %	1.23E+02	1.00

Reaction	σ_E(b)	$\Delta\sigma_E$(b)	σ_{T14}(b)	C/E
Th229(n,g) (M)	6.28E+01	9.6 %	6.53E+01	1.04
Th229(n,f)	3.08E+01	4.9 %	3.45E+01	1.12
Th230(n,f)	<1.20E-03	-	1.25E-03	-
Th230(n,g) (M)	2.29E+01	1.3 %	2.33E+01	1.02
Th232(n,g)	7.35E+00	0.4 %	7.35E+00	1.00
Th232(n,a)	<1.00E-03	-	9.70E-04	-
Th232(n,f)	5.20E-05	76.9 %	7.15E-04	13.75
Th233(n,f)	1.50E+01	13.3 %	1.86E+01	1.24
Th233(n,g) (M)	1.33E+03	3.8 %	2.16E+03	1.63
Th234(n,g) (M)	1.80E+00	27.8 %	1.79E+00	1.00
Th234(n,f)	<1.00E-02	-	9.95E-03	-
Pa225(n,f)	3.37E+01	-	1.62E+01	0.48
Pa227(n,f)	4.90E-01	-	4.35E+00	8.88
Pa229(n,f)	6.70E-02	-	6.75E-02	1.01
Pa230(n,f)	1.50E+03	16.7 %	4.66E+02	0.31
Pa231(n,f)	2.00E-02	5.0 %	1.99E-02	0.99
Pa231(n,g)	2.01E+02	1.1 %	2.00E+02	1.00
Pa232(n,f)	1.50E+03	1.9 %	1.51E+03	1.01
Pa232(n,g)	2.46E+02	12.2 %	2.46E+02	1.00
Pa233(n,g)	3.95E+01	3.0 %	3.93E+01	1.00
Pa233(n,g)g	1.94E+01	15.5 %	3.15E+01	1.62
Pa233(n,g)m	2.01E+01	15.9 %	7.83E+00	0.39
Pa233(n,f)	<1.00E-01	-	9.95E-02	-
Pa234(n,f)	<5.00E+03	-	6.77E+02	-
Pa234m(n,f)	<5.00E+02	-	2.61E+02	-
U230(n,f)	2.50E+01	40.0 %	2.49E+01	1.00
U231(n,f)	4.00E+02	75.0 %	2.46E+02	0.62
U232(n,f)	7.68E+01	6.2 %	1.28E+02	1.67
U232(n,g)	7.49E+01	2.1 %	7.59E+01	1.01
U233(n,g)	4.55E+01	1.5 %	4.52E+01	0.99
U233(n,a)	2.00E-04	-	1.82E-04	0.91
U233(n,f)	5.29E+02	0.2 %	5.31E+02	1.00
U234(n,f)	6.70E-02	20.9 %	6.71E-02	1.00
U234(n,g)	9.98E+01	1.3 %	1.01E+02	1.01
U235(n,g)	9.88E+01	0.8 %	9.87E+01	1.00
U235(n,f)	5.83E+02	0.2 %	5.85E+02	1.00
U236(n,g)	5.09E+00	2.0 %	5.30E+00	1.04
U236(n,f)	<1.30E-03	-	6.13E-02	-
U237(n,g) (M)	4.43E+02	37.7 %	3.52E+02	0.80
U237(n,f)	2.04E+00	82.8 %	3.74E+00	1.83
U238(n,f)	1.67E-05	82.0 %	1.68E-05	1.01
U238(n,g)	2.68E+00	0.7 %	2.68E+00	1.00
U239(n,f)	1.40E+01	21.4 %	1.40E+01	1.00
U239(n,g) (M)	2.20E+01	22.7 %	2.32E+01	1.06

Reaction	σ_E(b)	$\Delta\sigma_E$(b)	σ_{T14}(b)	C/E
Np231(n,f)	1.02E+02	-	8.05E+01	0.79
Np233(n,f)	5.60E+00	-	5.53E+00	0.99
Np234(n,f)	9.00E+02	33.3 %	6.10E+02	0.68
Np235(n,g) (M)	1.50E+02	1.3 %	1.40E+02	0.94
Np235(n,f)	5.10E-01	-	5.22E-01	1.02
Np236(n,g) (M)	1.42E+02	-	1.49E+02	1.05
Np237(n,f)	2.00E-02	5.0 %	2.00E-02	1.00
Np237(n,g) (M)	1.76E+02	1.6 %	1.75E+02	0.99
Np238(n,g) (M)	3.00E+02	-	2.98E+02	0.99
Np238(n,f)	2.09E+03	1.4 %	1.71E+03	0.82
Np239(n,f)	4.31E-01	140.8 %	4.32E-01	1.00
Np239(n,g)g	3.60E+01	22.2 %	5.18E+01	1.44
Np239(n,g)m	3.20E+01	18.8 %	1.60E+01	0.50
Np239(n,g) (M)	6.80E+01	14.7 %	6.48E+01	0.95
Pu234(n,f)	3.97E+02	-	1.27E+02	0.32
Pu236(n,f)	1.70E+02	-	1.77E+02	1.04
Pu236(n,g) (M)	1.59E+01	-	1.60E+01	1.00
Pu237(n,f)	2.46E+03	12.0 %	3.29E+03	1.34
Pu238(n,f)	1.79E+01	2.2 %	1.78E+01	0.99
Pu238(n,g)	5.40E+02	1.3 %	4.13E+02	0.77
Pu239(n,g)	2.69E+02	1.1 %	2.70E+02	1.00
Pu239(n,f)	7.48E+02	0.3 %	7.47E+02	1.00
Pu240(n,g)	2.90E+02	0.5 %	2.86E+02	0.99
Pu240(n,a)	3.00E-04	-	2.61E-04	0.87
Pu240(n,f)	5.60E-02	53.6 %	5.91E-02	1.06
Pu241(n,g)	3.62E+02	1.4 %	3.63E+02	1.00
Pu241(n,f)	1.01E+03	0.6 %	1.01E+03	1.00
Pu242(n,f)	1.80E-03	-	1.79E-03	0.99
Pu242(n,g)	1.85E+01	2.7 %	1.85E+01	1.00
Pu243(n,g) (M)	8.70E+01	11.5 %	8.63E+01	0.99
Pu243(n,f)	1.96E+02	8.2 %	2.17E+02	1.11
Pu244(n,g)	1.70E+00	5.9 %	1.71E+00	1.01
Pu244(n,f)	2.80E-03	-	1.71E-02	6.11
Pu245(n,g) (M)	1.50E+02	20.0 %	1.52E+02	1.01
Pu246(n,f)	8.50E-05	-	8.47E-05	1.00
Am237(n,f)	2.55E+02	-	6.79E+01	0.27
Am239(n,f)	2.90E+01	-	2.88E+01	0.99
Am241(n,f)	3.20E+00	2.8 %	3.17E+00	0.99
Am241(n,g)	5.87E+02	2.0 %	5.88E+02	1.00
Am241(n,g)g	5.33E+02	2.4 %	5.10E+02	0.96
Am241(n,g)m	5.40E+01	9.3 %	7.86E+01	1.45
Am242(n,g) (M)	3.30E+02	15.2 %	3.38E+02	1.02
Am242(n,f)	2.10E+03	9.5 %	2.10E+03	1.00
Am242m(n,f)	6.20E+03	3.2 %	5.59E+03	0.90

Reaction	σ_E(b)	$\Delta\sigma_E$(b)	σ_{T14}(b)	C/E
Am242m(n,g) (M)	1.29E+03	23.3 %	1.39E+03	1.07
Am243(n,f)	1.98E-01	2.2 %	1.96E-01	0.99
Am243(n,g)	7.51E+01	2.4 %	7.51E+01	1.00
Am243(n,g)g	2.01E+01	81.1 %	5.13E+01	2.55
Am243(n,g)m	5.50E+01	-	2.38E+01	0.43
Am244(n,f)	2.30E+03	13.0 %	2.75E+03	1.20
Am244m(n,f)	1.60E+03	18.8 %	1.42E+03	0.89
Am245(n,f)	1.40E-02	-	1.40E-02	1.00
Am247(n,f)	1.40E-03	-	1.40E-03	1.00
Cm240(n,f)	2.15E+03	-	8.76E+02	0.41
Cm241(n,f)	2.60E+03	-	2.92E+03	1.12
Cm242(n,g) (M)	1.60E+01	37.5 %	1.60E+01	1.00
Cm242(n,f)	<5.00E+00	-	6.41E+00	-
Cm243(n,f)	6.17E+02	3.2 %	6.20E+02	1.00
Cm243(n,g)	1.30E+02	7.7 %	1.30E+02	1.00
Cm244(n,g)	1.52E+01	7.9 %	1.52E+01	1.00
Cm244(n,f)	1.04E+00	19.2 %	1.03E+00	0.99
Cm245(n,f)	2.14E+03	2.7 %	2.16E+03	1.01
Cm245(n,g)	3.69E+02	4.6 %	3.70E+02	1.00
Cm246(n,f)	1.40E-01	35.7 %	1.50E-01	1.07
Cm246(n,g)	1.22E+00	13.1 %	1.23E+00	1.01
Cm247(n,g)	5.70E+01	17.5 %	5.72E+01	1.00
Cm247(n,f)	8.19E+01	5.4 %	8.57E+01	1.05
Cm248(n,g)	2.63E+00	9.9 %	2.63E+00	1.00
Cm248(n,f)	3.70E-01	13.5 %	3.85E-01	1.04
Cm249(n,g) (M)	1.60E+00	50.0 %	1.59E+00	0.99
Cm249(n,f)	2.50E+00	-	2.49E+00	1.00
Cm250(n,g) (M)	5.00E+01	-	4.98E+01	1.00
Cm250(n,f)	2.90E-03	-	2.89E-03	1.00
Bk243(n,f)	6.78E+02	-	1.74E+02	0.26
Bk245(n,f)	2.31E+02	-	2.14E+02	0.93
Bk247(n,f)	1.63E+01	-	1.71E+01	1.05
Bk249(n,f)	3.40E+00	0.8 %	4.17E+00	1.23
Bk249(n,g)	7.46E+02	5.4 %	7.46E+02	1.00
Bk250(n,g) (M)	3.50E+02	-	3.42E+02	0.98
Bk250(n,f)	9.60E+02	15.6 %	8.44E+02	0.88
Bk251(n,f)	5.20E-02	-	5.22E-02	1.00
Cf248(n,f)	7.30E+02	-	7.16E+02	0.98
Cf249(n,g) (M)	4.97E+02	4.2 %	4.83E+02	0.97
Cf249(n,f)	1.64E+03	2.0 %	1.65E+03	1.00
Cf250(n,g) (M)	2.03E+03	9.9 %	2.01E+03	0.99
Cf250(n,f)	1.10E+02	8.2 %	5.94E+01	0.54
Cf251(n,g) (M)	2.85E+03	5.3 %	3.11E+03	1.09
Cf251(n,f)	4.90E+03	5.1 %	4.88E+03	1.00

Reaction	σ_E(b)	$\Delta\sigma_E$(b)	σ_{T14}(b)	C/E
Cf252(n,f)	3.20E+01	12.5 %	3.19E+01	1.00
Cf252(n,g) (M)	2.04E+01	7.4 %	2.03E+01	1.00
Cf253(n,g) (M)	1.74E+01	10.3 %	1.85E+01	1.06
Cf253(n,f)	1.30E+03	18.5 %	8.73E+02	0.67
Cf254(n,g) (M)	4.50E+00	33.3 %	4.44E+00	0.99
Cf254(n,f)	2.00E+00	-	1.99E+00	1.00
Es251(n,f)	1.01E+02	-	1.00E+02	0.99
Es253(n,g) (M)	1.84E+02	8.2 %	1.87E+02	1.01
Es253(n,f)	8.70E+00	-	8.65E+00	0.99
Es254(n,g) (M)	2.83E+01	8.8 %	9.84E+01	3.48
Es254(n,f)	1.97E+03	15.2 %	1.35E+03	0.69
Es254m(n,g)	1.83E+03	4.4 %	7.82E+02	0.43
Es254m(n,f)	1.83E+03	4.4 %	1.76E+03	0.96
Es255(n,g) (M)	5.50E+01	18.2 %	6.10E+01	1.11
Es255(n,f)	1.50E+00	-	1.49E+00	1.00
Fm254(n,g) (M)	7.60E+01	-	5.05E+01	0.66
Fm254(n,f)	2.88E+03	-	2.02E+02	0.07
Fm255(n,f)	3.36E+03	5.1 %	1.66E+03	0.49
Fm255(n,g) (M)	2.60E+01	11.5 %	3.78E+01	1.45
Fm256(n,g) (M)	4.50E+01	-	4.55E+01	1.01
Fm257(n,f)	2.95E+03	5.4 %	7.46E+02	0.25

Integral resonance values

The data in Table 4 presents all of the integral resonance cross sections for reaction channels within the new UKAEA database. The experimental and TENDL-2014 cross sections are provided in barns, with C/E values in the last column. Note that all values which are given as inequalities have no C/E value or uncertainty and are not included in the statistical analysis of this dataset. The total absorption reaction channels are the sum of (n,γ), (n,p) and (n,α) channels.

Table 4: Summary of integral resonance cross section comparison.

Reaction	σ_E(b)	$\Delta\sigma_E$(b)	σ_{T14}(b)	C/E
H1(n,g)	1.49E-01	0.7 %	1.49E-01	1.00
H2(n,g)	2.30E-04	8.7 %	2.28E-04	0.99
He3(n,p)	2.40E+03	0.3 %	2.37E+03	0.99
Li6(n,abs)	4.25E+02	0.9 %	4.21E+02	0.99
Li6(n,g)	1.73E-02	8.1 %	1.73E-02	1.00

Reaction	σ_E(b)	$\Delta\sigma_E$(b)	σ_{T14}(b)	C/E
Li7(n,g)	2.20E-02	9.1 %	2.04E-02	0.93
Be7(n,p)	1.75E+04	2.9 %	1.75E+04	1.00
Be9(n,g)	3.80E-03	5.3 %	4.51E-03	1.19
B10(n,g)	1.30E-01	30.8 %	2.23E-01	1.72
B10(n,abs)	1.72E+03	0.0 %	1.72E+03	1.00
B11(n,g)	2.00E-03	5.0 %	2.74E-03	1.37
C12(n,g)	1.83E-03	27.3 %	1.76E-03	0.96
C13(n,g)	1.10E-03	18.2 %	6.14E-04	0.56
N14(n,g)	3.60E-02	2.8 %	3.36E-02	0.93
N14(n,p)	8.70E-01	3.4 %	8.19E-01	0.94
N15(n,g)	1.10E-04	27.3 %	3.21E-05	0.29
O16(n,g)	2.70E-04	11.1 %	1.59E-04	0.59
O17(n,abs)	1.10E-01	9.1 %	1.07E-01	0.98
O17(n,g)	3.90E-04	12.8 %	2.45E-04	0.63
O18(n,g)	8.10E-04	49.4 %	9.19E-04	1.13
F19(n,g)	2.00E-02	15.0 %	1.52E-02	0.76
Ne20(n,g)	1.77E-02	16.9 %	1.65E-02	0.93
Ne21(n,g)	2.96E-01	16.9 %	3.60E-01	1.21
Ne22(n,g)	2.20E-02	13.6 %	2.15E-02	0.98
Na22(n,p)	1.37E+05	8.8 %	1.25E+04	0.09
Na22(n,abs)	2.00E+05	25.0 %	3.12E+04	0.16
Na23(n,g)	3.11E-01	3.2 %	3.08E-01	0.99
Mg24(n,g)	3.70E-02	10.8 %	2.93E-02	0.79
Mg25(n,g)	1.95E-01	7.7 %	1.02E-01	0.52
Mg26(n,g)	2.40E-02	8.3 %	1.72E-02	0.72
Mg27(n,g)	3.00E-02	33.3 %	3.28E-02	1.09
Al27(n,g)	1.70E-01	5.9 %	1.27E-01	0.75
Si28(n,g)	8.00E-02	1.9 %	8.25E-02	1.03
Si29(n,g)	7.70E-02	19.5 %	7.51E-02	0.97
Si30(n,g)	6.30E-01	4.8 %	7.11E-02	0.11
Si31(n,g)	3.30E-02	9.1 %	3.83E-02	1.16
P31(n,g)	7.90E-02	2.5 %	7.64E-02	0.97
S32(n,g)	2.46E-01	4.1 %	2.42E-01	0.98
S33(n,g)	2.29E-01	6.6 %	2.22E-01	0.97
S34(n,g)	1.06E-01	47.2 %	1.05E-01	0.99
S36(n,g)	1.70E-01	23.5 %	1.06E-01	0.63
Cl35(n,p)	6.00E-01	-	2.26E-01	0.38
Cl35(n,g)	1.80E+01	11.1 %	1.82E+01	1.01
Cl36(n,p)	4.20E-02	-	7.04E-01	16.76
Cl36(n,g)	3.80E+00	-	4.71E+00	1.24
Cl37(n,g)	3.00E-01	13.3 %	2.07E-01	0.69
Cl37(n,g)g	2.60E-01	-	1.85E-01	0.71
Cl37(n,g)m	4.00E-02	-	2.15E-02	0.54
Ar36(n,g)	2.00E+00	50.0 %	2.47E+00	1.23

Reaction	σ_E(b)	$\Delta\sigma_E$(b)	σ_{T14}(b)	C/E
Ar40(n,g)	4.10E-01	7.3 %	2.95E-01	0.72
K39(n,g)	1.10E+00	9.1 %	9.84E-01	0.89
K40(n,p)	2.00E+00	10.0 %	2.17E+00	1.08
K40(n,g)	1.30E+01	30.8 %	1.32E+01	1.01
K41(n,g)	1.42E+00	4.2 %	9.13E-01	0.64
Ca40(n,g)	2.20E-01	9.1 %	2.07E-01	0.94
Ca42(n,g)	3.90E-01	10.3 %	3.62E-01	0.93
Ca43(n,g)	3.93E+00	3.8 %	4.24E+00	1.08
Ca44(n,g)	5.60E-01	1.8 %	4.21E-01	0.75
Ca46(n,g)	9.60E-01	10.4 %	8.13E-01	0.85
Ca48(n,g)	8.90E-01	20.2 %	9.62E-01	1.08
Sc45(n,g)	1.20E+01	4.2 %	1.18E+01	0.98
Sc45(n,g)g	6.40E+00	9.4 %	9.12E+00	1.43
Sc45(n,g)m	5.40E+00	11.1 %	2.66E+00	0.49
Ti46(n,g)	3.00E-01	30.0 %	3.52E-01	1.17
Ti47(n,g)	1.50E+00	13.3 %	1.52E+00	1.01
Ti48(n,g)	3.90E+00	5.1 %	3.77E+00	0.97
Ti49(n,g)	1.20E+00	16.7 %	9.52E-01	0.79
Ti50(n,g)	1.18E-01	9.3 %	8.92E-02	0.76
V50(n,g)	5.90E+01	25.4 %	6.07E+01	1.03
V51(n,g)	2.70E+00	3.7 %	2.58E+00	0.96
Cr50(n,g)	1.17E+01	1.7 %	7.21E+00	0.62
Cr52(n,g)	4.80E-01	4.2 %	4.91E-01	1.02
Cr53(n,g)	1.23E+01	24.4 %	8.68E+00	0.71
Cr54(n,g)	2.50E-01	16.0 %	1.99E-01	0.79
Mn53(n,g)	3.00E+01	16.7 %	3.63E+01	1.21
Mn54(n,g)	1.70E+01	-	2.11E+01	1.24
Mn55(n,g)	1.34E+01	3.7 %	1.35E+01	1.01
Fe54(n,g)	1.27E+00	7.9 %	1.18E+00	0.93
Fe55(n,g)	6.00E+00	16.7 %	6.82E+00	1.14
Fe56(n,g)	1.36E+00	11.0 %	1.33E+00	0.98
Fe57(n,g)	1.51E+00	9.9 %	1.59E+00	1.05
Fe58(n,g)	1.50E+00	4.7 %	1.35E+00	0.90
Fe59(n,g)	6.00E+00	16.7 %	5.91E+00	0.99
Co57(n,g)	2.00E+01	9.5 %	2.14E+01	1.07
Co58(n,g)	7.00E+03	14.3 %	6.67E+03	0.95
Co58m(n,g)	1.40E+05	7.1 %	4.06E+04	0.29
Co59(n,g)	7.40E+01	2.7 %	7.55E+01	1.02
Co59(n,g)g	3.50E+01	-	2.85E+01	0.81
Co59(n,g)m	3.90E+01	5.1 %	4.70E+01	1.20
Co60(n,g)	4.30E+00	20.9 %	4.46E+00	1.04
Co60m(n,g)	2.30E+02	21.7 %	1.95E+02	0.85
Ni58(n,g)	2.10E+00	1.0 %	1.98E+00	0.94
Ni59(n,abs)	1.38E+02	5.8 %	1.25E+02	0.91

Reaction	σ_E(b)	$\Delta\sigma_E$(b)	σ_{T14}(b)	C/E
Ni60(n,g)	1.40E+00	14.3 %	1.23E+00	0.88
Ni61(n,g)	2.10E+00	19.0 %	2.31E+00	1.10
Ni62(n,g)	6.80E+00	4.4 %	6.87E+00	1.01
Ni63(n,g)	9.00E+00	22.2 %	1.41E+01	1.57
Ni64(n,g)	1.07E+00	14.0 %	8.29E-01	0.77
Ni65(n,g)	1.00E+01	10.0 %	1.65E+02	16.55
Cu63(n,g)	4.97E+00	1.6 %	4.95E+00	1.00
Cu65(n,g)	2.19E+00	3.2 %	2.18E+00	0.99
Cu66(n,g)	6.00E+01	33.3 %	5.89E+01	0.98
Zn64(n,g)	1.37E+00	4.4 %	1.36E+00	0.99
Zn65(n,g)	3.00E+01	13.3 %	4.27E+01	1.42
Zn66(n,g)	1.10E+00	18.2 %	9.24E-01	0.84
Zn67(n,g)	2.40E+01	10.0 %	2.55E+01	1.06
Zn68(n,g)	3.50E+00	4.3 %	3.08E+00	0.88
Zn68(n,g)g	2.90E+00	-	2.74E+00	0.95
Zn68(n,g)m	2.06E-01	5.8 %	3.37E-01	1.63
Zn70(n,g)	8.60E-01	7.0 %	8.62E-01	1.00
Ga69(n,g)	1.56E+01	6.4 %	1.53E+01	0.98
Ga71(n,g)	3.11E+01	6.1 %	3.01E+01	0.97
Ge70(n,g)	2.22E+00	6.8 %	2.32E+00	1.04
Ge72(n,g)	7.20E-01	11.1 %	8.62E-01	1.20
Ge73(n,g)	6.30E+02	1.1 %	6.43E+01	0.10
Ge74(n,g)	1.00E+00	20.0 %	5.56E-01	0.56
Ge74(n,g)m	4.10E-01	17.1 %	1.38E-01	0.34
Ge76(n,g)	1.86E+00	12.9 %	1.36E+00	0.73
Ge76(n,g)g	6.60E-01	6.1 %	5.36E-01	0.81
Ge76(n,g)m	1.20E+00	16.7 %	8.25E-01	0.69
As75(n,g)	6.20E+01	3.2 %	6.27E+01	1.01
Se74(n,g)	5.76E+02	3.8 %	5.79E+02	1.00
Se76(n,g)	4.03E+01	-	3.42E+01	0.85
Se76(n,g)m	1.70E+01	11.8 %	8.72E+00	0.51
Se77(n,g)	3.00E+01	16.7 %	3.27E+01	1.09
Se78(n,g)	4.45E+00	10.1 %	4.65E+00	1.05
Se78(n,g)m	3.70E+00	16.2 %	2.69E+00	0.73
Se80(n,g)	2.00E+00	30.0 %	1.14E+00	0.57
Se80(n,g)g	9.94E-01	7.1 %	8.30E-01	0.83
Se80(n,g)m	1.47E-01	3.4 %	3.12E-01	2.12
Se82(n,g)	1.20E-01	16.7 %	1.03E-01	0.86
Br79(n,g)	1.27E+02	11.0 %	1.32E+02	1.04
Br79(n,g)g	9.50E+01	11.6 %	1.09E+02	1.15
Br79(n,g)m	3.20E+01	34.4 %	2.30E+01	0.72
Br81(n,g)	4.40E+01	11.4 %	4.62E+01	1.05
Kr78(n,g)	2.10E+01	14.3 %	2.31E+01	1.10
Kr80(n,g)	5.61E+01	10.0 %	5.95E+01	1.06

Reaction	σ_E(b)	$\Delta\sigma_E$(b)	σ_{T14}(b)	C/E
Kr82(n,g)	1.56E+02	12.8 %	8.63E+01	0.55
Kr83(n,g)	1.57E+02	15.9 %	1.67E+02	1.07
Kr84(n,g)	2.43E+00	8.2 %	2.15E+00	0.89
Kr85(n,g)	1.80E+00	55.6 %	1.58E+00	0.88
Kr86(n,g)	1.00E-03	-	1.35E-02	13.49
Rb85(n,g)	6.83E+00	3.2 %	7.53E+00	1.10
Rb86(n,g)	1.80E+01	16.7 %	2.70E+01	1.50
Rb87(n,g)	2.38E+00	5.0 %	2.36E+00	0.99
Rb88(n,g)	5.00E-01	20.0 %	1.30E+00	2.61
Sr84(n,g)	9.76E+00	11.3 %	1.04E+01	1.07
Sr84(n,g)g	7.40E-01	27.0 %	2.42E+00	3.27
Sr84(n,g)m	8.57E+00	4.9 %	7.99E+00	0.93
Sr86(n,g)m	4.80E+00	5.0 %	4.67E+00	0.97
Sr87(n,g)	1.17E+02	25.6 %	1.18E+02	1.01
Sr88(n,g)	6.50E-02	46.2 %	2.37E-02	0.37
Sr90(n,g)	1.04E-01	15.4 %	5.98E-02	0.58
Y89(n,g)	9.60E-01	6.2 %	8.44E-01	0.88
Zr90(n,g)	1.70E-01	11.8 %	1.31E-01	0.77
Zr91(n,g)	5.76E+00	6.9 %	6.05E+00	1.05
Zr92(n,g)	6.40E-01	31.2 %	6.40E-01	1.00
Zr93(n,g)	1.75E+01	28.6 %	1.97E+01	1.12
Zr94(n,g)	2.80E-01	3.6 %	2.73E-01	0.98
Zr96(n,g)	5.28E+00	2.1 %	5.13E+00	0.97
Nb93(n,g)	8.30E+00	4.8 %	9.23E+00	1.11
Nb94(n,g)	1.25E+02	6.4 %	1.30E+02	1.04
Nb95(n,g)	2.00E+02	-	1.69E+02	0.85
Mo92(n,g)	8.30E-01	-	8.43E-01	1.02
Mo94(n,g)	1.12E+00	-	1.32E+00	1.18
Mo95(n,g)	1.18E+02	5.9 %	1.18E+02	1.00
Mo96(n,g)	1.70E+01	17.6 %	1.78E+01	1.05
Mo97(n,g)	1.43E+01	21.0 %	1.69E+01	1.18
Mo98(n,g)	6.70E+00	4.5 %	6.82E+00	1.02
Mo100(n,g)	3.76E+00	4.0 %	3.91E+00	1.04
Tc99(n,g)	3.58E+02	5.6 %	3.44E+02	0.96
Ru96(n,g)	6.36E+00	3.6 %	7.34E+00	1.15
Ru99(n,g)	1.62E+02	12.3 %	1.70E+02	1.05
Ru100(n,g)	1.12E+01	9.8 %	1.22E+01	1.09
Ru101(n,g)	1.02E+02	9.8 %	1.12E+02	1.10
Ru102(n,g)	4.90E+00	6.1 %	5.73E+00	1.17
Ru103(n,g)	5.00E+00	-	4.73E+01	9.47
Ru104(n,g)	6.30E+00	3.2 %	6.77E+00	1.07
Ru106(n,g)	2.00E+00	30.0 %	3.22E+00	1.61
Rh103(n,g)	1.01E+03	5.0 %	9.70E+02	0.96
Rh103(n,g)m	7.50E+01	6.7 %	3.41E+01	0.45

Reaction	σ_E(b)	$\Delta\sigma_E$(b)	σ_{T14}(b)	C/E
Rh105(n,g)	1.70E+04	17.6 %	1.76E+04	1.04
Pd102(n,g)	1.20E+01	16.7 %	1.29E+01	1.08
Pd104(n,g)	1.90E+01	10.5 %	2.06E+01	1.08
Pd105(n,g)	9.00E+01	22.2 %	9.71E+01	1.08
Pd106(n,g)	6.65E+00	3.0 %	8.23E+00	1.24
Pd106(n,g)g	5.50E+00	-	8.21E+00	1.49
Pd106(n,g)m	2.00E-01	-	2.54E-02	0.13
Pd107(n,g)	1.05E+02	3.8 %	1.14E+02	1.09
Pd108(n,g)	2.44E+02	1.6 %	2.31E+02	0.95
Pd108(n,g)g	2.40E+02	-	2.30E+02	0.96
Pd108(n,g)m	2.00E+00	-	1.86E+00	0.93
Pd110(n,g)	3.10E+00	-	2.82E+00	0.91
Pd110(n,g)g	2.30E+00	13.0 %	2.81E+00	1.22
Pd110(n,g)m	6.60E-01	10.6 %	8.99E-03	0.01
Ag107(n,g)	1.07E+02	4.7 %	9.85E+01	0.92
Ag107(n,g)g	1.05E+02	-	9.73E+01	0.93
Ag107(n,g)m	1.20E+00	16.7 %	1.21E+00	1.01
Ag109(n,g)	1.47E+03	3.3 %	1.47E+03	1.00
Ag109(n,g)g	1.41E+03	-	1.40E+03	0.99
Ag109(n,g)m	6.51E+01	4.5 %	6.81E+01	1.05
Ag110m(n,g)	2.00E+01	20.0 %	8.21E+01	4.11
Ag111(n,g)	1.05E+02	19.0 %	1.16E+02	1.10
Cd106(n,g)	4.10E+00	24.4 %	7.02E+00	1.71
Cd108(n,g)	1.07E+01	28.0 %	1.36E+01	1.27
Cd109(n,g)	6.70E+03	17.9 %	5.22E+03	0.78
Cd110(n,g)	3.94E+01	-	3.92E+01	1.00
Cd110(n,g)g	3.40E+01	-	3.83E+01	1.13
Cd110(n,g)m	3.90E+00	2.6 %	9.24E-01	0.24
Cd111(n,g)	4.17E+01	7.2 %	5.24E+01	1.26
Cd112(n,g)	1.25E+01	8.0 %	1.30E+01	1.04
Cd113(n,g)	3.90E+02	10.3 %	3.94E+02	1.01
Cd114(n,g)	1.26E+01	7.9 %	1.30E+01	1.03
Cd116(n,g)	1.50E+00	13.3 %	1.70E+00	1.13
In113(n,g)	3.20E+02	9.4 %	3.33E+02	1.04
In113(n,g)m	2.20E+02	13.6 %	2.62E+02	1.19
In115(n,g)	3.30E+03	3.0 %	3.22E+03	0.98
In115(n,g)g	6.50E+02	4.6 %	2.85E+01	0.04
In115(n,g)m	2.65E+03	3.8 %	1.23E+04	4.64
In115(n,g)n	1.50E+03	-	4.93E+02	0.33
Sn112(n,g)	2.90E+01	6.9 %	2.87E+01	0.99
Sn112(n,g)g	1.90E+01	-	1.74E+01	0.92
Sn112(n,g)m	8.00E+00	-	1.12E+01	1.41
Sn113(n,g)	2.17E+02	2.3 %	2.46E+02	1.13
Sn114(n,g)	6.30E+00	23.8 %	6.75E+00	1.07

Reaction	σ_E(b)	$\Delta\sigma_E$(b)	σ_{T14}(b)	C/E
Sn115(n,g)	2.39E+01	25.1 %	1.96E+01	0.82
Sn116(n,g)	1.19E+01	8.4 %	1.22E+01	1.02
Sn116(n,g)m	4.90E-01	32.7 %	1.14E-01	0.23
Sn117(n,g)	1.57E+01	15.9 %	1.81E+01	1.16
Sn118(n,g)	3.40E+00	11.8 %	3.49E+00	1.03
Sn119(n,g)	2.90E+00	17.2 %	4.37E+00	1.51
Sn120(n,g)	1.14E+00	26.3 %	1.06E+00	0.93
Sn122(n,g)	8.10E-01	4.9 %	6.42E-01	0.79
Sn124(n,g)	8.04E+00	5.0 %	8.15E+00	1.01
Sn124(n,g)g	8.30E-02	30.1 %	3.56E-01	4.29
Sn124(n,g)m	7.80E+00	2.6 %	7.80E+00	1.00
Sb121(n,g)	2.02E+02	9.9 %	2.06E+02	1.02
Sb121(n,g)m	1.30E+01	7.7 %	3.74E-01	0.03
Sb123(n,g)	1.26E+02	15.9 %	1.27E+02	1.01
Te120(n,g)	1.00E+00	-	7.25E+00	7.25
Te122(n,g)	2.80E+01	35.7 %	8.92E+01	3.19
Te123(n,g)	5.63E+03	5.8 %	5.64E+03	1.00
Te124(n,g)	5.30E+00	13.2 %	5.15E+00	0.97
Te125(n,g)	2.07E+01	14.5 %	2.28E+01	1.10
Te126(n,g)	8.00E+00	7.5 %	7.53E+00	0.94
Te126(n,g)g	7.40E+00	-	7.20E+00	0.97
Te126(n,g)m	6.00E-01	-	3.30E-01	0.55
Te127(n,g)	1.14E+03	14.9 %	1.99E+02	0.17
Te128(n,g)	1.24E+00	-	1.22E+00	0.99
Te128(n,g)g	1.58E+00	3.8 %	1.20E+00	0.76
Te128(n,g)m	7.75E-02	6.5 %	2.50E-02	0.32
Te130(n,g)	4.00E-01	12.5 %	2.41E-01	0.60
I125(n,g)	1.37E+04	14.6 %	1.17E+04	0.85
I126(n,g)	4.06E+04	-	2.64E+04	0.65
I127(n,g)	1.55E+02	4.5 %	1.61E+02	1.04
I129(n,g)	3.38E+01	4.1 %	3.37E+01	1.00
I129(n,g)g	1.56E+01	4.5 %	1.89E+01	1.21
I129(n,g)m	1.82E+01	4.4 %	1.48E+01	0.81
I131(n,g)	8.00E+00	5.0 %	9.60E+01	12.00
Xe124(n,g)	3.60E+03	19.4 %	3.18E+03	0.88
Xe124(n,g)g	3.00E+03	-	2.80E+03	0.93
Xe124(n,g)m	6.00E+02	16.7 %	3.78E+02	0.63
Xe126(n,g)	6.10E+01	9.8 %	6.62E+01	1.09
Xe126(n,g)g	5.20E+01	-	6.20E+01	1.19
Xe126(n,g)m	8.00E+00	25.0 %	4.23E+00	0.53
Xe128(n,g)	1.14E+01	-	1.21E+01	1.06
Xe129(n,g)	2.52E+02	6.0 %	2.55E+02	1.01
Xe130(n,g)	4.80E+00	-	4.55E+00	0.95
Xe131(n,g)	8.90E+02	5.6 %	8.78E+02	0.99

Reaction	σ_E(b)	$\Delta\sigma_E$(b)	σ_{T14}(b)	C/E
Xe132(n,g)	5.00E+00	12.0 %	4.38E+00	0.88
Xe132(n,g)m	9.00E-01	22.2 %	3.39E-02	0.04
Xe134(n,g)	3.80E-01	10.5 %	2.05E-01	0.54
Xe135(n,g)	7.60E+03	6.6 %	7.89E+03	1.04
Xe136(n,g)	7.40E-01	28.4 %	7.09E-01	0.96
Cs133(n,g)	4.37E+02	5.9 %	4.08E+02	0.93
Cs133(n,g)m	2.90E+01	3.8 %	2.69E+00	0.09
Cs134(n,g)	7.60E+01	-	9.99E+01	1.31
Cs135(n,g)	3.79E+01	7.1 %	5.36E+01	1.41
Cs137(n,g)	3.60E-01	19.4 %	2.75E-01	0.76
Ba130(n,g)	1.76E+02	4.0 %	1.74E+02	0.99
Ba130(n,g)g	2.30E+01	4.3 %	1.69E+02	7.34
Ba130(n,g)m	1.53E+02	4.6 %	5.00E+00	0.03
Ba132(n,g)	3.50E+01	-	5.63E+01	1.61
Ba132(n,g)m	2.80E+00	-	1.30E+00	0.46
Ba133(n,g)	1.10E+02	27.3 %	9.92E+01	0.90
Ba134(n,g)	2.10E+01	14.3 %	2.16E+01	1.03
Ba134(n,g)m	2.39E+01	15.9 %	7.82E-01	0.03
Ba135(n,g)	9.70E+01	7.2 %	9.93E+01	1.02
Ba135(n,g)m	4.65E-01	15.1 %	1.78E-01	0.38
Ba136(n,g)	1.70E+00	17.6 %	1.70E+00	1.00
Ba136(n,g)g	1.50E+00	-	1.65E+00	1.10
Ba136(n,g)m	1.00E-01	-	4.89E-02	0.49
Ba137(n,g)	4.30E+00	23.3 %	3.55E+00	0.83
Ba138(n,g)	2.80E-01	14.3 %	2.62E-01	0.94
Ba139(n,g)	2.20E+00	22.7 %	8.96E+00	4.07
Ba140(n,g)	1.36E+01	10.3 %	2.02E+01	1.49
La138(n,g)	4.09E+02	22.0 %	3.74E+02	0.91
La139(n,g)	1.21E+01	0.5 %	1.22E+01	1.01
La140(n,g)	6.90E+01	5.8 %	7.38E+01	1.07
Ce136(n,g)	7.70E+01	15.6 %	7.65E+01	0.99
Ce138(n,g)	6.70E+00	50.7 %	7.33E+00	1.09
Ce138(n,g)g	5.20E+00	-	7.21E+00	1.39
Ce138(n,g)m	1.50E+00	-	1.19E-01	0.08
Ce140(n,g)	5.40E-01	9.3 %	2.75E-01	0.51
Ce141(n,g)	1.51E+02	1.3 %	1.54E+02	1.02
Ce142(n,g)	1.15E+00	4.3 %	7.84E-01	0.68
Ce143(n,g)	2.70E+00	11.1 %	5.23E+00	1.94
Ce144(n,g)	2.60E+00	11.5 %	2.26E+00	0.87
Pr141(n,g)	1.74E+01	24.1 %	1.75E+01	1.01
Pr142(n,g)	9.00E+00	11.1 %	1.55E+01	1.72
Pr143(n,g)	1.90E+02	13.2 %	1.54E+02	0.81
Nd142(n,g)	3.40E+01	32.4 %	6.13E+00	0.18
Nd143(n,g)	1.29E+02	23.3 %	1.30E+02	1.01

Reaction	σ_E(b)	$\Delta\sigma_E$(b)	σ_{T14}(b)	C/E
Nd144(n,g)	4.20E+00	11.9 %	4.38E+00	1.04
Nd145(n,g)	2.30E+02	15.2 %	2.33E+02	1.01
Nd146(n,g)	2.57E+00	5.4 %	3.01E+00	1.17
Nd147(n,g)	4.30E+02	-	5.10E+02	1.19
Nd148(n,g)	1.55E+01	9.7 %	1.61E+01	1.04
Nd150(n,g)	1.52E+01	5.3 %	1.69E+01	1.11
Pm147(n,g)	2.06E+03	4.9 %	2.12E+03	1.03
Pm147(n,g)g	1.28E+03	5.2 %	1.42E+03	1.11
Pm147(n,g)m	7.90E+02	12.7 %	6.97E+02	0.88
Pm148(n,g)	2.60E+03	92.3 %	1.43E+03	0.55
Pm148m(n,g)	3.60E+03	66.7 %	2.09E+03	0.58
Sm144(n,g)	2.38E+00	7.1 %	1.90E+00	0.80
Sm145(n,g)	6.00E+02	15.0 %	2.89E+03	4.81
Sm147(n,g)	7.77E+02	3.9 %	7.79E+02	1.00
Sm148(n,g)	2.70E+01	51.9 %	3.83E+01	1.42
Sm149(n,g)	3.39E+03	14.7 %	3.47E+03	1.02
Sm150(n,g)	3.58E+02	14.0 %	3.33E+02	0.93
Sm151(n,g)	3.77E+03	4.2 %	3.49E+03	0.93
Sm152(n,g)	2.97E+03	3.4 %	2.98E+03	1.00
Sm154(n,g)	3.60E+01	11.1 %	3.60E+01	1.00
Eu151(n,g)	3.30E+03	9.1 %	3.25E+03	0.98
Eu151(n,g)g	1.51E+03	21.9 %	2.21E+03	1.46
Eu151(n,g)m	1.79E+03	-	1.03E+03	0.58
Eu152(n,g)	1.58E+03	12.7 %	2.85E+03	1.81
Eu152m(n,g)	1.00E+05	-	4.57E+04	0.46
Eu153(n,g)	1.42E+03	7.0 %	1.23E+03	0.87
Eu154(n,g)	8.02E+02	24.9 %	1.88E+03	2.35
Eu155(n,g)	2.32E+04	1.3 %	2.34E+04	1.01
Gd152(n,g)	2.02E+03	7.9 %	1.03E+03	0.51
Gd154(n,g)	2.45E+02	12.2 %	2.16E+02	0.88
Gd155(n,g)	1.54E+03	6.5 %	1.51E+03	0.98
Gd156(n,g)	1.04E+02	14.4 %	1.06E+02	1.02
Gd157(n,g)	7.54E+02	2.7 %	8.48E+02	1.12
Gd158(n,g)	7.70E+01	9.1 %	6.81E+01	0.88
Gd160(n,g)	7.40E+00	13.5 %	7.98E+00	1.08
Tb159(n,g)	4.18E+02	4.8 %	4.04E+02	0.97
Dy156(n,g)	8.70E+02	9.2 %	1.02E+03	1.17
Dy158(n,g)	1.20E+02	16.7 %	2.06E+02	1.72
Dy160(n,g)	1.12E+03	8.0 %	1.11E+03	0.99
Dy161(n,g)	1.08E+03	7.4 %	1.08E+03	1.00
Dy162(n,g)	2.74E+03	9.9 %	2.75E+03	1.00
Dy163(n,g)	1.47E+03	6.8 %	1.49E+03	1.02
Dy164(n,g)	3.41E+02	5.9 %	3.42E+02	1.00
Dy165(n,g)	2.20E+04	13.6 %	1.20E+04	0.54

Reaction	σ_E(b)	$\Delta\sigma_E$(b)	σ_{T14}(b)	C/E
Ho165(n,g)	6.65E+02	3.0 %	6.89E+02	1.04
Ho165(n,g)g	6.50E+02	3.4 %	6.21E+02	0.96
Ho166m(n,g)	1.00E+04	27.0 %	1.18E+03	0.12
Er162(n,g)	4.80E+02	10.4 %	5.09E+02	1.06
Er164(n,g)	1.05E+02	9.5 %	1.50E+02	1.43
Er166(n,g)	9.50E+01	7.4 %	9.70E+01	1.02
Er167(n,g)	2.97E+03	2.4 %	2.98E+03	1.00
Er168(n,g)	3.70E+01	13.5 %	3.76E+01	1.02
Er170(n,g)	3.54E+01	16.7 %	4.16E+01	1.18
Er171(n,g)	1.70E+02	11.8 %	1.42E+03	8.35
Tm169(n,g)	1.66E+03	3.0 %	1.63E+03	0.98
Tm170(n,g)	4.60E+02	10.9 %	1.66E+03	3.60
Tm171(n,g)	4.60E+02	10.9 %	9.73E+02	2.12
Yb168(n,g)	2.13E+04	4.7 %	2.15E+04	1.01
Yb169(n,g)	5.20E+03	9.6 %	2.45E+03	0.47
Yb170(n,g)	3.10E+02	9.7 %	3.11E+02	1.00
Yb171(n,g)	3.18E+02	9.4 %	3.23E+02	1.01
Yb172(n,g)	2.50E+01	12.0 %	2.71E+01	1.09
Yb173(n,g)	3.80E+02	7.9 %	3.86E+02	1.01
Yb174(n,g)	6.00E+01	16.7 %	4.44E+01	0.74
Yb176(n,g)	6.90E+00	8.7 %	6.48E+00	0.94
Lu175(n,g)	6.20E+02	8.1 %	6.16E+02	0.99
Lu175(n,g)m	5.50E+02	5.5 %	5.07E+02	0.92
Lu176(n,g)	1.10E+03	-	9.81E+02	0.89
Lu176(n,g)g	1.87E+03	2.1 %	9.76E+02	0.52
Lu176(n,g)m	4.70E+00	29.8 %	5.08E+00	1.08
Lu177m(n,g)	1.40E+00	14.3 %	1.43E+01	10.20
Hf174(n,g)	3.07E+02	4.9 %	4.81E+02	1.57
Hf176(n,g)	7.08E+02	2.1 %	5.26E+02	0.74
Hf177(n,g)	7.20E+03	2.8 %	7.21E+03	1.00
Hf178(n,g)	1.88E+03	1.1 %	1.87E+03	0.99
Hf178(n,g)g	8.50E+02	-	3.89E+02	0.46
Hf178(n,g)m	1.00E+03	-	1.48E+03	1.48
Hf179(n,g)	6.30E+02	4.8 %	5.57E+02	0.88
Hf179(n,g)g	6.20E+02	4.8 %	5.49E+02	0.89
Hf179(n,g)m	6.90E+00	87.0 %	7.72E+00	1.12
Hf180(n,g)	3.30E+01	3.0 %	3.67E+01	1.11
Ta180(n,g)	1.35E+03	7.4 %	6.70E+03	4.96
Ta181(n,g)	6.55E+02	3.1 %	6.60E+02	1.01
Ta181(n,g)g	6.50E+02	-	4.21E+02	0.65
Ta181(n,g)n	4.15E-01	26.5 %	3.24E-02	0.08
Ta182(n,g)	9.43E+02	5.3 %	1.13E+03	1.20
W180(n,g)	2.14E+02	14.0 %	6.36E+02	2.97
W182(n,g)	6.00E+02	10.0 %	6.02E+02	1.00

Reaction	σ_E(b)	$\Delta\sigma_E$(b)	σ_{T14}(b)	C/E
W183(n,g)	3.55E+02	8.5 %	3.63E+02	1.02
W184(n,g)	1.47E+01	10.2 %	1.66E+01	1.13
W185(n,g)	1.16E+02	43.1 %	1.37E+02	1.18
W186(n,g)	4.80E+02	3.1 %	4.77E+02	0.99
W187(n,g)	2.76E+03	19.9 %	1.53E+03	0.55
Re185(n,g)	1.73E+03	2.9 %	1.73E+03	1.00
Re187(n,g)	3.00E+02	6.7 %	3.03E+02	1.01
Os184(n,g)	6.01E+02	8.5 %	6.77E+02	1.13
Os186(n,g)	2.54E+02	11.8 %	8.06E+00	0.03
Os187(n,g)	5.07E+02	13.8 %	5.68E+02	1.12
Os188(n,g)	1.52E+02	13.2 %	1.54E+02	1.01
Os189(n,g)	6.60E+02	6.1 %	7.76E+02	1.18
Os190(n,g)	2.10E+01	-	3.01E+01	1.43
Os190(n,g)m	2.20E+01	7.7 %	2.68E+01	1.22
Os191(n,g)	1.70E+02	17.6 %	5.84E+02	3.43
Os192(n,g)	7.00E+00	57.1 %	1.08E+01	1.54
Ir191(n,g)	3.55E+03	2.8 %	3.32E+03	0.94
Ir192(n,g)	3.41E+03	-	3.69E+03	1.08
Ir193(n,g)	1.35E+03	7.4 %	1.35E+03	1.00
Ir194(n,g)	7.00E+02	28.6 %	8.19E+02	1.17
Pt190(n,g)	7.20E+01	13.9 %	1.30E+02	1.80
Pt192(n,g)	1.18E+02	25.4 %	1.87E+01	0.16
Pt194(n,g)	4.00E+00	25.0 %	6.59E+00	1.65
Pt194(n,g)m	1.00E+00	10.0 %	2.37E-02	0.02
Pt195(n,g)	3.67E+02	6.8 %	3.74E+02	1.02
Pt196(n,g)	7.10E+00	4.2 %	5.88E+00	0.83
Pt196(n,g)m	3.50E-01	20.0 %	9.78E-02	0.28
Pt198(n,g)	6.20E+01	3.2 %	4.84E+01	0.78
Pt198(n,g)m	6.00E+00	11.7 %	1.37E-03	0.00
Pt199(n,g)	7.00E+00	-	4.64E+01	6.63
Au197(n,g)	1.56E+03	1.8 %	1.57E+03	1.01
Au197(n,g)m	6.00E-02	33.3 %	7.55E-03	0.13
Au198(n,g)	4.00E+04	-	4.98E+04	1.25
Hg196(n,g)	4.63E+02	-	4.43E+02	0.96
Hg196(n,g)g	4.13E+02	3.6 %	4.42E+02	1.07
Hg196(n,g)m	5.89E+01	4.1 %	9.54E-01	0.02
Hg198(n,g)	7.20E+01	2.8 %	6.27E+01	0.87
Hg198(n,g)g	7.00E+01	-	6.26E+01	0.89
Hg198(n,g)m	1.80E+00	16.7 %	9.18E-02	0.05
Hg199(n,g)	4.34E+02	4.6 %	4.39E+02	1.01
Hg200(n,g)	1.50E+00	33.3 %	4.28E+01	28.53
Hg201(n,g)	3.00E+01	10.0 %	3.47E+01	1.16
Hg202(n,g)	2.90E+00	6.9 %	2.76E+00	0.95
Hg204(n,g)	8.50E-01	23.5 %	8.52E-01	1.00

Reaction	σ_E(b)	$\Delta\sigma_E$(b)	σ_{T14}(b)	C/E
Tl203(n,g)	3.96E+01	5.1 %	3.93E+01	0.99
Tl204(n,g)	9.40E+01	0.2 %	1.05E+02	1.12
Tl205(n,g)	6.60E-01	15.2 %	8.28E-01	1.25
Pb204(n,g)	2.23E+00	9.0 %	2.04E+00	0.91
Pb205(n,g)	2.00E+00	-	7.90E+00	3.95
Pb206(n,g)	2.23E-01	62.8 %	9.12E-02	0.41
Pb207(n,g)	3.20E-01	6.2 %	3.45E-01	1.08
Pb208(n,g)	1.10E-03	18.2 %	9.70E-04	0.88
Bi209(n,g)	1.40E-01	14.3 %	1.92E-01	1.37
Bi210m(n,g)	2.00E-01	15.0 %	1.04E-01	0.52
Ra226(n,g)	2.80E+02	17.9 %	2.83E+02	1.01
Ac227(n,g)	1.66E+03	4.8 %	4.89E+02	0.29
Th228(n,g)	1.01E+03	39.6 %	1.05E+03	1.04
Th229(n,f)	4.05E+02	18.5 %	5.48E+02	1.35
Th229(n,g)	9.70E+02	18.0 %	1.21E+03	1.25
Th230(n,g)	9.93E+02	3.0 %	9.73E+02	0.98
Th231(n,f)	1.56E+02	-	4.99E+02	3.20
Th232(n,g)	8.33E+01	1.8 %	8.52E+01	1.02
Th232(n,f)	7.46E-02	2.1 %	8.34E-03	0.11
Th233(n,g)	1.70E+03	54.7 %	1.23E+03	0.72
Th233(n,f)	8.40E+01	-	2.12E+02	2.53
Pa231(n,g)	5.25E+02	11.4 %	5.37E+02	1.02
Pa231(n,f)	5.00E-02	20.0 %	9.57E-02	1.91
Pa232(n,g)	1.17E+02	25.6 %	1.22E+02	1.05
Pa232(n,f)	1.08E+03	2.0 %	7.78E+02	0.72
Pa233(n,g)	8.60E+02	4.1 %	8.83E+02	1.03
Pa233(n,g)g	4.32E+02	16.2 %	7.07E+02	1.64
Pa233(n,g)m	4.38E+02	16.0 %	1.75E+02	0.40
Pa233(n,g)g	4.32E+02	16.2 %	7.07E+02	1.64
Pa233(n,g)m	4.38E+02	16.0 %	1.75E+02	0.40
Pa233(n,f)	3.00E+00	-	1.88E+00	0.63
U232(n,f)	3.50E+02	8.6 %	3.59E+02	1.02
U232(n,g)	2.80E+02	5.4 %	1.83E+02	0.65
U233(n,g)	1.38E+02	4.3 %	1.41E+02	1.02
U233(n,abs)	8.97E+02	2.2 %	1.41E+02	0.16
U233(n,f)	7.75E+02	2.2 %	7.65E+02	0.99
U234(n,f)	5.60E-01	-	7.03E-01	1.26
U234(n,g)	6.40E+02	3.1 %	6.31E+02	0.99
U235(n,f)	2.75E+02	1.8 %	2.69E+02	0.98
U235(n,g)	1.46E+02	41.1 %	1.40E+02	0.96
U235(n,abs)	4.19E+02	1.9 %	1.40E+02	0.33
U236(n,f)	4.10E+00	24.4 %	4.34E+00	1.06
U236(n,g)	3.45E+02	4.3 %	3.45E+02	1.00
U237(n,f)	1.40E+01	-	1.03E+01	0.74

Reaction	σ_E(b)	$\Delta\sigma_E$(b)	σ_{T14}(b)	C/E
U237(n,g)	1.20E+03	16.7 %	1.53E+03	1.28
U238(n,f)	1.63E-03	9.8 %	2.35E-03	1.44
U238(n,g)	2.77E+02	1.1 %	2.75E+02	0.99
Np236m(n,f)	1.35E+03	6.4 %	3.94E+02	0.29
Np237(n,f)	4.70E+00	4.9 %	5.49E-01	0.12
Np237(n,g)	6.52E+02	3.7 %	6.98E+02	1.07
Np238(n,f)	8.83E+02	7.9 %	6.14E+02	0.70
Np238(n,abs)	1.50E+03	33.3 %	2.44E+02	0.16
Pu236(n,f)	9.90E+02	3.0 %	6.55E+02	0.66
Pu236(n,g)	5.60E+01	-	9.41E+01	1.68
Pu238(n,g)	1.62E+02	9.3 %	1.47E+02	0.91
Pu238(n,f)	3.30E+01	15.2 %	2.41E+01	0.73
Pu238(n,abs)	1.95E+02	8.2 %	1.47E+02	0.75
Pu239(n,f)	3.03E+02	3.3 %	2.93E+02	0.97
Pu239(n,g)	1.80E+02	11.1 %	1.81E+02	1.01
Pu240(n,f)	3.16E+00	-	3.36E+00	1.06
Pu240(n,g)	8.45E+03	3.6 %	8.48E+03	1.00
Pu241(n,f)	5.70E+02	2.6 %	5.60E+02	0.98
Pu241(n,g)	1.62E+02	6.2 %	1.80E+02	1.11
Pu241(n,abs)	7.32E+02	2.3 %	1.80E+02	0.25
Pu242(n,f)	1.20E-01	-	2.25E-01	1.88
Pu242(n,g)	1.12E+03	3.6 %	1.12E+03	1.00
Pu243(n,f)	5.50E+02	14.5 %	3.65E+02	0.66
Pu243(n,g)	2.70E+02	13.0 %	1.47E+02	0.55
Pu244(n,g)	4.06E+01	7.1 %	4.38E+01	1.08
Pu245(n,g)	2.20E+02	18.2 %	1.73E+02	0.79
Am241(n,f)	1.44E+01	6.9 %	7.27E+00	0.50
Am241(n,g)	1.43E+03	7.0 %	1.40E+03	0.98
Am241(n,g)g	1.23E+03	8.1 %	1.21E+03	0.99
Am241(n,g)m	1.95E+02	10.3 %	1.87E+02	0.96
Am242(n,f)	3.00E+02	-	9.91E+02	3.30
Am242(n,g)	1.50E+02	-	1.99E+02	1.33
Am242m(n,f)	1.57E+03	5.1 %	3.72E+02	0.24
Am242m(n,g)	2.11E+02	-	6.80E+01	0.32
Am243(n,g)	1.82E+03	3.8 %	1.80E+03	0.99
Am243(n,g)g	9.40E+01	9.6 %	1.23E+03	13.08
Am243(n,g)m	1.73E+03	4.0 %	5.70E+02	0.33
Am243(n,f)	8.50E+00	5.9 %	2.48E+00	0.29
Cm242(n,g)	1.10E+02	18.2 %	1.08E+02	0.98
Cm242(n,f)	1.29E+01	5.4 %	7.90E+00	0.61
Cm243(n,g)	2.15E+02	9.3 %	1.94E+02	0.90
Cm243(n,f)	1.57E+03	6.4 %	1.54E+03	0.98
Cm244(n,f)	1.25E+01	20.0 %	6.04E+00	0.48
Cm244(n,g)	6.55E+02	4.6 %	6.57E+02	1.00

Reaction	σ_E(b)	$\Delta\sigma_E$(b)	σ_{T14}(b)	C/E
Cm245(n,g)	1.01E+02	7.9 %	1.10E+02	1.09
Cm245(n,f)	8.40E+02	47.6 %	7.35E+02	0.87
Cm246(n,f)	1.02E+01	3.9 %	9.95E+00	0.98
Cm246(n,g)	1.22E+02	5.7 %	1.03E+02	0.84
Cm247(n,f)	7.60E+02	6.6 %	6.28E+02	0.83
Cm247(n,g)	5.30E+02	5.7 %	5.44E+02	1.03
Cm248(n,f)	1.31E+01	11.5 %	2.89E+00	0.22
Cm248(n,g)	2.70E+02	5.6 %	2.67E+02	0.99
Bk249(n,g)	1.11E+03	9.0 %	1.19E+03	1.07
Cf249(n,f)	2.38E+03	3.6 %	2.32E+03	0.98
Cf249(n,g)	7.65E+02	4.6 %	6.13E+02	0.80
Cf250(n,g)	1.16E+04	4.3 %	1.17E+04	1.01
Cf250(n,f)	1.60E+02	25.0 %	7.68E+02	4.80
Cf251(n,g)	1.60E+03	1.9 %	1.98E+03	1.24
Cf251(n,f)	5.90E+03	1.7 %	1.31E+03	0.22
Cf252(n,g)	4.25E+01	7.1 %	6.71E+01	1.58
Cf252(n,f)	1.10E+02	27.3 %	1.06E+02	0.97
Cf253(n,f)	2.00E+03	20.0 %	2.02E+02	0.10
Cf253(n,g)	8.00E+00	12.5 %	4.79E+00	0.60
Cf254(n,g)	2.00E+00	-	1.03E+01	5.17
Cf254(n,f)	2.80E+01	-	3.42E+01	1.22
Es253(n,g)	3.86E+03	5.2 %	2.02E+03	0.52
Es253(n,g)g	1.14E+02	6.1 %	8.54E+02	7.49
Es253(n,g)m	3.75E+03	5.3 %	7.25E+02	0.19
Es254(n,f)	1.20E+03	20.8 %	1.66E+03	1.39
Es254(n,g)	1.82E+01	8.2 %	2.59E+01	1.42
Es254m(n,g)	1.00E+03	-	1.48E+02	0.15
Fm255(n,g)	1.40E+01	14.3 %	2.65E+01	1.89
Fm257(n,abs)	5.00E+00	-	6.06E+00	1.21

30 keV MACS values

The data in Table 5 presents all of the integral resonance cross sections for capture reactions within the KADoNiS database. The experimental and TENDL-2014 cross sections are provided in barns, with C/E values in the last column.

Table 5: Summary of 30 keV Maxwellian-averaged cross section comparison.

Reaction	σ_E(b)	$\Delta\sigma_E$(b)	σ_{T14}(b)	C/E
H001(n,g)	2.54E-04	2.0E-05	1.52E-04	0.60

Reaction	σ_E(b)	$\Delta\sigma_E$(b)	σ_{T14}(b)	C/E
H002(n,g)	3.00E-06	2.0E-07	2.00E-06	0.67
He003(n,g)	7.60E-06	6.0E-07	2.13E-05	2.80
Li007(n,g)	4.20E-05	3.0E-06	4.64E-05	1.11
Be009(n,g)	1.02E-05	1.6E-06	9.29E-06	0.91
C012(n,g)	1.54E-05	1.0E-06	1.62E-05	1.05
C013(n,g)	2.10E-05	4.0E-06	1.40E-05	0.67
C014(n,g)	8.48E-06	5.7E-07	1.49E-08	0.00
N014(n,g)	4.10E-05	6.0E-05	6.68E-05	1.63
N015(n,g)	5.80E-06	6.0E-07	9.20E-06	1.59
O016(n,g)	3.80E-05	4.0E-06	3.16E-05	0.83
O018(n,g)	8.90E-06	8.0E-07	4.89E-04	54.92
F019(n,g)	3.20E-03	1.0E-04	4.36E-03	1.36
Ne020(n,g)	1.19E-04	1.1E-05	1.19E-04	1.00
Ne021(n,g)	1.50E-03	9.0E-04	1.71E-03	1.14
Ne022(n,g)	5.80E-05	4.0E-06	8.34E-05	1.44
Na023(n,g)	2.10E-03	2.0E-04	2.00E-03	0.95
Mg024(n,g)	3.30E-03	4.0E-04	3.90E-03	1.18
Mg025(n,g)	6.40E-03	4.0E-04	5.86E-03	0.91
Mg026(n,g)	1.26E-04	9.0E-06	9.74E-05	0.77
Al026(n,g)	3.70E-03	0.0E+00	3.12E-03	0.84
Al027(n,g)	3.74E-03	3.0E-04	3.30E-03	0.88
Si028(n,g)	1.42E-03	1.3E-04	5.80E-03	4.09
Si029(n,g)	6.58E-03	6.6E-04	6.44E-03	0.98
Si030(n,g)	1.82E-03	3.3E-04	1.81E-03	0.99
P031(n,g)	1.74E-03	9.0E-05	2.10E-03	1.20
S032(n,g)	4.10E-03	2.0E-04	5.81E-03	1.42
S033(n,g)	7.40E-03	1.5E-03	6.33E-03	0.86
S034(n,g)	2.26E-04	1.0E-05	3.13E-04	1.38
S036(n,g)	1.71E-04	1.4E-05	7.60E-04	4.45
Cl035(n,g)	9.70E-03	2.1E-04	9.24E-03	0.95
Cl036(n,g)	1.20E-02	1.0E-03	6.13E-03	0.51
Cl037(n,g)	2.12E-03	7.0E-05	3.44E-03	1.62
Ar036(n,g)	9.00E-03	1.5E-03	8.70E-03	0.97
Ar038(n,g)	3.00E-03	3.0E-04	2.21E-03	0.74
Ar039(n,g)	8.00E-03	2.0E-03	1.50E+00	187.60
Ar040(n,g)	2.55E-03	1.0E-04	2.37E-03	0.93
K039(n,g)	1.18E-02	4.0E-04	1.03E-02	0.87
K040(n,g)	3.10E-02	7.0E-03	3.07E-02	0.99
K041(n,g)	2.20E-02	7.0E-04	1.99E-02	0.90
Ca040(n,g)	5.73E-03	3.4E-04	5.46E-03	0.95
Ca041(n,g)	3.00E-02	7.0E-03	3.67E-02	1.22
Ca042(n,g)	1.56E-02	2.0E-03	1.31E-02	0.84
Ca043(n,g)	5.10E-02	6.0E-03	4.99E-02	0.98
Ca044(n,g)	9.40E-03	1.3E-03	7.63E-03	0.81

Reaction	σ_E(b)	$\Delta\sigma_E$(b)	σ_{T14}(b)	C/E
Ca045(n,g)	1.75E-02	3.5E-03	1.72E-02	0.98
Ca046(n,g)	5.30E-03	5.0E-04	6.17E-03	1.16
Ca048(n,g)	8.70E-04	9.0E-05	8.60E-04	0.99
Sc045(n,g)	6.90E-02	5.0E-03	6.45E-02	0.93
Ti046(n,g)	2.68E-02	3.2E-03	2.60E-02	0.97
Ti047(n,g)	6.44E-02	7.7E-03	5.82E-02	0.90
Ti048(n,g)	3.18E-02	5.1E-03	2.65E-02	0.83
Ti049(n,g)	2.21E-02	2.1E-03	1.32E-02	0.60
Ti050(n,g)	3.60E-03	4.0E-04	3.43E-03	0.95
V050(n,g)	5.00E-02	9.0E-03	4.28E-02	0.86
V051(n,g)	3.80E-02	4.0E-03	3.17E-02	0.83
Cr050(n,g)	4.90E-02	1.3E-02	3.82E-02	0.78
Cr051(n,g)	8.70E-02	1.6E-02	8.29E-02	0.95
Cr052(n,g)	8.80E-03	2.3E-03	9.06E-03	1.03
Cr053(n,g)	5.80E-02	1.0E-02	4.15E-02	0.71
Cr054(n,g)	6.70E-03	1.6E-03	4.78E-03	0.71
Mn055(n,g)	3.96E-02	3.0E-03	3.28E-02	0.83
Fe054(n,g)	2.96E-02	1.3E-03	2.16E-02	0.73
Fe055(n,g)	7.50E-02	1.2E-02	8.47E-02	1.13
Fe056(n,g)	1.17E-02	5.0E-04	1.18E-02	1.01
Fe057(n,g)	4.00E-02	4.0E-03	6.05E-02	1.51
Fe058(n,g)	1.35E-02	7.0E-04	1.40E-02	1.04
Fe060(n,g)	5.15E-03	1.4E-03	6.09E-03	1.18
Co059(n,g)	3.96E-02	2.7E-03	4.06E-02	1.03
Ni058(n,g)	3.87E-02	1.5E-03	3.39E-02	0.87
Ni059(n,g)	8.70E-02	1.4E-02	6.51E-02	0.75
Ni060(n,g)	2.99E-02	7.0E-04	2.67E-02	0.89
Ni061(n,g)	8.20E-02	8.0E-03	9.90E-02	1.21
Ni062(n,g)	2.23E-02	1.6E-03	1.92E-02	0.86
Ni063(n,g)	3.10E-02	6.0E-03	3.04E-02	0.98
Ni064(n,g)	8.00E-03	7.0E-04	1.44E-02	1.80
Cu063(n,g)	5.57E-02	2.2E-03	9.16E-02	1.65
Cu065(n,g)	2.98E-02	1.3E-03	3.84E-02	1.29
Zn064(n,g)	5.90E-02	5.0E-03	6.00E-02	1.02
Zn065(n,g)	1.62E-01	2.7E-02	3.23E-01	1.99
Zn066(n,g)	3.50E-02	3.0E-03	3.60E-02	1.03
Zn067(n,g)	1.53E-01	1.5E-02	1.11E-01	0.72
Zn068(n,g)	1.92E-02	2.4E-03	2.10E-02	1.09
Zn070(n,g)	2.15E-02	2.0E-03	2.03E-02	0.95
Ga069(n,g)	1.39E-01	6.0E-03	1.22E-01	0.88
Ga071(n,g)	1.23E-01	8.0E-03	9.80E-02	0.80
Ge070(n,g)	8.80E-02	5.0E-03	6.19E-02	0.70
Ge072(n,g)	7.30E-02	7.0E-03	6.63E-02	0.91
Ge073(n,g)	2.43E-01	4.7E-02	2.35E-01	0.97

Reaction	σ_E(b)	$\Delta\sigma_E$(b)	σ_{T14}(b)	C/E
Ge074(n,g)	3.76E-02	3.9E-03	3.62E-02	0.96
Ge076(n,g)	2.15E-02	1.8E-03	1.97E-02	0.92
As075(n,g)	3.62E-01	1.9E-02	4.17E-01	1.15
Se074(n,g)	2.71E-01	1.5E-02	2.59E-01	0.96
Se076(n,g)	1.64E-01	8.0E-03	1.39E-01	0.85
Se077(n,g)	4.18E-01	7.1E-02	4.61E-01	1.10
Se078(n,g)	6.00E-02	9.6E-03	6.03E-02	1.00
Se079(n,g)	2.63E-01	4.6E-02	2.73E-01	1.04
Se080(n,g)	4.20E-02	3.0E-03	3.99E-02	0.95
Se082(n,g)	9.00E-03	8.0E-03	4.00E-03	0.44
Br079(n,g)	6.28E-01	3.4E-02	6.37E-01	1.01
Br081(n,g)	2.39E-01	7.0E-03	2.35E-01	0.98
Kr078(n,g)	3.21E-01	2.6E-02	2.71E-01	0.84
Kr079(n,g)	9.59E-01	1.6E-01	8.84E-01	0.92
Kr080(n,g)	2.67E-01	1.4E-02	2.52E-01	0.94
Kr081(n,g)	6.07E-01	1.0E-01	6.22E-01	1.02
Kr082(n,g)	9.00E-02	6.0E-03	7.85E-02	0.87
Kr083(n,g)	2.43E-01	1.5E-02	3.49E-01	1.44
Kr084(n,g)	3.80E-02	4.0E-03	3.18E-02	0.84
Kr085(n,g)	5.50E-02	4.5E-02	5.06E-02	0.92
Kr086(n,g)	3.40E-03	3.0E-04	4.08E-03	1.20
Rb085(n,g)	2.34E-01	7.0E-03	2.57E-01	1.10
Rb086(n,g)	2.02E-01	1.6E-01	1.99E-01	0.98
Rb087(n,g)	1.57E-02	8.0E-04	1.68E-02	1.07
Sr084(n,g)	3.00E-01	1.7E-02	2.57E-01	0.86
Sr086(n,g)	6.40E-02	3.0E-03	5.63E-02	0.88
Sr087(n,g)	9.20E-02	4.0E-03	7.42E-02	0.81
Sr088(n,g)	6.13E-03	1.1E-04	5.37E-03	0.88
Sr089(n,g)	1.90E-02	1.4E-02	1.43E-02	0.75
Y089(n,g)	1.90E-02	6.0E-04	2.31E-02	1.21
Zr090(n,g)	1.93E-02	9.0E-04	1.93E-02	1.00
Zr091(n,g)	6.20E-02	3.4E-03	6.57E-02	1.06
Zr092(n,g)	3.01E-02	1.7E-03	4.53E-02	1.51
Zr093(n,g)	9.50E-02	1.0E-02	8.87E-02	0.93
Zr094(n,g)	2.60E-02	1.0E-03	2.90E-02	1.12
Zr095(n,g)	7.90E-02	1.2E-02	8.35E-02	1.06
Zr096(n,g)	1.07E-02	5.0E-04	1.07E-02	1.00
Nb093(n,g)	2.66E-01	5.0E-03	2.88E-01	1.08
Nb094(n,g)	4.82E-01	9.2E-02	5.49E-01	1.14
Nb095(n,g)	3.10E-01	6.5E-02	5.14E-01	1.66
Mo100(n,g)	1.08E-01	1.4E-02	1.07E-01	0.99
Mo092(n,g)	7.00E-02	1.0E-02	5.33E-02	0.76
Mo094(n,g)	1.02E-01	2.0E-02	1.10E-01	1.08
Mo095(n,g)	2.92E-01	1.2E-02	3.68E-01	1.26

Reaction	σ_E(b)	$\Delta\sigma_E$(b)	σ_{T14}(b)	C/E
Mo096(n,g)	1.12E-01	8.0E-03	1.05E-01	0.94
Mo097(n,g)	3.39E-01	1.4E-02	3.45E-01	1.02
Mo098(n,g)	9.90E-02	7.0E-03	8.97E-02	0.91
Mo099(n,g)	2.40E-01	4.0E-02	2.68E-01	1.12
Tc099(n,g)	7.81E-01	4.7E-02	8.82E-01	1.13
Ru100(n,g)	2.06E-01	1.3E-02	1.82E-01	0.88
Ru101(n,g)	9.96E-01	4.0E-02	1.05E+00	1.05
Ru102(n,g)	1.51E-01	7.0E-03	2.56E-01	1.70
Ru103(n,g)	3.43E-01	5.2E-02	4.36E-01	1.27
Ru104(n,g)	1.56E-01	6.0E-03	2.35E-01	1.50
Ru096(n,g)	2.07E-01	8.0E-03	1.86E-01	0.90
Ru098(n,g)	1.73E-01	3.6E-02	1.70E-01	0.98
Ru099(n,g)	6.31E-01	9.9E-02	6.75E-01	1.07
Rh103(n,g)	8.11E-01	1.4E-02	1.02E+00	1.26
Pd102(n,g)	3.69E-01	1.7E-02	3.66E-01	0.99
Pd104(n,g)	2.89E-01	2.9E-02	2.84E-01	0.98
Pd105(n,g)	1.20E+00	6.0E-02	1.21E+00	1.01
Pd106(n,g)	2.52E-01	2.5E-02	2.86E-01	1.14
Pd107(n,g)	1.34E+00	6.0E-02	1.41E+00	1.05
Pd108(n,g)	2.03E-01	2.0E-02	1.98E-01	0.98
Pd110(n,g)	1.46E-01	2.0E-02	1.56E-01	1.07
Ag107(n,g)	7.92E-01	3.0E-02	6.99E-01	0.88
Ag109(n,g)	7.88E-01	3.0E-02	9.04E-01	1.15
Ag110(n,g)	1.17E+00	1.9E-01	1.15E+00	0.98
Cd106(n,g)	3.02E-01	2.4E-02	3.48E-01	1.15
Cd108(n,g)	2.02E-01	9.0E-03	2.04E-01	1.01
Cd110(n,g)	2.37E-01	2.0E-03	2.33E-01	0.98
Cd111(n,g)	7.54E-01	1.2E-02	8.41E-01	1.11
Cd112(n,g)	1.88E-01	1.7E-03	1.98E-01	1.05
Cd113(n,g)	6.67E-01	1.1E-02	6.34E-01	0.95
Cd114(n,g)	1.29E-01	1.3E-03	1.17E-01	0.91
Cd115(n,g)	2.90E-01	6.2E-02	6.17E-01	2.13
Cd115m(n,g)	6.01E-01	2.0E-01	6.92E-01	1.15
Cd116(n,g)	7.48E-02	9.0E-04	8.63E-02	1.15
In113(n,g)	7.87E-01	7.0E-02	9.06E-01	1.15
In114m(n,g)	2.60E+00	1.3E+00	2.42E+00	0.93
In115(n,g)	7.06E-01	7.0E-02	7.50E-01	1.06
Sn112(n,g)	2.10E-01	1.2E-02	1.83E-01	0.87
Sn114(n,g)	1.34E-01	1.8E-03	1.17E-01	0.87
Sn115(n,g)	3.42E-01	8.7E-03	3.45E-01	1.01
Sn116(n,g)	9.16E-02	6.0E-04	9.59E-02	1.05
Sn117(n,g)	3.19E-01	4.8E-03	3.24E-01	1.02
Sn118(n,g)	6.21E-02	6.0E-04	5.30E-02	0.85
Sn119(n,g)	1.80E-01	1.0E-02	1.64E-01	0.91

Reaction	σ_E(b)	$\Delta\sigma_E$(b)	σ_{T14}(b)	C/E
Sn120(n,g)	3.60E-02	3.0E-04	3.81E-02	1.06
Sn121(n,g)	1.67E-01	3.0E-02	3.60E-01	2.16
Sn122(n,g)	2.19E-02	1.5E-03	1.97E-02	0.90
Sn124(n,g)	1.20E-02	1.8E-03	1.91E-02	1.59
Sn125(n,g)	5.90E-02	9.0E-03	6.60E-02	1.12
Sn126(n,g)	1.00E-02	4.0E-03	9.91E-03	0.99
Sb121(n,g)	5.32E-01	1.6E-02	5.33E-01	1.00
Sb122(n,g)	8.94E-01	1.6E-01	8.51E-01	0.95
Sb123(n,g)	3.03E-01	9.0E-03	3.10E-01	1.02
Sb125(n,g)	2.60E-01	7.0E-02	2.29E-01	0.88
Te120(n,g)	5.19E-01	2.6E-02	5.11E-01	0.98
Te122(n,g)	2.95E-01	3.0E-03	2.64E-01	0.89
Te123(n,g)	8.32E-01	8.0E-03	1.20E+00	1.44
Te124(n,g)	1.55E-01	2.0E-03	1.06E-01	0.68
Te125(n,g)	4.31E-01	4.0E-03	3.96E-01	0.92
Te126(n,g)	8.13E-02	1.4E-03	6.98E-02	0.86
Te128(n,g)	4.44E-02	1.3E-03	3.12E-02	0.70
Te130(n,g)	1.47E-02	2.8E-03	1.11E-02	0.75
I127(n,g)	6.35E-01	3.0E-02	6.58E-01	1.04
I129(n,g)	4.41E-01	2.2E-02	4.12E-01	0.93
Xe124(n,g)	6.44E-01	8.3E-02	6.93E-01	1.08
Xe126(n,g)	3.59E-01	5.1E-02	3.72E-01	1.04
Xe128(n,g)	2.63E-01	3.7E-03	2.96E-01	1.13
Xe129(n,g)	6.17E-01	1.2E-02	5.74E-01	0.93
Xe130(n,g)	1.32E-01	2.1E-03	1.48E-01	1.12
Xe131(n,g)	3.40E-01	6.5E-02	3.49E-01	1.03
Xe132(n,g)	6.46E-02	5.3E-03	7.14E-02	1.10
Xe133(n,g)	1.27E-01	3.4E-02	1.20E-01	0.95
Xe134(n,g)	2.02E-02	1.7E-03	1.60E-02	0.79
Xe136(n,g)	9.10E-04	8.0E-05	9.64E-04	1.06
Cs133(n,g)	5.09E-01	2.1E-02	5.21E-01	1.02
Cs134(n,g)	7.24E-01	6.5E-02	7.34E-01	1.01
Cs135(n,g)	1.60E-01	1.0E-02	1.64E-01	1.02
Ba130(n,g)	7.46E-01	3.4E-02	8.14E-01	1.09
Ba132(n,g)	3.97E-01	1.6E-02	3.98E-01	1.00
Ba134(n,g)	1.76E-01	5.6E-03	1.81E-01	1.03
Ba135(n,g)	4.55E-01	1.5E-02	5.01E-01	1.10
Ba136(n,g)	6.12E-02	2.0E-03	6.10E-02	1.00
Ba137(n,g)	7.63E-02	2.4E-03	7.44E-02	0.97
Ba138(n,g)	4.00E-03	2.0E-04	3.60E-03	0.90
La138(n,g)	4.19E-01	5.9E-02	5.00E-01	1.19
La139(n,g)	3.24E-02	3.1E-03	4.68E-02	1.44
Ce132(n,g)	1.57E+00	4.2E-01	1.53E+00	0.98
Ce133(n,g)	2.60E+00	4.0E-01	2.47E+00	0.95

Reaction	σ_E(b)	$\Delta\sigma_E$(b)	σ_{T14}(b)	C/E
Ce134(n,g)	9.67E-01	3.5E-01	9.00E-01	0.93
Ce135(n,g)	1.32E+00	2.6E-01	1.26E+00	0.96
Ce136(n,g)	3.00E-01	2.1E-02	2.89E-01	0.96
Ce137(n,g)	9.73E-01	2.6E-01	9.36E-01	0.96
Ce138(n,g)	1.79E-01	5.0E-03	1.72E-01	0.96
Ce139(n,g)	2.14E-01	1.2E-01	2.31E-01	1.08
Ce140(n,g)	1.10E-02	4.0E-04	8.83E-03	0.80
Ce141(n,g)	7.60E-02	3.3E-02	1.02E-01	1.34
Ce142(n,g)	2.80E-02	1.0E-03	2.21E-02	0.79
Pr141(n,g)	1.11E-01	1.4E-03	9.68E-02	0.87
Pr142(n,g)	4.15E-01	1.8E-01	3.85E-01	0.93
Pr143(n,g)	3.50E-01	8.6E-02	2.68E-01	0.77
Nd142(n,g)	3.50E-02	7.0E-04	3.56E-02	1.02
Nd143(n,g)	2.45E-01	3.0E-03	2.53E-01	1.03
Nd144(n,g)	8.13E-02	1.5E-03	7.63E-02	0.94
Nd145(n,g)	4.25E-01	5.0E-03	4.22E-01	0.99
Nd146(n,g)	9.12E-02	1.0E-03	1.29E-01	1.41
Nd147(n,g)	5.44E-01	9.0E-02	5.32E-01	0.98
Nd148(n,g)	1.47E-01	2.0E-03	1.26E-01	0.86
Nd150(n,g)	1.59E-01	1.0E-02	1.45E-01	0.91
Pm147(n,g)	7.09E-01	1.0E-01	8.71E-01	1.23
Pm148(n,g)	2.97E+00	5.0E-01	1.67E+00	0.56
Pm148m(n,g)	2.45E+00	1.2E+00	4.96E+00	2.02
Pm149(n,g)	2.51E+00	7.5E-01	1.72E+00	0.68
Sm144(n,g)	9.20E-02	6.0E-03	4.41E-02	0.48
Sm147(n,g)	9.73E-01	1.0E-02	1.06E+00	1.09
Sm148(n,g)	2.41E-01	2.0E-03	2.47E-01	1.03
Sm149(n,g)	1.82E+00	1.7E-02	2.28E+00	1.25
Sm150(n,g)	4.22E-01	4.0E-03	4.23E-01	1.00
Sm151(n,g)	3.03E+00	6.8E-02	2.97E+00	0.98
Sm152(n,g)	4.73E-01	4.0E-03	4.59E-01	0.97
Sm153(n,g)	1.09E+00	1.7E-01	1.46E+00	1.33
Sm154(n,g)	2.06E-01	9.0E-03	2.03E-01	0.98
Eu151(n,g)	3.48E+00	7.7E-02	3.82E+00	1.10
Eu152(n,g)	7.60E+00	1.2E+00	7.02E+00	0.92
Eu153(n,g)	2.56E+00	4.6E-02	2.42E+00	0.95
Eu154(n,g)	4.42E+00	6.7E-01	5.29E+00	1.20
Eu155(n,g)	1.32E+00	8.4E-02	1.75E+00	1.32
Gd152(n,g)	1.05E+00	1.7E-02	1.09E+00	1.04
Gd153(n,g)	4.55E+00	7.0E-01	5.14E+00	1.13
Gd154(n,g)	1.03E+00	1.2E-02	1.09E+00	1.06
Gd155(n,g)	2.65E+00	3.0E-02	2.81E+00	1.06
Gd156(n,g)	6.15E-01	5.0E-03	6.10E-01	0.99
Gd157(n,g)	1.37E+00	1.5E-02	1.35E+00	0.98

Reaction	σ_E(b)	$\Delta\sigma_E$(b)	σ_{T14}(b)	C/E
Gd158(n,g)	3.24E-01	3.0E-03	2.97E-01	0.92
Gd160(n,g)	1.54E-01	2.0E-02	1.55E-01	1.01
Tb159(n,g)	1.58E+00	1.5E-01	1.60E+00	1.01
Tb160(n,g)	3.24E+00	5.1E-01	5.88E+00	1.81
Dy156(n,g)	1.61E+00	9.2E-02	1.80E+00	1.12
Dy158(n,g)	1.06E+00	4.0E-01	1.29E+00	1.22
Dy160(n,g)	8.90E-01	1.2E-02	8.26E-01	0.93
Dy161(n,g)	1.96E+00	1.9E-02	1.98E+00	1.01
Dy162(n,g)	4.46E-01	4.0E-03	4.96E-01	1.11
Dy163(n,g)	1.11E+00	1.1E-02	1.12E+00	1.00
Dy164(n,g)	2.12E-01	3.0E-03	2.11E-01	0.99
Ho163(n,g)	2.12E+00	9.5E-02	5.97E+00	2.81
Ho165(n,g)	1.28E+00	1.0E-01	1.38E+00	1.07
Er162(n,g)	1.62E+00	1.2E-01	1.82E+00	1.12
Er164(n,g)	1.08E+00	5.1E-02	1.34E+00	1.23
Er166(n,g)	5.63E-01	5.6E-02	5.20E-01	0.92
Er167(n,g)	1.43E+00	1.4E-01	1.45E+00	1.02
Er168(n,g)	3.38E-01	4.4E-02	3.22E-01	0.95
Er169(n,g)	6.53E-01	1.1E-01	6.47E-01	0.99
Er170(n,g)	1.70E-01	7.0E-03	1.77E-01	1.04
Tm169(n,g)	1.13E+00	5.6E-02	1.17E+00	1.03
Tm170(n,g)	1.87E+00	3.3E-01	2.06E+00	1.10
Tm171(n,g)	4.86E-01	1.4E-01	9.93E-01	2.04
Yb168(n,g)	1.21E+00	4.9E-02	1.24E+00	1.02
Yb170(n,g)	7.68E-01	7.0E-03	7.72E-01	1.01
Yb171(n,g)	1.21E+00	1.2E-02	1.22E+00	1.01
Yb172(n,g)	3.41E-01	3.0E-03	3.96E-01	1.16
Yb173(n,g)	7.54E-01	7.0E-03	8.44E-01	1.12
Yb174(n,g)	1.51E-01	1.7E-03	1.62E-01	1.07
Yb175(n,g)	5.58E-01	8.3E-02	7.93E-01	1.42
Yb176(n,g)	1.16E-01	2.0E-03	1.01E-01	0.87
Lu175(n,g)	1.22E+00	1.0E-02	1.26E+00	1.04
Lu176(n,g)	1.64E+00	1.4E-02	1.90E+00	1.16
Hf174(n,g)	9.83E-01	4.6E-02	1.02E+00	1.04
Hf176(n,g)	6.26E-01	1.1E-02	5.58E-01	0.89
Hf177(n,g)	1.54E+00	1.2E-02	1.62E+00	1.05
Hf178(n,g)	3.19E-01	3.0E-03	3.18E-01	1.00
Hf179(n,g)	9.22E-01	8.0E-03	9.70E-01	1.05
Hf180(n,g)	1.57E-01	2.0E-03	1.41E-01	0.90
Hf181(n,g)	1.94E-01	3.1E-02	3.84E-01	1.98
Hf182(n,g)	1.41E-01	8.0E-03	1.44E-01	1.02
Ta179(n,g)	1.33E+00	4.2E-01	3.13E+00	2.34
Ta180m(n,g)	1.47E+00	1.0E-01	1.65E+00	1.13
Ta181(n,g)	7.66E-01	1.5E-02	7.74E-01	1.01

Reaction	σ_E(b)	$\Delta\sigma_E$(b)	σ_{T14}(b)	C/E
Ta182(n,g)	1.12E+00	1.8E-01	1.20E+00	1.07
W180(n,g)	6.60E-01	5.3E-02	5.59E-01	0.85
W182(n,g)	2.74E-01	8.0E-03	3.23E-01	1.18
W183(n,g)	5.15E-01	1.5E-02	5.80E-01	1.13
W184(n,g)	2.23E-01	5.0E-03	2.72E-01	1.22
W185(n,g)	5.84E-01	5.3E-02	8.28E-01	1.42
W186(n,g)	2.35E-01	9.0E-03	1.99E-01	0.85
Re185(n,g)	1.53E+00	6.2E-02	1.70E+00	1.11
Re186(n,g)	1.55E+00	2.5E-01	1.91E+00	1.23
Re187(n,g)	1.16E+00	5.7E-02	1.16E+00	1.00
Os184(n,g)	5.90E-01	3.9E-02	5.86E-01	0.99
Os186(n,g)	4.10E-01	1.7E-02	3.86E-01	0.94
Os187(n,g)	9.66E-01	3.1E-02	1.10E+00	1.13
Os188(n,g)	2.93E-01	1.4E-02	2.52E-01	0.86
Os189(n,g)	1.17E+00	4.7E-02	1.26E+00	1.08
Os190(n,g)	2.74E-01	1.2E-02	3.10E-01	1.13
Os191(n,g)	1.29E+00	2.8E-01	1.22E+00	0.95
Os192(n,g)	1.55E-01	7.0E-03	1.59E-01	1.03
Ir191(n,g)	1.35E+00	4.3E-02	1.34E+00	0.99
Ir192(n,g)	2.08E+00	4.5E-01	2.38E+00	1.15
Ir193(n,g)	9.94E-01	7.0E-02	9.17E-01	0.92
Pt190(n,g)	5.08E-01	4.4E-02	9.31E-01	1.83
Pt192(n,g)	5.90E-01	1.2E-01	4.29E-01	0.73
Pt193(n,g)	1.12E+00	2.4E-01	8.08E-01	0.72
Pt194(n,g)	3.65E-01	8.5E-02	3.20E-01	0.88
Pt195(n,g)	8.60E-01	2.0E-01	8.00E-01	0.93
Pt196(n,g)	1.83E-01	1.6E-02	2.00E-01	1.09
Pt198(n,g)	9.22E-02	4.6E-03	1.19E-01	1.29
Au197(n,g)	5.82E-01	9.0E-03	6.30E-01	1.08
Au198(n,g)	8.40E-01	1.5E-01	9.01E-01	1.07
Hg196(n,g)	2.04E-01	8.0E-03	2.14E-01	1.05
Hg198(n,g)	1.73E-01	1.5E-02	2.43E-01	1.41
Hg199(n,g)	3.74E-01	2.3E-02	3.34E-01	0.89
Hg200(n,g)	1.15E-01	1.2E-02	1.19E+00	10.34
Hg201(n,g)	2.64E-01	1.4E-02	3.28E-01	1.24
Hg202(n,g)	6.32E-02	1.9E-03	3.11E-02	0.49
Hg203(n,g)	9.80E-02	1.7E-02	3.86E-01	3.94
Hg204(n,g)	4.20E-02	4.0E-03	4.74E-02	1.13
Tl203(n,g)	1.24E-01	8.0E-03	9.32E-02	0.75
Tl204(n,g)	2.15E-01	3.8E-02	5.04E-01	2.34
Tl205(n,g)	5.40E-02	4.0E-03	1.09E-01	2.01
Pb204(n,g)	8.10E-02	2.3E-03	1.07E-01	1.32
Pb205(n,g)	1.25E-01	2.2E-02	2.13E-01	1.70
Pb206(n,g)	1.45E-02	3.0E-04	1.36E-02	0.94

Reaction	σ_E(b)	$\Delta\sigma_E$(b)	σ_{T14}(b)	C/E
Pb207(n,g)	9.90E-03	5.0E-04	1.18E-02	1.19
Pb208(n,g)	3.60E-04	3.0E-05	6.45E-04	1.79
Bi209(n,g)	2.56E-03	3.0E-04	2.90E-03	1.13
Bi210(n,g)	6.00E-03	5.0E-03	9.77E-03	1.63

B Systematics

All of the systematics used in previous EAF validations [24] have been reproduced below. Note that only a subset of the 14 and 20 MeV systematics are used for comparisons in this report. Those are generally the more robust systematics for major channels, but as demonstrated in the report they fail to reproduce many of the global, physical features of the TENDL-2014 nuclear data and are simply used as checks for logical behaviour and outliers. In all equation,

$$A = N + Z$$

is the sum of the neutron N and proton Z numbers, known as the mass number, and

$$S = \frac{N - Z}{A}$$

is the asymmetry, which describes how neutron-rich/poor the nuclide is.

B.1 14.5 MeV systematics

(n,p) systematics

Systematics for (n,p) reactions are taken from [32] and [33].

$$\begin{aligned} \sigma_{(n,p)} &= 7.657\left(A^{1/3}+1\right)^2 \exp\left\{-28.80S - 59.24S^2 + 0.2365A^{1/2}\right\} && Z \geq 40 \\ \sigma_{(n,p)} &= 23.659\left(A^{1/3}+1\right)^2 \exp\left\{-23.041\left(S+S^2\right)\right\} && Z<40 \end{aligned}$$

(n,α) systematics

Systematics for (n,α) reactions are taken from [31].

$$\sigma_{(n,\alpha)} = 15.0678\left(A^{1/3}+1\right)^2 \exp\left\{-27.55\left(S+S^2\right)\right\}$$

(n,d+np), (n,d) and (n,np) systematics

Systematics for (n,d+np), (n,d) and (n,np) reactions are taken from [32, 36]. For light nuclei with $S \leq 0.125$ the following systematics are used:

$$\sigma_{(n,d)} = 9.94 \exp\{-0.11S\}$$
$$\sigma_{(n,np+d)} = 900.9 \left(A^{1/3}+1\right)^2 (1 - 0.4828\tanh(\xi+1)) \exp\left\{-52.3S - 135.7A^{-1}\right\}$$

where ξ is the difference between proton and neutron separation energies. For nuclides with S>0.125 an alternative form for the (n,d) is used:

$$\sigma_{(n,d)} = 53.066 \left(A^{1/3}+1\right)^2$$

Generally the (n,np) cross section should be given by the difference,

$$\sigma_{(n,np)} = \sigma_{(n,np+d)} - \sigma_{(n,d)},$$

but whenever the systematic for the (n,d) happens to be greater than the sum systematic, the (n,p) is instead replaced by

$$\sigma_{(n,np)} = 0.1\sigma_{(n,d)}$$

(n,t) systematics

Systematics for (n,t) reactions are taken from [36].

$$\sigma_{(n,t)} = 53.066 \left(A^{1/3}+1\right)^2 A^{-1/3} \left(-0.35627S + 0.0045118ZA^{-1/3} + 0.047995 + \Delta\right)^3$$

$$\Delta = \begin{cases} 0 & \text{for even-even target nuclei} \\ 4.7774A^{-3/4} - 1.0881A^{-1/2} & \text{for odd } A \text{ nuclei} \\ 9.5548A^{-3/4} - 2.1762A^{-1/2} & \text{for odd-odd target nuclei} \end{cases}$$

(n,nd) systematics

Systematics for (n,nd) reactions are taken from [36].

$$\sigma_{(n,nd)} = \begin{cases} 0.1516 \left(A^{1/3}+1\right)^2 \exp\left\{-24.35S + 0.2670A^{1/2}\right\} & \text{for even } A \\ 440.21 \exp\{-20.509S\} & \text{for odd } A \end{cases}$$

(n,h) systematics

Systematics for (n,h) reactions are taken from [39].

$$\sigma_{(n,h)} = 0.75 \left(A^{1/3} + 1\right)^2 \exp\{-11.338S\}$$

(n,n') systematics

Systematics for (n,n') reactions are taken from [40]. These data depend on the product spin states and are held in tabulated data instead of analytic formulae.

(n,γ) systematics

Systematics for (n,γ) reactions are taken from [30].

$$\sigma_{(n,\gamma)} = 1.18 - 1.13 \exp\{-0.01338A\}$$

(n,2n) systematics

Systematics for (n,2n) reactions are taken from [34].

$$\sigma_{(n,2n)} = 47.015 \left(A^{1/3} + 1\right)^2 (1 - 3.9777 \exp\{-24.116S\})$$

(n,2p) systematics

Systematics for (n,2p) reactions are taken from [41].

$$\sigma_{(n,2p)} = 48.49 \exp\{-2.99S\}$$

(n,nα) systematics

Systematics for (n,nα) reactions are taken from [35].

$$\sigma_{(n,n\alpha)} = 17.48 \exp\{-24.2S\}$$

B.2 20 MeV systematics

These systematics are taken from [36] and are used for nuclei with A>40.

(n,p) systematics

For Z<50 the following systematic is used:

$$\sigma_{(n,p)} = 53.066 \left(A^{1/3}+1\right)^2 \exp\Big\{ -47.384\left(S+A^{-1}\right)^2 - 2.3294\left(S+0.5A^{-1}\right) - 0.10405ZA^{-1/3} - 2.3483\Big\}$$

while for $Z \geq 50$ the following systematic is used:

$$\sigma_{(n,p)} = 53.066 \left(A^{1/3}+1\right)^2 \left(-1.2477(S+A^{-1}) + 0.4087\right)^3$$

(n,np) systematics

$$\sigma_{(n,np)} = 53.066 \left(A^{1/3}+1\right)^2 \left(A^{-1/3}\Big(-2.7098\big(S+1.5A^{-1}\big) + 0.67115\Big)^2 + \exp\left\{-496.74\left(S+1.5A^{-1}\right)^2 + 48.162\left(S+1.5A^{-1}\right) - 1.6714\right\}\right)$$

(n,d) systematics

$$\sigma_{(n,d)} = 53.066 \left(A^{1/3}+1\right)^2 A^{-1/3}\left(-1.3107S + 0.0019167ZA^{-1/3} + 0.48491\right)^3$$

(n,t) systematics

$$\sigma_{(n,t)} = 53.066 \left(A^{1/3}+1\right)^2 A^{-1/3}\left(-0.1506S + 0.000306ZA^{-1/3} + 0.19566 + \Delta\right)^3$$

$$\Delta = \begin{cases} 0 & \text{for even-even target nuclei} \\ 0.89317A^{-3/4} - 1.0839A^{-1/2} & \text{for odd } A \text{ nuclei} \\ 1.78634A^{-3/4} - 0.21678A^{-1/2} & \text{for odd-odd target nuclei} \end{cases}$$

(n,α) systematics

The following systematic is only used for Z<50:

$$\begin{aligned}\sigma_{(n,\alpha)} =& 53.066 \left(A^{1/3}+1\right)^2 \Big\{ -37.317 \left(S+A^{-1}\right)^2 - 7.2027 \left(S+0.5A^{-1}\right) \\ & -0.22669 Z A^{-1/3} - 2.027 \Big\}\end{aligned}$$

B.3 3.0 MeV inelastic systematics

Systematics for (n,n') reactions are taken from [42].

$$\sigma_{(n,n')} = \left(A^{1/3}+1\right)^2 \exp\left\{-0.110\Delta^2 + 0.0686\Delta + 4.21\right\}$$

where Δ is the difference between excited and ground spin states.

B.4 30 keV capture systematics

Systematics for (n,γ) reactions at 30 keV are taken from [41].

$$\sigma_{(n,\gamma)} = C_1 \left(\mu U\right)^{C_2}$$

where μ are parameter values depending on N, U is defined as

$$U = Q(n,\gamma) - P(Z) - P(N),$$

where $P(Z)$ and $P(N)$ are the pairing energies and the constants are given by:

$$\begin{aligned} C_1 &= 8.236E-8, \quad C_2 = 4.827 \quad \text{for odd } Z \\ C_1 &= 6.995E-7, \quad C_2 = 4.287 \quad \text{for even } Z. \end{aligned}$$

B.5 Non-elastic systematics

Systematics for total nonelastic reactions are taken from [43] and are applicable for incident neutron energies between 1 and 50 MeV.

$$\sigma_{nonel} = E\left(31.05A^{-1/3} - 25.91\right) + 342A^{1/3} + 21.89A^{2/3} + E^{-1}\left(0.223A^{4/3} + 0.673A^{2/3} + 617.4\right)$$

References

[1] A. Koning, S. Hilaire, and S. Goriely, "TALYS-1.6, User Manual," *Nuclear Research and Consultancy Group NRG, Petten*, 2013.

[2] A. Koning and D. Rochman, "Modern Nuclear Data Evaluation with the TALYS Code System," *Nuclear Data Sheets*, vol. 113, no. 12, pp. 2841 – 2934, 2012. Special Issue on Nuclear Reaction Data.

[3] A. Koning *et al.*, "TENDL-2014: TALYS-based Evaluated Nuclear Data Library." http://www.talys.eu/tendl-2014, 2014.

[4] S. F. Mughabghab, *Atlas of Neutron Resonances: Resonance Parameters and Thermal Cross Sections. Z=1-100.* Elsevier, 5 ed., April 2006.

[5] W. M. Haynes, ed., *Handbook of Chemistry and Physics*. CRC Press, 96 ed., June 2015.

[6] J. Kopecky. Private communication, February 2015.

[7] M. Fleming, J.-Ch. Sublet, and J. Kopecky, "Integro-Differential Verification and Validation, FISPACT-II & TENDL-2014 nuclear data libraries," Tech. Rep. CCFE-R(15)27, CCFE, March 2015. http://www.ccfe.ac.uk/EASY.aspx.

[8] J.-Ch. Sublet and M. Fleming, "Maxwellian-Averaged Neutron-Induced Cross Sections for kT=1 keV to 100 keV, KADoNiS, TENDL-2014, ENDF/B-VII.1 and JENDL-4.0u nuclear data libraries," Tech. Rep. UKAEA-R(15)29, UKAEA, March 2015. http://www.ccfe.ac.uk/EASY.aspx.

[9] R. Werner and D. Santry, "Neutron capture cross sections of ^{22}Na and ^{58}Co, url = http://www.sciencedirect.com/science/article/pii/0022310772900561, volume = 26, year = 1972, bdsk-url-1 = http://www.sciencedirect.com/science/article/pii/0022310772900561, bdsk-url-2 = http://dx.doi.org/10.1016/0022-3107(72)90056-1," *Journal of Nuclear Energy*, no. 8, pp. 403 – 408.

[10] K. S. Krane and J. Sylvester, "Neutron capture cross sections of ^{112,116,122,124}Sn," *Phys. Rev. C*, vol. 73, p. 054312, May 2006.

[11] M. C. Eastman and K. S. Krane, "Neutron capture cross sections of even-mass tellurium isotopes," *Phys. Rev. C*, vol. 77, p. 024303, Feb 2008.

[12] S. Karamian, J. Carroll, J. Adam, E. Kulagin, and E. Shabalin, "Production of long-lived hafnium isomers in reactor irradiations," *High Energy Density Physics*, vol. 2, no. 1–2, pp. 48 – 56, 2006.

[13] I. Dillmann, M. Heil, F. Käppeler, and T. Rauscher, "KADoNiS v0.3 - The third update of the Karlsruhe Astrophysical Database of Nucleosynthesis in Stars," in *Proceeding of the workshop EFNUDAT Fast Neutrons - scientific workshop on neutron measurements, theory and applications*, (Geel, Belgium), April 2009.

[14] Z. Bao, H. Beer, F. Käppeler, F. Voss, K. Wisshak, and T. Rauscher, "Neutron Cross Sections for Nucleosynthesis Studies," *Atomic Data and Nuclear Data Tables*, vol. 76, no. 1, pp. 70 – 154, 2000.

[15] M. Chadwick, M. Herman, P. Obloainske, M. Dunn, Y. Danon, A. Kahler, D. Smith, B. Pritychenko, G. Arbanas, R. Arcilla, R. Brewer, D. Brown, R. Capote, A. Carlson, Y. Cho, H. Derrien, K. Guber, G. Hale, S. Hoblit, S. Holloway, T. Johnson, T. Kawano, B. Kiedrowski, H. Kim, S. Kunieda, N. Larson, L. Leal, J. Lestone, R. Little, E. McCutchan, R. MacFarlane, M. MacInnes, C. Mattoon, R. McKnight, S. Mughabghab, G. Nobre, G. Palmiotti, A. Palumbo, M. Pigni, V. Pronyaev, R. Sayer, A. Sonzogni, N. Summers, P. Talou, I. Thompson, A. Trkov, R. Vogt, S. van der Marck, A. Wallner, M. White, D. Wiarda, and P. Young, "ENDF/B-VII.1 Nuclear Data for Science and Technology: Cross Sections, Covariances, Fission Product Yields and Decay Data ," *Nuclear Data Sheets*, vol. 112, no. 12, pp. 2887 – 2996, 2011. Special Issue on ENDF/B-VII.1 Library.

[16] K. Shibata, O. Iwamoto, T. Nakagawa, N. IWAMOTO, A. ICHIHARA, S. KUNIEDA, S. CHIBA, K. FURUTAKA, N. OTUKA, T. OHASAWA, T. MURATA, H. MATSUNOBU, A. ZUKERAN, S. KAMADA, and J.-i. KATAKURA, "JENDL-4.0: A New Library for Nuclear Science and Engineering," *Journal of Nuclear Science and Technology*, vol. 48, no. 1, pp. 1–30, 2011.

[17] D. E. Cullen, "PREPRO 2015: 2015 ENDF/B Pre-processing codes (ENDF/B-VII tested)," Tech. Rep. IAEA-NDS-39 (Rev. 16), IAEA, 2015. `http://www-nds.iaea.org/ndspub/endf/prepro/`.

[18] K. Shibata. Private communication, December 2014.

[19] T. Nakagawa, S. Chiba, T. Hayakawa, and T. Kajino, "Maxwellian-averaged neutron-induced reaction cross sections and astrophysical reaction rates for kT = 1 keV to 1 MeV calculated from microscopic neutron cross section library JENDL-3.3," *Atomic Data and Nuclear Data Tables*, vol. 91, no. 2, pp. 77 – 186, 2005.

[20] C. Dunford and A. Trkov, "Endf utility codes version 7.02." `http://www.nndc.bnl.gov/nndcscr/endf/endf-util/index.html`.

[21] J.-C. Sublet, P. Ribon, and M. Coste-Delclaux, "CALENDF-2010: User Manual," Tech. Rep. CEA-R-6277, ISSN 0429-3460, CEA, 2011.

[22] R. Capote, M. Herman, P. Obložinský, P. Young, S. Goriely, T. Belgya, A. Ignatyuk, A. Koning, S. Hilaire, V. Plujko, M. Avrigeanu, O. Bersillon, M. Chadwick, T. Fukahori, Z. Ge, Y. Han, S. Kailas, J. Kopecky, V. Maslov, G. Reffo, M. Sin, E. Soukhovitskii, and P. Talou, "RIPL – Reference Input Parameter Library for Calculation of Nuclear Reactions and Nuclear Data Evaluations," *Nuclear Data Sheets*, vol. 110, no. 12, pp. 3107 – 3214, 2009. Special Issue on Nuclear Reaction Data.

[23] S. van der Marck, A. Koning, and D. Rochman, "Benchmarking TENDL-2012," *Nuclear Data Sheets*, vol. 118, pp. 446 – 449, 2014.

[24] R. A. Forrest, J. Kopecky, and J.-Ch. Sublet, "The European Activation File: EAF-2007 neutron-induced cross section library," Tech. Rep. UKAEA FUS 535, UKAEA, March 2007.

[25] R. R. Winters, R. F. Carlton, C. H. Johnson, N. W. Hill, and M. R. Lacerna, "Total cross section and neutron resonance spectroscopy for $n + ^{40}$Ar," *Phys. Rev. C*, vol. 43, pp. 492–509, Feb 1991.

[26] D. Rochman, A. Koning, J. Kopecky, J.-C. Sublet, P. Ribon, and M. Moxon, "From average parameters to statistical resolved resonances," *Annals of Nuclear Energy*, vol. 51, pp. 60 – 68, 2013.

[27] A. Koning and J. Delaroche, "Local and global nucleon optical models from 1 keV to 200 MeV," *Nuclear Physics A*, vol. 713, no. 34, pp. 231 – 310, 2003.

[28] A. Koning, S. Hilaire, and S. Goriely, "Global and local level density models," *Nuclear Physics A*, vol. 810, no. 14, pp. 13 – 76, 2008.

[29] Y. Dukarevich, A. Dyumin, and D. Kaminker, "Total neutron cross sections of isotopes and the isobaric spin term of the nuclear potential," *Nuclear Physics A*, vol. 92, no. 2, pp. 433 – 448, 1967.

[30] J. Kopecky, H. A. J. van der Kamp, H. Gruppelaar, and D. Nierop, "Development of a European Activation File by extending and updating the REAC-ECN data file," Tech. Rep. ECN-89-75, 1989.

[31] A. D. Majdeddin, V. Semkova, R. Dóczi, C. M. Buczkó, and J. Csikai, "Investigations on (n,α) Cross Sections in the 14 MeV Region," Tech. Rep. INDC(HUN)-031, IAEA, July 1997.

[32] R. A. Forrest, "Systematics of neutron-induced threshold reactions with charged products at about 14.5 MeV," Tech. Rep. AERE-R–12419, UK Atomic Energy Research Establishment, December 1986.

[33] R. Dóczi, V. Semkova, A. D. Majdeddin, C. M. Buczkó, and J. Csikai, "Investigations on (n,p) Cross Sections in the 14 MeV Region," Tech. Rep. INDC(HUN)-032, IAEA, October 1997.

[34] S. A. Badikov, O. T. Grudzevich, A. V. Ignatyuk, A. B. Pashchenko, A. V. Zelenetsky, and K. I. Zolotarev, "Cross-section evaludations for activation data library," in *Nuclear Data for Science and Technology* (S. M. Qaim, ed.), pp. 930–932, 1992.

[35] R. A. Forrest and J. Kopecky, "The European Activation File: EAF-2003 cross section library," Tech. Rep. UKAEA FUS 486, UKAEA, 2002.

[36] A. Y. Konobeev and Y. A. Korovin, "Use of systematics to estimate neutron reaction cross-sections," *Atomic Energy*, vol. 85, pp. 556–563, August 1998.

[37] M. Herman, R. Capote, B. Carlson, P. Obloinsk, M. Sin, A. Trkov, H. Wienke, and V. Zerkin, "EMPIRE: Nuclear Reaction Model Code System for Data Evaluation," *Nuclear Data Sheets*, vol. 108, no. 12, pp. 2655 – 2715, 2007. Special Issue on Evaluations of Neutron Cross Sections.

[38] P. G. Young, E. D. Arthur, and M. B. Chadwick, "Comprehensive Nuclear Model Calculations: Introduction to the Theory and Use of the GNASH Code," Tech. Rep. LA–12343-MS, LANL, 1992.

[39] Y. Lishan and J. Yuling, "Systematics of the (n,3He) reaction cross sections at 14 MeV," *Chinese Journal of Nuclear Physics*, vol. 14, no. 95, 1992.

[40] H. Vonach, "Excitation of Isomeric States in (n,n') Reactions," Tech. Rep. IAEA-TECDOC-457, IAEA, 1988.

[41] R. A. Forrest and J. Kopecky, "The European Activation File: EAF-2001 cross section library," Tech. Rep. UKAEA FUS 451, UKAEA, 2001.

[42] T. Shimizu, I. Miyazaki, K. Arakita, M. Shibata, K. Kawade, J. Hori, and T. Nishitani, "Measurement of (n,n') reaction cross-sections of 79Br, 90Zr, 197Au and 207Pb with pulsed d-D neutrons," *Annals of Nuclear Energy*, vol. 32, pp. 949–963, 2005.

[43] A. Chatterjee, K. H. N. Murthy, and S. K. Gupta, "Optical Reaction Cross Sections for Light Projectiles," Tech. Rep. INDC(IND)-27/GJ, IAEA, November 1980.